DISSERTATION

DOES ORIENTATION MATTER?

CONTROLLING LACCASE ORIENTATION ON PLANAR GOLD ELECTRODES.

Submitted by

Collin Perry

Department of Chemistry

In partial fulfillment of the requirements

For the Degree of Doctor of Philosophy

Colorado State University

Fort Collins, Colorado

Fall 2024

Doctoral Committee:

Advisor: Christopher Ackerson

Christopher Snow

David Dandy

Nathan Neale

ABSTRACT

DOES ORIENTATION MATTER?

CONTROLLING LACCASE ORIENTATION ON PLANAR GOLD ELECTRODES.

Enzyme electronics are becoming more common in modern life. Even though these technologies have been integrated into everyday life, the fundamental understanding of how an enzymes' orientation at the electrode surfaces affects the enzymes catalysis is still unknown. To understand this more we designed a library of laccase mutants, all with a single solvent exposed cysteine. These cysteine residues are used to bind to a gold electrode modified with a monolayer of sulfhydryl molecules capped with a maleimide binding group. Each mutants' single cysteine will bind to the maleimide group orienting each mutant differently at the electrode surface. The wild type enzyme (WT) and all the mutants, D113C, N264C, H470C all show activity toward a common substrate 2,2'-azino-bis(3-ethylbenzothiazoline-6-sulfonic acid) (ABTS). Although each mutant does show catalytic activity in solution, we were unable to obtain an electrochemical response from the laccase library using the maleimide capped electrodes for either ABTS or oxygen. Modification of the electrodes via the deposition gold clusters makes the electrode surface more topographically complex. The cluster modified electrodes bound with WT laccase displayed an electrochemical response for the reduction of oxygen to water. The increased topography from using gold clusters allows for electron transfer with laccase enzymes, while the planar

electrodes modified with the laccase enzymes in which we achieved an electrochemical response.

ACKNOWLEDGEMENTS

I never thought I would have PI as great as Chris Ackerson. The culture of “play” he instills into his lab is truly unique and creates a fabulous place to work. I have never been afraid to have ideas or speak my mind in the lab and I am so happy to have that. Chris deserves every scientific, intellectual, and pedagogical award that ever comes his way and many more. Thank you so much for your grace, patience, nurturing, and care as it came to me and this project.

When I joined the Ackerson lab I had never worked with gold or any thiols before. Luckily my project had a tremendous level of overlap with the areas of expertise of much of the lab. I would have achieved nothing if it were not for my colleagues and mentors. Chris Hosier and Ian Anderson were tremendous help when it came to finding resources as well as handling materials and reagents in the lab. Gold is not as inert as the world likes to think and thiols follow you home.

Also, when joining the Ackerson Lab I never had any training in biology, chemical biology, or biochemistry. I had never even taken a class in the field. Zach Butz, thankfully, showed me how to work with DNA, design plasmids, and keep sterile conditions in the lab. All my initial DNA sequences were fixed and then eventually approved by him to move forward with laccase enzymes. Alex Hendricks similarly was immensely helpful when it came to protein expression and purification. My talks with him were philosophically profound, applicable, and helpful in all areas of life. A special thanks to Ryan Riskowski for always being there to bounce ideas off and for always being a great example of an excited

and creative scientist. Your enthusiasm is contagious, and you were an amazing post doc and mentor to me and the entire Ackerson Lab.

My parents have always supported me. I can not remember a time when I was scared to ask questions or speak my mind around my parents. As I grow up, I now realize how much of a gift this truly is to have. Not many people get to share genuine conversations with their parents, and I am proud to have parents willing to share opinions with me. Growing up I was never afraid of failure. I was not raised in a "failure is not an option" home. I recall my father telling me that when you are learning how to do something, failure is the most likely option. Losing my father while in grad school was not expected or planned. It was the hardest thing I have ever had to overcome. I miss him every day and am very proud to be his son.

My mother has always been a supporting person when it came to me chasing my skills and passions. I am very lucky to have a parent that will support me in whatever endeavors I choose. I love you very much and am proud to have you as a mother.

I would be nothing if it were not for my siblings Brittany and Brandon. Brittany taught me how to ride a bike and knew my schedule for me all the way up into high school. Brandon taught me how to throw a football and was a great example of someone being able to teach themselves anything, as long as you are passionate. They have been great support throughout my life and I hope I can be the same to them. You were my first friends and foes and will forever be my family.

TABLE OF CONTENTS

Chapter 1: Introduction

Electron transfer is inescapable within biochemical systems. Electron transfer events can occur between different substrates, proteins, and enzymes in which the electrons are moved heterogeneously or internally within a single protein homogenously.[1] Enzymes are naturally occurring cellular workhorses, catalyzing reactions and shuttling electrons between molecules to aid in maintaining homeostasis. In order to utilize these natural functions of life for use in molecular synthesis, catalysis, and biosensing more must be done to understand these electron transfer events in vivo and in vitro. [2,3]

Enzymes catalyzing useful reactions for synthesis, sensing, remediation, and energy production are potentially powerful scientific endeavors. Nitrogenases, for example, catalyze the formation of ammonia by reducing elemental nitrogen from the atmosphere using electrons provided by Adenine triphosphate (ATP). Performing this reaction abiotically via the Haber-Bosch process utilizes up to 2% of the world's total energy. To clean up the production of ammonia, nitrogenases have been studied to either inspire new catalysts to perform this reaction or to utilize them more directly to produce ammonia with lower energy needs. [4]

Background

Inducing and tracking enzymatic processes can become quite complex, often requiring either coenzyme(s) and/or redox active molecules, like FAD, NADPH, or ATP. In Fig. 1, this is represented by the redox active enzyme, hydrogenase, reacting with its electron donor NADPH, and its namesake substrate hydrogen, incoming as solvated protons. For this

reaction to occur the hydrogenase enzyme must react with NADPH, obtain its two electrons, transport them to a ligated proton, bound at a separate active site. Finally, this hydride reacts with another proton in solution to form hydrogen. The reaction within hydrogenase happens very fast, but at low concentrations this reaction is limited by the rate in which the three reactants collide together in solution.[5] This reliance on redox active biochemical substrates makes in vivo experiments with redox active enzymes to be quite demanding in terms of capital and time. These biological reagents are expensive to make and difficult to store, since they are very sensitive towards oxidation. One way to avoid the use of expensive reagents and coenzymes is by utilizing electrodes to provide the electromotive forces and electrons required for redox chemistries to take place. For this reason, enzymes have been studied in coordination with electrochemistry for well over half a century.[3,6] The body of literature surrounding enzyme electronics is quite vast and well established. Now, enzyme

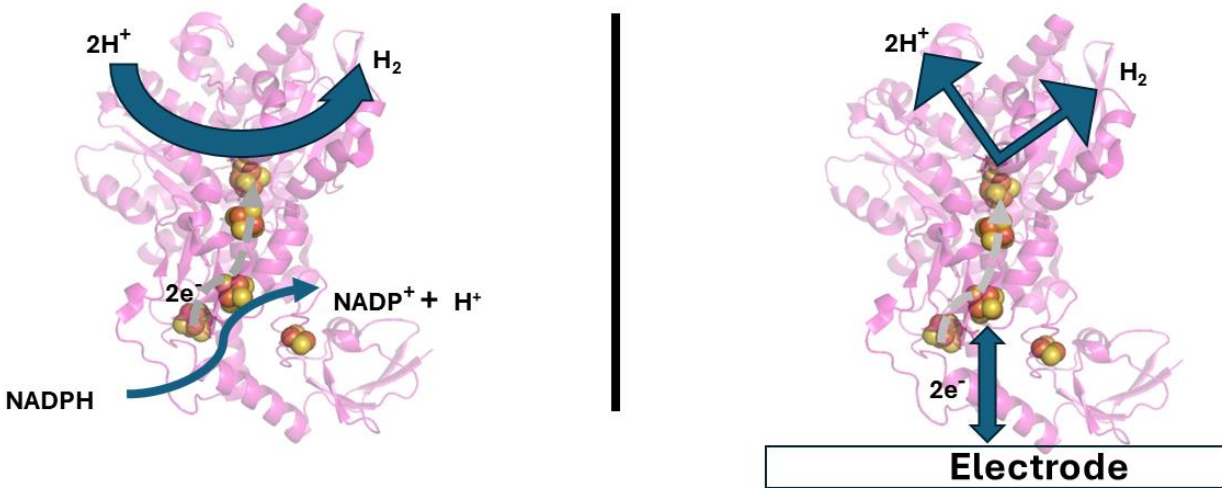

Figure 1 Hydrogenase enzyme reacting with its native substrates NADPH and hydrogen(Left) and using and electrode for electron transfer processes

modified electrodes are already commercially available products totaling billions in sales every year in the form of diabetes test kits alone, monitoring a patient's blood sugar levels. [7]

However, with all this commercial success with bioelectronics there are still many questions surrounding these technologies that must be answered for enzymatic electrodes to continue to evolve as increasingly useful technologies. [2,8,9] The most interesting questions are those surrounding the three-dimensional (3D) structure of proteins with respect to on electrode for better control of catalysis. An enzyme's 3D structure is very important to its biochemical function and many diseases and ailments can be linked to misfolded or mutated proteins. Known 3D crystal structures of proteins with angstrom(Å) resolution have grown exponentially for the past three decades thanks to the advances in computing power and electron microscopy.[10] While there has been great success attaching enzymes to electrode surfaces to probe or control its catalytic function,[2] their orientations on the electrode surface have not been fully studied.[8] By immobilizing enzymes onto electrode surfaces one can control where reactions take place and monitor them precisely with the aid of sensitive electronics. There are three main questions in enzyme electronics and biosensors that must be answered for these technologies to evolve that we are most intrigued by.

1. For Oxidoreductase enzymes which take part in both reduction and oxidation reactions: Does one active site respond more favorably to electron transfer with an electrode surface over the other?
2. Which orientation of an enzyme's allows for the greatest packing density of enzymes on the electrode surface?

3. How much does packing density and orientation affect flux of substrates, limiting the reaction rate and currents achievable?

Probing these questions further requires choosing a model system enzyme. The ideal enzyme for answering these questions would belong to the oxidoreductase class of enzymes. The enzyme should have substrate promiscuity to probe different levels of steric hinderance that could occur at the electrode surface. This is a possible consequence of overpacking enzymes in a non-ideal orientation onto and around the electrode surface. Thus, commonly studied enzymes like nitrogenases and hydrogenases are not the ideal candidates for this study since diatomic nitrogen and hydrogen would not experience much steric hinderance and they have very specific electron sources in the form of ATP or NADPH. It's also important to note that hydrogenase enzymes are very oxygen sensitive and are inactivated by even small levels of oxygen.[11,12] Laccase enzymes, however, react with oxygen as a substrate and appear to meet the criteria required to answer these questions.[13,14] Laccases are oxidoreductases that contain two catalytically active sites; one catalyzes the reduction of diatomic oxygen to water, while the other active site oxidizes a myriad of amino and phenol containing substrates. Laccase substrate promiscuity allows for the study of steric effects on molecules as small as hydroquinone ranging up to large dyes and soluble lignin-based materials. Therefore, laccase has been chosen for use as our model enzyme to study the effects of orientation on enzyme modified electrodes.

Laccase enzymes belong to the multi-copper oxidase family of oxidoreductase enzymes. They have been found in nearly every branch of life so there are many well-known

sequences and structures. The two active sites within laccases are denoted the T1 site for the phenol oxidizing active site and the trinuclear cluster site used to reduce oxygen. Natively they are separated by a 13Å cysteine-histidine bridge allowing for the two active sites to be isolated electronically. Fig 2 shows the structure of laccase enzymes with the two copper active sites. Chapter 2 is devoted entirely to the experimentation involving laccase enzymes. More on its structure, mechanism, and its engineering can be found there.

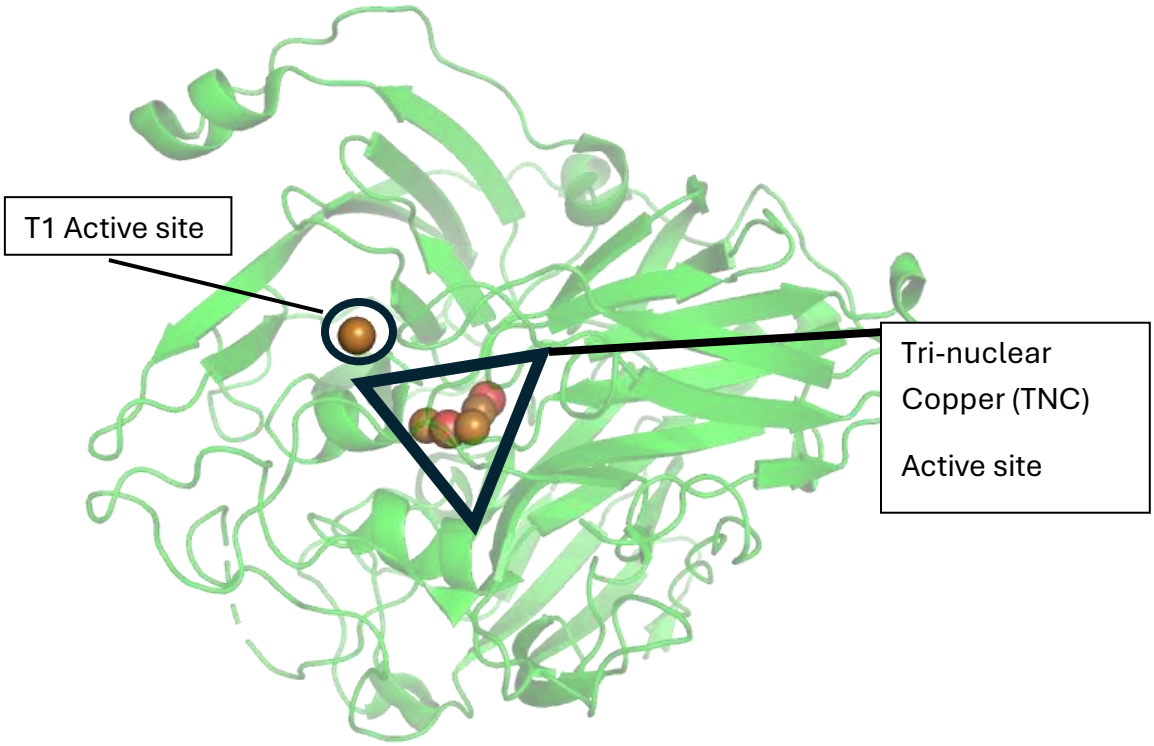

Figure 2 Laccase crystal structure from Bacillus Subtillis. T1 phenol oxidizing copper active site (circle) and the Tri-nuclear copper (TNC) oxygen reducing active site (Triangle)

Choosing an immobilization strategy for attaching our model enzyme laccase onto the surface of electrodes will be very important. There are many ways to engineer an enzyme onto an electrode surface. Typical methods for protein immobilization are via adsorption,

entrapment, or covalent-bond based attachments.[15] Adsorption and covalent attachment strategies can be seen in figure 3. Adsorption often involves weak electrostatic interactions between the electrode surface, sometimes modified by a molecular monolayer, and the solvent exposed regions of a protein. Entrapment utilizes nanomaterials, salts, or gels to immobilize proteins within a matrix or precipitate from which proteins have trouble dissociating through. Sometimes entrapped enzymes are stabilized by certain electrostatic or hydrogen bonds, but encapsulation of the enzyme is the largest factor holding the protein in place. Covalent attachment uses at least one covalent bond between the protein, another protein, a molecular monolayer, or the electrode surface. These can be non-specific binding, where a bifunctional molecule is able to bind to certain common moieties (e.g. carbonyl or amino groups) abundant in all proteins and will thus bind together in a matrix similar to a polymer on an electrode surface. Specific interactions can also be isolated and promoted with a peptide tag (e.g. His or strep tag) or by using unique, low-occurring amino acids (e.g. cysteine or methionine). Each of these techniques has their benefits and shortfalls and all of which must be considered in making an immobilization strategy.

Enzyme Immobilization Techniques

Of the main enzyme immobilization techniques (adsorption, covalent, and entrapment) only adsorption and covalent attachments offer any control over the protein orientation at the electrode surface. Electrodes using entrapment have been shown to be good biosensors with great detection limits and for tracking electrochemically active enzymes, but they have little control over the enzymes interactions with the electrode surface.[16–18]

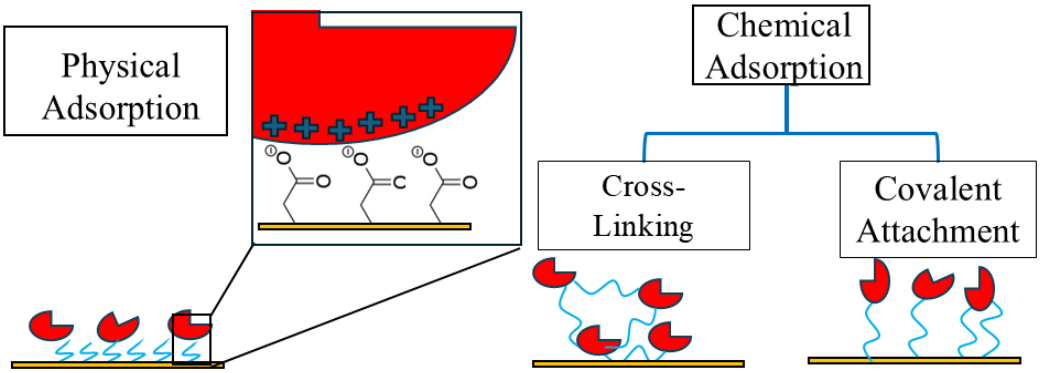

Figure 3 Two different immobilization techniques physical adsorption(left) and covalent attachments (right)

Adsorption- Orientation Control

Adsorption of enzymes onto electrodes has been a common practice for studying their electrochemical properties.[6] Adsorption does not involve the introduction of a formal chemical bond, but instead relies on the weaker intermolecular interactions between the electrode surface and the solvent exposed regions of a protein or enzyme. These interactions can be governed by hydrogen bonding, pi-pi interactions, attractive forces from opposing charges, or even metallophilic interactions between specific amino acids moieties and different conductive architectures. The goal is to have areas of the protein with charge to be attracted to opposing charges provided by a self-assembled monolayer (SAM) of molecules on the electrode surface. Adsorption of enzymes can make very useful electrodes: they can be quickly produced and provide meaningful information about an attached enzyme or substrate; however, they are limited by their stability. Since there is no permanent bond between the electrode and the adsorbed substrate the risk of losing the enzyme of interest is high.[19] First, the pH at the electrode surface is not static. In the case of a linear sweep electrochemical experiment, the charge building up at the electrode surface

will alter the solvent and electrolyte structure at the interface of the electrode surface.[20] The electrolyte rearranges into a charged double-layer which greatly changes the pH near the electrode surface, this can disrupt any weak interactions between the enzyme and the electrode. If stirring or agitation is involved in these experiments the loss of enzyme is even greater. The act of adsorption is typically non-specific in its binding, but many clever techniques have been developed for a myriad of enzymes with different electrode materials.

Taniguchi et al[21] adsorbed commercially available bilirubin oxidase, an enzyme very close to laccases in both structure and function, onto Au(111) and Au(100) single crystal gold electrodes functionalized with self-assembled monolayers of short chain hydrocarbon thiol SAMs capped with sulfate, ammonia, alcohol and carboxylic acids. With control of the pH these moieties can provide different charged surfaces at the electrode solvent interface. The goal is to have areas of the protein with charge to be attracted opposing charges provided by the respective SAM's. It was found that bilirubin oxidase adsorbed onto -NH2, -OH, and -CH3 capped SAM's did not show much if any electrocatalytic current. This showed that positive, electronegative, and nonpolar surfaces either do not orient BOD in a way that facilitates electron transfer or do not attract BOD strongly at all. Sulfate and carboxylic acid capped SAM's did show electrocatalytic currents towards the reduction of oxygen to water. They estimated the distance between the electrode and the enzyme at 17Å. This distance is approaching the limits of electron tunnelling established by Marcus theory for electron transfer at 20Å. These experiments successfully showed that the surface conditions of an electrode can dictate the orientation and binding of certain enzymes.

Blanford et al. engineered a pyrolytic graphite electrode(PGE) functionalized with a monolayer of anthracene with the goal of orienting laccase enzymes with its T1 active site nearest the electrode surface.[22] Anthracene shares a similar structure to many of laccase substrates and can bind to the T1 active site through hydrophobic interactions. Comparing just PGE+laccase versus the anthracene modified PGE+laccase electrode the modified electrode showed a 6x increase in current density, 650μA/cm^2, with a rotating disc electrode. Anthracene modified electrodes maintained 80% of its activity after 60 days while the unmodified electrode lost all its catalytic activity after 20 days. Suggesting the T1 active site anthracene binding is strong and favored interaction with the electrode overcoming repeated uses.

Giroud and Minteer[23] designed a way to adsorb commercially available laccase from *trametes versicolor* onto modified multi-walled carbon nanotubes (MWCNT) with its T1 active site oriented towards the electrode surface. The modified MWCNT electrode had pyrene derivatives adsorbed onto the MWCNT via pi-pi stacking. Bound to the pyrene molecules is an anthracene moiety which has a similar backbone structure as many laccase phenolic substrates. The T1 active site was predicted to be binding to the anthracene backbone through hydrophobic interactions, without a formal bond being made. They discovered that the oriented laccase enzyme using anthracene was obtaining steady-state current densities of 180μA/cm2. These were more than double that of the laccase enzymes adsorbed onto MWCNT with just pyrene molecules to help aid in electron transfer. This experiment suggests that oriented attachment of laccase is still very important even when the electrode is not uniform due to the nature of how MWCNT lay on the electrode.

Controlling the stacking of MWCNT is very complicated and most MWCNT arrays have cluttered and random 3-dimensional structure and act similarly to entrapment methods. Using small molecules to help orient the laccase enzyme in a preferred direction. Coincidentally, Bourourou et al.[24] the same month published a very similar experimental design. Here, instead of an anthracene functional group bound to the pyrene they instead used an anthraquinone moiety. This moiety induces interactions with the T1 active site but instead using an anthraquinone to take part in the hydrophobic interactions with the active site. They achieved current densities of 800μA/cm^2 with a doubly functionalized pyrene with two anthraquinone moieties. This was almost double that of the singly functionalized electrode, which in turn had double the current densities of randomly oriented laccase molecules on MWCNT. They also found that these electrodes lost 50% of their activity over a 10 day period. This is much less stable than the electrodes produced by Blanford et al. These together show that short linkers like anthracene and anthraquinones at around 1nm away from the electrode surface are interacting with the T1 active site. This with closer packing interactions caused by bifunctional linker moieties will allow for higher current densities.[25]

Most recently, Rizzo et al. engineered a laccase enzyme, using directed evolution, originally from the *aquifex aeolicus* with an amino acid loop rich in methionine residues that naturally adsorb onto gold surfaces.[26,27] The sulfur on methionine already has both of its bonds in the form of C-S bonds. Even with this the methionine amino acids will still adsorb preferentially to gold surface metallophilically. This methionine rich loop is located very close to the T1 active site of the laccase enzyme and will orient this T1 site closer to the

electrode surface. The addition of the laccase enzymes on this gold electrode showed 40% higher oxygen reduction currents when compared to the wild type and 3-times greater than that of the looped mutant attached to a glassy carbon electrode. The electrochemical activity of laccase was tested at different pH's, pH 4-7, and even at a higher pH the looped laccase still had profound activity towards oxygen reduction, although requiring more negative potentials to achieve reduction. The long-term stability of these electrodes was not discussed in this paper.

Clearly, adsorption is a valid technique to immobilize enzymes, and in particular laccases, onto different electrode support systems. Even with weaker intermolecular interaction lacking a chemical bond, researchers have been able to optimize activities by orienting the T1 active site closest to the electrode surface. However, we have seen these electrodes suffer from stability over a few days and up to a few weeks. Covalent attachment allows for greater control over interactions with atomic precision and with chemical bonds holding things in place.

Covalent Attachment

Covalently attaching enzymes onto electrodes involves forming at least one chemical bond between the electrode surface and the enzyme. There are a myriad of techniques, reagents, and moieties engineered to interact with common amino acid features that make up proteins.[15] Primary amines, thiols, and amino acid tags (His and Strep tags) have been used to attach enzymes to electrode surfaces. This can often be specific or non-specific binding depending on the solvent exposed residues on the enzyme. If an enzyme possesses multiple binding sites, then the atomic precision wanted in an enzyme's

orientation goes away. Depending on the linker this can also result in the crosslinking of enzymes to each other as well as the electrode. Crosslinked electrodes have shown great promise in making functional devices.[18] However, the random orientation of enzymes makes this technique not applicable to the scope of this research. Crosslinking can also occur after immobilization. This has been shown to be beneficial to electrode stability.

Mena et al.[28] attached commercially available laccase enzymes to gold electrode using mercaptopropionic acid (MPA) and N-succinimidyl propionate (NTSP) SAM modified using the now common biological reagents 1-(3-dimethylaminopropyl)-3-ethylcarbodiimide (EDC) and N-hydroxysulfosuccinimide (NHS) to bind primary amines to the electrode surface. Both techniques resulted in the same interfaces of a propane-thiol separating the gold electrode from the binding amino acid residue. Glutaraldehyde was used to compare just SAM bound enzymes to ones also cross-linked together. Results show that between the two SAM techniques, the MPA SAM was more insulating towards electron transfer than the technique using NTSP monolayers. This is attributed to denser packing on MPA possibly caused by its smaller size while forming the SAM. Thus, NTSP SAMs were used to compare the electrochemical activities of laccase just bound to the electrode versus those linked together by the polymerization of glutaraldehyde. The cross-linked electrode showed a 3-fold increase in stability of 9 days compared to the non-linked electrode. This was attributed to the increase of bonds formed between the enzymes so that even if the SAM degrades laccase enzymes will be stuck in place rather than drifting into solution. This experiment showed that more densely packed SAM could be a hinderance to proper electron transfer in

covalently bound enzymes. This method does not allow for site specific binding since both lysine and the N-terminus have primary amines that can bind via this technique.

Li et al[29] attached laccase to gold using a cysteine modified at the end of a His-tag allowing it to bind to a bare gold electrode. They genetically designed two variants one with Cys-His-tag at the C and N terminus, respectively. The C-terminus of this laccase would orient the enzymes T1 active site closer to the electrode while the N-terminus location is closer to the TNC active site. Oxygen reduction was obtained by both methods, however, the C-terminus Cys-His-tag presented with a lower overpotential and a higher current density. This suggests the T1 site allows for better electron transfer between the enzyme and the electrode. The two termini of most enzymes tend to allow for more degrees of freedom than amino acids held tightly within secondary structures, but with a 50mV difference in onset potentials for oxygen reduction and double the current densities, clearly there is a preferential orientation demonstrated here within.

Later, Ran et al[30] covalently immobilized the redox active horseradish peroxidase (HRP) to gold electrodes using a 1,4 dialkynylbenzene SAM to bind to an azido modified lysine residues on the enzyme. Unfortunately, this cannot be seen as site-specific since any reactions that can bind to the primary amine on lysine can also bind to the N-terminus of the protein.[31] A copper catalyzed azide-alkyne cycloaddition (CuAAC) reaction was performed to link the HRP to the gold surface and was successful in obtaining direct electron transfer between the electrode surface and the HRP. This experiment was significant because this was the first time CuAAC was used on gold electrodes for DET and catalysis with redox

enzymes. This powerful reaction has been used quite frequently in biosensors and enzyme electrochemistry over the past decade. [32,33]

In 2020 Gentil et al.[34] announced they successfully covalently attached laccase to MWCNT using a SAM capped with an azido group that was able to bind to single alkyne functionalized amino acid residue. To make the library of laccases with a single lysine residue they needed to first remove the original two lysine residues expressed in trametes versicolor naturally. After this they focused on expressing 4 mutants, the original two location K71 and K40 near the T2/T3 active site and then two near the T1 active site at location 157 and 161, respectively. After the library was expressed, the enzymes were attached to the MWCNT functionalized with 4-azidobenzene using 4-ethynylbenzaldehyde as a bridge connecting the lysine to the 4-azidobenzene functionalized MWCNT via the copper catalyzed alkyne-azide cycloaddition reaction. They found that the coordinating laccase through its K71 lysine near the TNC reduced diatomic oxygen with the highest current densities than the other mutations near the T1 active site. Even using the WT laccase from trametes versicolor, with two lysine residues, possessed higher current densities than the K161 location at the T1 active site. This is unique since much of the work in orienting laccase enzymes to the electrode surface focuses on orienting the T1 active site closest to the electrode surface for the fastest and most stable electron transfer. Clearly, direct electron transfer can occur at the TNC with great efficiency.

Finally, Elizabeth Schneider in her dissertation[35] attempted to orient a library of cytochrome p450 redox active proteins to a planar gold electrode with a SAM of

Dithiobismalaimidoethane (DTME) and propyl amines, respectively. This DTME SAM is capped with a maleimide group attached to an ethane thiol making it a short linker between the electrode and the enzyme cytochrome p450. The maleimide group binds preferentially to the thiols bound to cysteine amino acid residues. After many attempts at achieving an electrochemical response, it appears as if this combination of protein, electrode, and linker molecules ended with never achieving any meaningful currents from the cytochrome p450 enzymes. There have been reports of specific SAMs, gold surfaces, and certain enzymes of different species having problems with showing electrochemical catalysis showing how many unknowns and pitfalls in this site-specific immobilization on gold electrodes.[36] These must be considered, and flexibility is required within experimental designs to help overcome these.

Planar Electrode Materials

Planar electrodes and those approaching atomically flat will give the clearest look into enzyme orientation.[8] The materials for planar electrode production have diversified greatly over the past decades.[8] With the inventions of large crystalline semiconductors and new nanomaterials the landscape for electrode architectures is broad. Yet to date there are only a few electrode materials that could be truly considered planar or even atomically flat over longer distances(microns). Basal plane graphite electrodes considered planar in small electrodes, leave a plane of graphite on the electrode surface. Unfortunately, the carbon electrode makes other analytical techniques complicated.[8] IR-ATR, AFM, and other surface characterization techniques are more challenging or not an option with graphite-based electrodes since they do not form plasmon like metal based electrodes. Silicon has been

made so successfully that you can purchase commercially available atomically flat silicon wafer of a variety of surface orientations (e.g. (111) and (101)).[37,38] It does allow for many surface characterization techniques owing to more confidence in the SAM structure. However, semiconductor electrodes are much more nuanced than a typical metal or carbon-based electrode. Band bending, and control over the lighting in the laboratory make some data deconvoluting more complicated.[39] Aside from that, the cleaning and working with pure silicon surfaces requires hydrofluoric acid (HF). HF is quite dangerous to have and store in the lab and the silicon surfaces themselves are prone to oxidation. Truly dangerous chemicals and such sensitive surfaces like silicon should be avoided, if at all possible, unless proper lab conditions can be maintained.

The use of gold as an electrode support could prove to be ideal for protein immobilization and obtaining electrochemical measurements.[8] Gold, as a noble metal, is inert toward oxidation by many chemistries in biological conditions and the conditions required to modify gold are well established.[40–42] Gold can form stable bonds with thiols, alkynes, and phosphine groups which can be modified with proteins or as bifunctional SAM's with multiple reactive groups, allowing for further functionalization.[43] Gold is very conductive and can be modified to control topology and therefore the surface area. Much of the research conducted with gold electrodes utilize bulk gold, gold nanoparticles, or nanoporous gold electrodes.[44,45] Bulk gold features many surface defects that can contribute to an increased surface area which provides better interactions with proteins and enzymes. Pits, stair steps, terraces, valleys, and a non-uniform surface have been shown to promote molecular binding and electron transfer.[46] The use of single crystalline

gold is ideal for use as a planar electrode. Single crystal gold can be purchased or engineered to have a known crystalline structure, typically in the 111 or 100 crystal planes. These crystalline features can be consistent over microns of space. Yet with larger electrodes (millimeter or greater) there is no consistent atomically flat surface. Because of this we will explore using thin film gold electrodes with 10nm thick gold. With such a thin film of gold, we hope to limit large surface features to below 3 nm in size.

Synopsis

Given the established literature it is clear that more work needs to be done anchoring laccase enzymes onto planar gold electrodes with more atomic precision than the current literature. For site specific control over the orientation of the laccase enzyme the amino acid cysteine gives better control than amine-based techniques that bind to lysine and the N terminus. Aside from the enzyme's cysteine forming stable bonds directly with gold, which would place the laccase enzyme closest to the electrode surface, the cysteines native sulfhydryl would also bind to maleimide groups capping SAMs. Using SAM's to attach enzymes to electrodes allows for control over the distance between the electrode and the laccase active sites.

To study the orientation of laccase enzymes on planar gold electrodes a library of laccase enzymes from *Bacillus subtilis* will be engineered genetically to have a single solvent exposed cysteine residue. This library will comprise of 4 different laccase enzymes all mutated to have only one solvent exposed cysteine residue in a different location on the laccase enzymes surface. The cysteine residues will offer a variety of binding locations so

that the T1 and TNC can be isolated for DET. This way the catalysis of oxygen at the TNC and ABTS/phenols at the T1 site can be probed individually and more can be determined about the steric hinderance at the individual active sites. Laccase library design and experiments can be found in chapter 2.

Self-assembled monolayers formed using modified alkane thiols containing tail group moieties that allow for the laccase's cysteine to bind will be used. This is done using maleimide binding groups that preferentially bind strongly to sulfhydryl groups (thiols). The bifunctional molecule used will be dithiobismaleimidoethane(DTME) where a disulfide, each of which is bound to an ethyl group which is bound to the nitrogen of the maleimide group. The sulfhydryl side group on the cysteine can bind to either of the sp^2 carbons on the maleimide structure. In order to control the distance between the electrode and the laccase enzyme further a second SAM immobilization technique is engineered. The second bifunctional SAM consists of azido propyl thioacetate. The thioacetate of the molecule is deprotected in-situ during SAM formation and leaves a thiol functionalized gold surface with a propyl group attached to an azido moiety, which can further be functionalized by an alkynyl group. Using the CuAAC reaction, propargyl maleimide can be attached to this azido capped SAM and leave a terminally bound maleimide exposed into the solvent. The Azido-alkyl-thioacetate class of molecules comes with various alkyl lengths from propane to octane. Controlling the hydrocarbon linker length will position the laccase enzyme further away from the electrode surface. The aim is to increase the tunnelling distance for electrons, which would generally lower the currents achieved in most electrochemical processes. However, with large carbon-based catalysts like enzymes reacting with large molecular substrate,

there could be a preference for having more degrees of freedom to accommodate catalysis with minimal steric hinderance. These electrodes will be studied by cyclic voltammetry in order to find the onset potentials and currents achieved by these systems with different substrates. Mainly oxygen and ABTS will be studied as laccase preferred substrates for catalysis. The overall scheme for electrode functionalization and enzyme immobilization are shown below in figure 4. More on the electrode design and the subsequent electrochemical experiments will be covered in chapter 3.

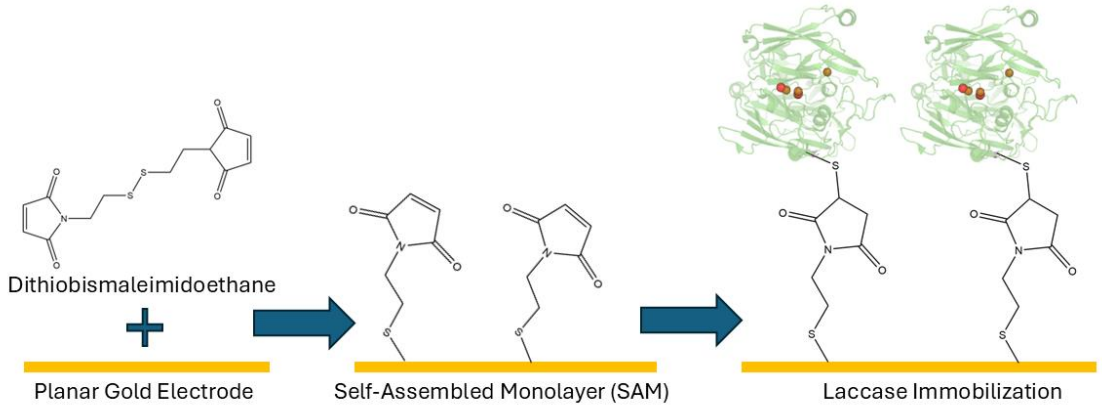

Figure 4 The immobilization scheme for the attachment of laccase onto gold electrodes using dithiobismaleimidoethane (DTME) as a self-assembled monolayer.

Conclusion

Protein and enzyme voltammetry is nearly a century old.[47] Even with the large body of knowledge, we still have much to learn about the interactions between enzymes and the electrodes. Since there are enzymes that carry out every biosynthesis within cells the applications for sensing, catalysis, and synthesis seem endless. Recent advances in chemical biology and proteomics allow for the engineering of proteins with relative ease. This engineering gives rise to the capabilities of adding or removing parts of a protein that

can help bind to electrode surfaces in different ways. Modifying electrodes to bind to proteins through various means allows for meticulous control over and careful measuring of the catalytic rates of reactions. Out of all the commonly studied enzymes in the literature (nitrogenase, hydrogenase, and laccases), laccases are readily expressed, operable under normal atmospheric conditions and display oxidation toward a number of substrates with various sizes. Like hydrogenases and nitrogenases, laccase, and other multicopper oxidases, possess multiple different metal sites within their structure that facilitate catalysis and electron transfer. This makes laccases analogs for studying electron transfer with metalloenzymes, even if they do not react with the same substrates. More electrode architectures need to be engineered to study electron transfer processes with greater atomic precision and more laccase enzymes should be modified and studied on electrode surfaces to understand the nuances surrounding enzyme orientation and how it affects the enzymes catalysis. For this reason, we pursued a series of experiments immobilizing laccase enzymes onto planar gold electrodes to allow for a greater clarity surrounding the enzymes orientation with respect to the electrode surface. Using electrochemical experimentations, our aim is to find orientations that promote enzyme stability and overall catalysis.

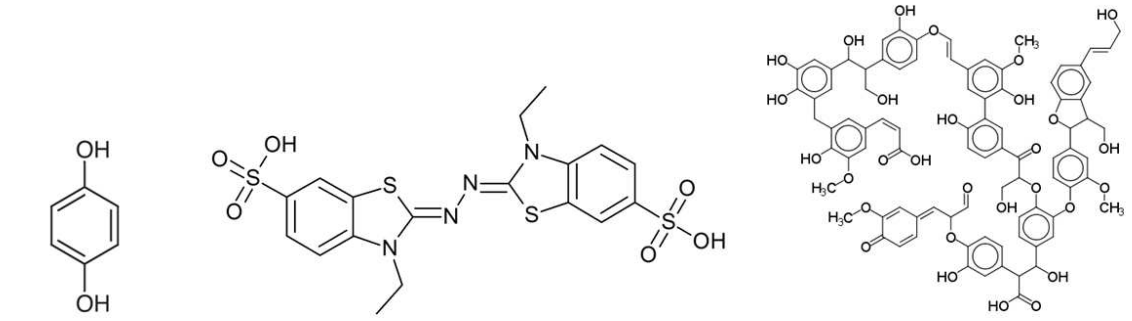

Hydroquinone 2,2'-azino-bis(3-ethylbenzothiazoline-6-sulfonic acid) Lignin

Figure 5 Some known laccase substrates and their general structure. Lignin has no unique structure.

References

(1) Gray, H. B.; Winkler, J. R. Electron Transfer in Proteins. *Annual Review of Biochemistry* **1996**, *65* (1), 537–561. https://doi.org/10.1146/annurev.bi.65.070196.002541.

(2) Bollella, P.; Katz, E. Enzyme-Based Biosensors: Tackling Electron Transfer Issues. *Sensors* **2020**, *20* (12), 3517. https://doi.org/10.3390/s20123517.

(3) Rasmussen, M.; Abdellaoui, S.; Minteer, S. D. Enzymatic Biofuel Cells: 30 Years of Critical Advancements. *Biosensors and Bioelectronics* **2016**, *76*, 91–102. https://doi.org/10.1016/j.bios.2015.06.029.

(4) D. Milton, R.; Abdellaoui, S.; Khadka, N.; R. Dean, D.; Leech, D.; C. Seefeldt, L.; D. Minteer, S. Nitrogenase Bioelectrocatalysis: Heterogeneous Ammonia and Hydrogen Production by MoFe Protein. *Energy & Environmental Science* **2016**, *9* (8), 2550–2554. https://doi.org/10.1039/C6EE01432A.

(5) Peters, J. W.; Schut, G. J.; Boyd, E. S.; Mulder, D. W.; Shepard, E. M.; Broderick, J. B.; King, P. W.; Adams, M. W. W. [FeFe]- and [NiFe]-Hydrogenase Diversity, Mechanism, and Maturation. *Biochimica et Biophysica Acta (BBA) - Molecular Cell Research* **2015**, *1853* (6), 1350–1369. https://doi.org/10.1016/j.bbamcr.2014.11.021.

(6) Updike, S. J.; Hicks, G. P. The Enzyme Electrode. *Nature* **1967**, *214* (5092), 986–988. https://doi.org/10.1038/214986a0.

(7) Bhatia, D.; Paul, S.; Acharjee, T.; Ramachairy, S. S. Biosensors and Their Widespread Impact on Human Health. *Sensors International* **2024**, *5*, 100257. https://doi.org/10.1016/j.sintl.2023.100257.

(8) Hitaishi, V. P.; Clement, R.; Bourassin, N.; Baaden, M.; de Poulpiquet, A.; Sacquin-Mora, S.; Ciaccafava, A.; Lojou, E. Controlling Redox Enzyme Orientation at Planar Electrodes. *Catalysts* **2018**, *8* (5), 192. https://doi.org/10.3390/catal8050192.

(9) Blout, A.; Billon, F.; Calers, C.; Méthivier, C.; Pailleret, A.; Perrot, H.; Jolivalt, C. Orientation of a Trametes Versicolor Laccase on Amorphous Carbon Nitride Coated Graphite Electrodes for Improved Electroreduction of Dioxygen to Water. *Electrochimica Acta* **2018**, *277*, 255–267. https://doi.org/10.1016/j.electacta.2018.04.145.

(10) Gore, S.; García, E. S.; Hendrickx, P. M.; Gutmanas, A.; Westbrook, J. D.; Yang, H.; Feng, Z.; Baskaran, K.; Berrisford, J. M.; Hudson, B. P.; Ikegawa, Y.; Kobayashi, N.; Lawson, C. L.; Mading, S.; Mak, L.; Mukhopadhyay, A.; Oldfield, T. J.; Patwardhan, A.; Peisach, E.; Sahni, G.; Sekharan, M. R.; Sen, S.; Shao, C.; Smart, O. S.; Ulrich, E. L.; Yamashita, R.; Quesada, M.; Young, J. Y.; Nakamura, H.; Markley, J. L.; Berman, H. M.; Burley, S. K.; Velankar, S.; Kleywegt, G. J. Validation of Structures in the Protein Data Bank. *Structure(London, England:1993)* **2017**, *25* (12), 1916. https://doi.org/10.1016/j.str.2017.10.009.

(11) Artz, J. H.; Mulder, D. W.; Ratzloff, M. W.; Lubner, C. E.; Zadvornyy, O. A.; LeVan, A. X.; Williams, S. G.; Adams, M. W. W.; Jones, A. K.; King, P. W.; Peters, J. W. Reduction Potentials of [FeFe]-Hydrogenase Accessory Iron–Sulfur Clusters Provide Insights into the Energetics of Proton Reduction Catalysis. *Journal of the American Chemical Society* **2017**, *139* (28), 9544–9550. https://doi.org/10.1021/jacs.7b02099.

(12) Madden, C.; Vaughn, M. D.; Díez-Pérez, I.; Brown, K. A.; King, P. W.; Gust, D.; Moore, A. L.; Moore, T. A. Catalytic Turnover of [FeFe]-Hydrogenase Based on Single-Molecule Imaging. *Journal of the American Chemical Society* **2012**, *134* (3), 1577–1582. https://doi.org/10.1021/ja207461t.
(13) Morozova, O. V.; Shumakovich, G. P.; Gorbacheva, M. A.; Shleev, S. V.; Yaropolov, A. I. "Blue" Laccases. *Biochemistry Moscow* **2007**, *72* (10), 1136–1150. https://doi.org/10.1134/S0006297907100112.
(14) Giardina, P.; Faraco, V.; Pezzella, C.; Piscitelli, A.; Vanhulle, S.; Sannia, G. Laccases: A Never-Ending Story. *Cell. Mol. Life Sci.* **2010**, *67* (3), 369–385. https://doi.org/10.1007/s00018-009-0169-1.
(15) Dwevedi, A. Basics of Enzyme Immobilization. In *Enzyme Immobilization: Advances in Industry, Agriculture, Medicine, and the Environment*; Dwevedi, A., Ed.; Springer International Publishing: Cham, 2016; pp 21–44. https://doi.org/10.1007/978-3-319-41418-8_2.
(16) Kaur, G.; Adhikari, R.; Cass, P.; Bown, M.; Gunatillake, P. Electrically Conductive Polymers and Composites for Biomedical Applications. *RSC Advances* **2015**, *5* (47), 37553–37567. https://doi.org/10.1039/C5RA01851J.
(17) Holzinger, M.; Le Goff, A.; Cosnier, S. Nanomaterials for Biosensing Applications: A Review. *Frontiers in Chemistry* **2014**, *2*.
(18) Fischback, M.; Kwon, K. Y.; Lee, I.; Shin, S. J.; Park, H. G.; Kim, B. C.; Kwon, Y.; Jung, H.-T.; Kim, J.; Ha, S. Enzyme Precipitate Coatings of Glucose Oxidase onto Carbon Paper for Biofuel Cell Applications. *Biotechnol Bioeng* **2012**, *109* (2), 318–324. https://doi.org/10.1002/bit.23317.
(19) Talbert, J. N.; Goddard, J. M. Enzymes on Material Surfaces. *Colloids and Surfaces B: Biointerfaces* **2012**, *93*, 8–19. https://doi.org/10.1016/j.colsurfb.2012.01.003.
(20) Kuhn, A. T.; Chan, C. Y. pH Changes at Near-Electrode Surfaces. *J Appl Electrochem* **1983**, *13* (2), 189–207. https://doi.org/10.1007/BF00612481.
(21) Tominaga, M.; Ohtani, M.; Taniguchi, I. Gold Single-Crystal Electrode Surface Modified with Self-Assembled Monolayers for Electron Tunneling with Bilirubin Oxidase. *Phys. Chem. Chem. Phys.* **2008**, *10* (46), 6928–6934. https://doi.org/10.1039/B809737B.
(22) Blanford, C. F.; Heath, R. S.; Armstrong, F. A. A Stable Electrode for High-Potential, Electrocatalytic O2 Reduction Based on Rational Attachment of a Blue Copper Oxidase to a Graphite Surface. *Chem. Commun.* **2007**, No. 17, 1710. https://doi.org/10.1039/b703114a.
(23) Giroud, F.; Minteer, S. D. Anthracene-Modified Pyrenes Immobilized on Carbon Nanotubes for Direct Electroreduction of O2 by Laccase. *Electrochemistry Communications* **2013**, *34*, 157–160. https://doi.org/10.1016/j.elecom.2013.06.006.
(24) Bourourou, M.; Elouarzaki, K.; Lalaoui, N.; Agnès, C.; Le Goff, A.; Holzinger, M.; Maaref, A.; Cosnier, S. Supramolecular Immobilization of Laccase on Carbon Nanotube Electrodes Functionalized with (Methylpyrenylaminomethyl)Anthraquinone for Direct Electron Reduction of Oxygen. *Chemistry – A European Journal* **2013**, *19* (28), 9371–9375. https://doi.org/10.1002/chem.201301043.

(25) Giroud, F.; Milton, R. D.; Tan, B.-X.; Minteer, S. D. Simplifying Enzymatic Biofuel Cells: Immobilized Naphthoquinone as a Biocathodic Orientational Moiety and Bioanodic Electron Mediator. *ACS Catal.* **2015**, *5* (2), 1240–1244. https://doi.org/10.1021/cs501940g.
(26) Rizzo, F.; Brissos, V.; Villain, S.; Martins, L. O.; Conzuelo, F. Simple and Directed Immobilization of a Multicopper Oxidase on Flat Bare Gold Electrodes Provides High Catalytic Currents for O2 Reduction. *ACS Catal.* **2024**, *14* (7), 4760–4767. https://doi.org/10.1021/acscatal.4c00516.
(27) Cooper, E.; Krebs, F.; Smith, McD.; Raval, R. The Interaction of Amino Acids with Metals: Methionine on Gold. *Journal of Electron Spectroscopy and Related Phenomena* **1993**, *64–65*, 469–475. https://doi.org/10.1016/0368-2048(93)80111-X.
(28) Mena, M. L.; Carralero, V.; González-Cortés, A.; Yáñez-Sedeño, P.; Pingarrón, J. M. Laccase Biosensor Based on N-Succinimidyl-3-Thiopropionate-Functionalized Gold Electrodes. *Electroanalysis* **2005**, *17* (23), 2147–2155. https://doi.org/10.1002/elan.200503345.
(29) Li, Y.; Zhang, J.; Huang, X.; Wang, T. Construction and Direct Electrochemistry of Orientation Controlled Laccase Electrode. *Biochemical and Biophysical Research Communications* **2014**, *446* (1), 201–205. https://doi.org/10.1016/j.bbrc.2014.02.084.
(30) Ran, Q.; Peng, R.; Liang, C.; Ye, S.; Xian, Y.; Zhang, W.; Jin, L. Covalent Immobilization of Horseradish Peroxidase via Click Chemistry and Its Direct Electrochemistry. *Talanta* **2011**, *83* (5), 1381–1385. https://doi.org/10.1016/j.talanta.2010.11.024.
(31) van Dongen, S. F. M.; Teeuwen, R. L. M.; Nallani, M.; van Berkel, S. S.; Cornelissen, J. J. L. M.; Nolte, R. J. M.; van Hest, J. C. M. Single-Step Azide Introduction in Proteins via an Aqueous Diazo Transfer. *Bioconjugate Chemistry* **2009**, *20* (1), 20–23. https://doi.org/10.1021/bc8004304.
(32) Jangid, V.; Brunel, D.; Sanchez-Adaime, E.; Bharwal, A. K.; Dumur, F.; Duché, D.; Abel, M.; Koudia, M.; Buffeteau, T.; Nijhuis, C. A.; Berginc, G.; Lebouin, C.; Escoubas, L. Improving Orientation, Packing Density, and Molecular Arrangement in Self-Assembled Monolayers of Bianchoring Ferrocene–Triazole Derivatives by "Click" Chemistry. *Langmuir* **2022**, *38* (11), 3585–3596. https://doi.org/10.1021/acs.langmuir.2c00215.
(33) Brunel, D.; Jangid, V.; Sanchez Adaime, E.; Duché, D.; Bharwal, A. K.; Abel, M.; Koudia, M.; Buffeteau, T.; Lebouin, C.; Simon, J. J.; Sauvage, R. M.; Berginc, G.; Escoubas, L.; Gigmes, D.; Dumur, F. Click Chemistry: An Efficient Tool to Control the Functionalization of Metallic Surfaces with Alkyl Chains Possessing Two Reactive End Groups. *Applied Surface Science* **2021**, *566*, 150731. https://doi.org/10.1016/j.apsusc.2021.150731.
(34) Gentil, S.; Rousselot-Pailley, P.; Sancho, F.; Robert, V.; Mekmouche, Y.; Guallar, V.; Tron, T.; Le Goff, A. Efficiency of Site-Specific Clicked Laccase–Carbon Nanotubes Biocathodes towards O_2 Reduction. *Chem. Eur. J.* **2020**, *26* (21), 4798–4804. https://doi.org/10.1002/chem.201905234.

(35) Schneider, E. Oriented Attachment of Cytochrome P450 2C9 to a Self-Assembled Monolayer on a Gold Electrode as a Biosensor Design, UC Berkeley, 2011. https://escholarship.org/uc/item/1m67k8mm (accessed 2019-09-18).
(36) Pita, M.; Shleev, S.; Ruzgas, T.; Fernández, V. M.; Yaropolov, A. I.; Gorton, L. Direct Heterogeneous Electron Transfer Reactions of Fungal Laccases at Bare and Thiol-Modified Gold Electrodes. *Electrochemistry Communications* **2006**, *8* (5), 747–753. https://doi.org/10.1016/j.elecom.2006.03.008.
(37) Ng, A.; Ciampi, S.; James, M.; Harper, J. B.; Gooding, J. J. Comparing the Reactivity of Alkynes and Alkenes on Silicon (100) Surfaces †. *Langmuir* **2009**, *25* (24), 13934–13941. https://doi.org/10.1021/la901526e.
(38) Finocchio, E.; Macis, E.; Raiteri, R.; Busca, G. Adsorption of Trimethoxysilane and of 3-Mercaptopropyltrimethoxysilane on Silica and on Silicon Wafers from Vapor Phase: An IR Study. *Langmuir* **2007**, *23* (5), 2505–2509. https://doi.org/10.1021/la062972b.
(39) Tapia, C.; Shleev, S.; Conesa, J. C.; De Lacey, A. L.; Pita, M. Laccase-Catalyzed Bioelectrochemical Oxidation of Water Assisted with Visible Light. *ACS Catal.* **2017**, *7* (7), 4881–4889. https://doi.org/10.1021/acscatal.7b01556.
(40) Béthencourt, M. I.; Srisombat, L.; Chinwangso, P.; Lee, T. R. SAMs on Gold Derived from the Direct Adsorption of Alkanethioacetates Are Inferior to Those Derived from the Direct Adsorption of Alkanethiols. *Langmuir* **2009**, *25* (3), 1265–1271. https://doi.org/10.1021/la803179q.
(41) Pensa, E.; Cortés, E.; Corthey, G.; Carro, P.; Vericat, C.; Fonticelli, M. H.; Benítez, G.; Rubert, A. A.; Salvarezza, R. C. The Chemistry of the Sulfur–Gold Interface: In Search of a Unified Model. *Acc. Chem. Res.* **2012**, *45* (8), 1183–1192. https://doi.org/10.1021/ar200260p.
(42) Srisombat, L.; Jamison, A. C.; Lee, T. R. Stability: A Key Issue for Self-Assembled Monolayers on Gold as Thin-Film Coatings and Nanoparticle Protectants. *Colloids and Surfaces A: Physicochemical and Engineering Aspects* **2011**, *390* (1), 1–19. https://doi.org/10.1016/j.colsurfa.2011.09.020.
(43) Abroshan, H.; Li, G.; Lin, J.; Kim, H. J.; Jin, R. Molecular Mechanism for the Activation of Au25(SCH2CH2Ph)18 Nanoclusters by Imidazolium-Based Ionic Liquids for Catalysis. *Journal of Catalysis* **2016**, *337*, 72–79. https://doi.org/10.1016/j.jcat.2016.01.011.
(. *Biosensors and Bioelectronics* **2013**, *42*, 242–247. https://doi.org/10.1016/j.bios.2012.10.087.
(45) Qiu, H.; Xu, C.; Huang, X.; Ding, Y.; Qu, Y.; Gao, P. Immobilization of Laccase on Nanoporous Gold: Comparative Studies on the Immobilization Strategies and the Particle Size Effects. *J. Phys. Chem. C* **2009**, *113* (6), 2521–2525. https://doi.org/10.1021/jp8090304.
(46) Che, G.; Li, Z.; Zhang, H.; Cabrera, C. R. Voltammetry of Defect Sites at a Self-Assembled Monolayer on a Gold Surface. *Journal of Electroanalytical Chemistry* **1998**, *453* (1), 9–17. https://doi.org/10.1016/S0022-0728(97)00246-5.

Chapter Two- Laccase Library and Activity

Laccase Structure and mechanism

Laccases belong to the multi-copper oxidases family of the oxidoreductase family of enzymes. They have been discovered to be expressed naturally in nearly every form of life but were first identified in the sap of Japanese Lacquer trees in the late 19th century.[1] They contain a single coordinated copper ion (T1) active site oxidizing a variety of aromatic substrates and a tri-nuclear copper(TNC) cluster active site reducing molecular oxygen to water through 4 electron exchange events. With hundreds of oxidases identified, still only a small minority can catalyze the Oxygen Reduction Reaction (ORR) effectively.[2] This reaction is coveted for use as the cathode in biofuel cells or in self-powered biosensors.[3] The laccase T1 active sites substrate promiscuity has led towards its investigation for uses in water remediation, pulp degradation, and use within organic synthesis.[4–6]

The non-specific T1 active site is based around a single copper ion coordinated to four amino acids, 2 histidine, a methionine, and a cysteine residue.[7] For some species this methionine residue is substituted for another residue, typically phenylalanine or histidine.[8,9] Due to the copper's coordination with cysteine and resting charge (2+) this active site has a strong blue color and maintains a maximum absorption (ABS_{max}) at ~600nm. This site directly oxidizes polyphenols including both para and ortho polyphenols, aminophenols, poly and aryl amines in a single electron exchange event among others.[10] This single electron oxidation reaction generally forms radical species that must continue to react and rearrange

to accommodate this unstable change. This electron is passed through the T1 coordinated cysteine to a histidine bound to the enzyme's second catalytic site where oxygen is reduced. This cysteine-histidine bridge is found in most multi-copper oxidase and separates the two active sites by approximately 13Å on average between species.[11]

The TNC catalytic active site reduces atmospheric oxygen to water via three copper atoms arranged in a triangular cluster stabilized by eight coordinated histidine residues, one of which is part of the cysteine-histidine bridge mentioned above.[7] This tri-nuclear copper cluster can be further differentiated as a single T2-type copper atom and two T3-type copper atoms. The two T3 copper atoms are coordinated by 3 histidine residues each and a hydroxide ion shared between them. The T2 copper atom is coordinated by only two histidine residues and a single water molecule that it does not have to share. The active sites and some of the binding amino acids can be seen in figure 6.

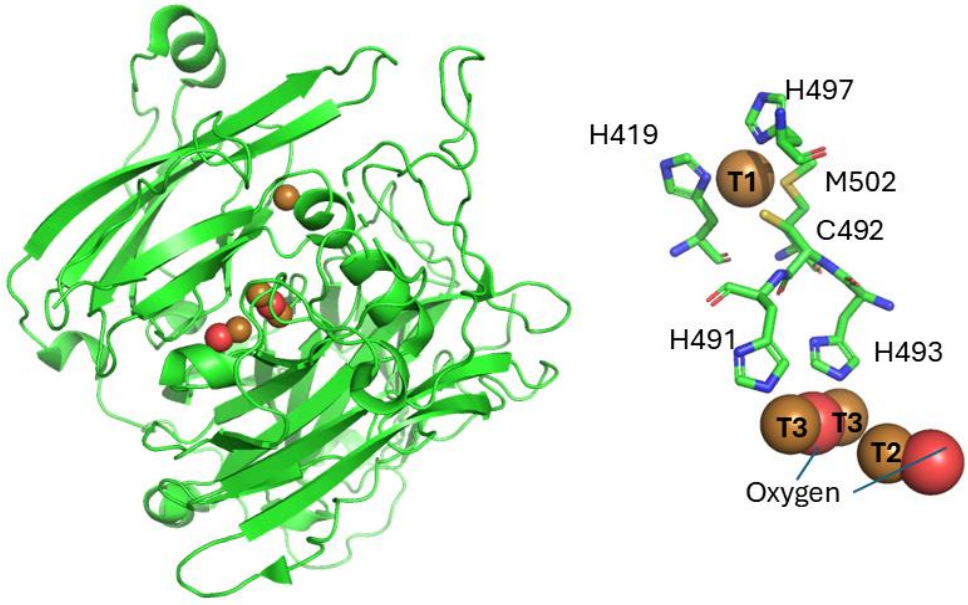

Figure 6 Laccase enzyme from Bacillus Subtillis and its active site(left) with some of the binding amino acids, including the Cys-Hys bridge connecting the active sites.

The overall (ORR) chemical reaction, using a phenol as the sample substrate, can be written as

$$\mathbf{4ArOH + O_2 \rightarrow 4ArO^{\bullet} + 2\,H2O}$$

There is some nuance to this balanced chemical equation. The protons added to the oxygen are not from the T1 substrate. The distance between the two active sites does not permit this at the same rate as electron transfer.

The reduction potential of the T1 copper active site is not uniform between species. Subsequently, high and low potential laccases have been identified and engineered. The potentials range from 800mV to 300mV vs NHE.[12–14] The T1 active site can only be reduced by substrates with lower reduction potential than the active site, sometimes this limits the laccase signature substrate promiscuity for low redox species. Since the redox potential of oxygen in pH 5 is 0.95V vs NHE, the high redox potential laccases are operating at very close to the formal reduction potential of O_2.

The mechanism for substrate oxidation at the T1 active site is described mathematically by a semi-classical Marcus theory for electron transfer (ET), often used for metalloenzymes. The electron transfer rate k_{ET} (s^{-1}) is described by [15]

$$k_{ET} = k_A S \cdot \sqrt{\frac{4\pi^3}{h^2 \lambda k_B T}} |H_{DA}|^2 \, exp\left(\frac{-(\Delta G^o + \lambda)^2}{4\lambda k_B T}\right) \qquad \text{Eq. 1}$$

In this case k_A is the equilibrium constant for the electron donor-acceptor complex, S is the steric term to account for asymmetry in the complex formation allowing for electron transfer. λ, appearing twice, is the reorganization energy of the protein, this involves the energy required for ligand and solvent rearrangements between initial and final states during electron transfer. H_{DA} is the electronic coupling between the donor and acceptor, and ΔG^o is the Gibbs free energy difference for electron transfer.

Structural data show only minimal differences between the oxidized and reduced structures of T1 sites in most copper oxidases.[16] The only changes observed involve a slight shortening of the ligand-Cu bonds. The coppers coordination allows the T1 active site to be studied via electron paramagnetic resonance (EPR). Substrates initially bind to the solvent exposed histidine residue near the T1 active site, before interacting with the T1 site and being oxidized. This reduces the T1 copper from 2+ to a 1+ oxidation state and the electron is passed to the TNC reducing each copper to the 1+ charge. To fully be reduced to +1, 4 substrates must be oxidized before any oxygen binding takes place at the TNC.

The full catalytic cycle can be seen in figure 7. During ORR catalysis, starting in a fully reduced state (all red), all four copper metals comprising both active sites are resting under a (1+) oxidation state. Upon binding with molecular oxygen at the tri nuclear copper site, a two-electron transfer event forms a peroxide intermediate. The first two electrons are transferred from the T2 and one of the T3 copper ions. Next, a second two electron transfer event reduces the peroxide into two hydroxide ions with an electron from the remaining T3 copper and the electron held by the T1 copper active site. Protons are shuttled at least

partially by neighboring aspartic acid residues near the TNC. Hydroxide ions sit in the native intermediate state until the next four electron transfer events take place, and the fully reduced state is reformed. If there is no further reduction of a substrate at the T1 site, the enzyme will transition into its resting oxidized state until substrate oxidation occurs. Entering the fully reduced state from the resting state has been shown to take longer than from the native intermediate state. The rates of electron transfer can change between species and are very susceptible to nearby amino acids.

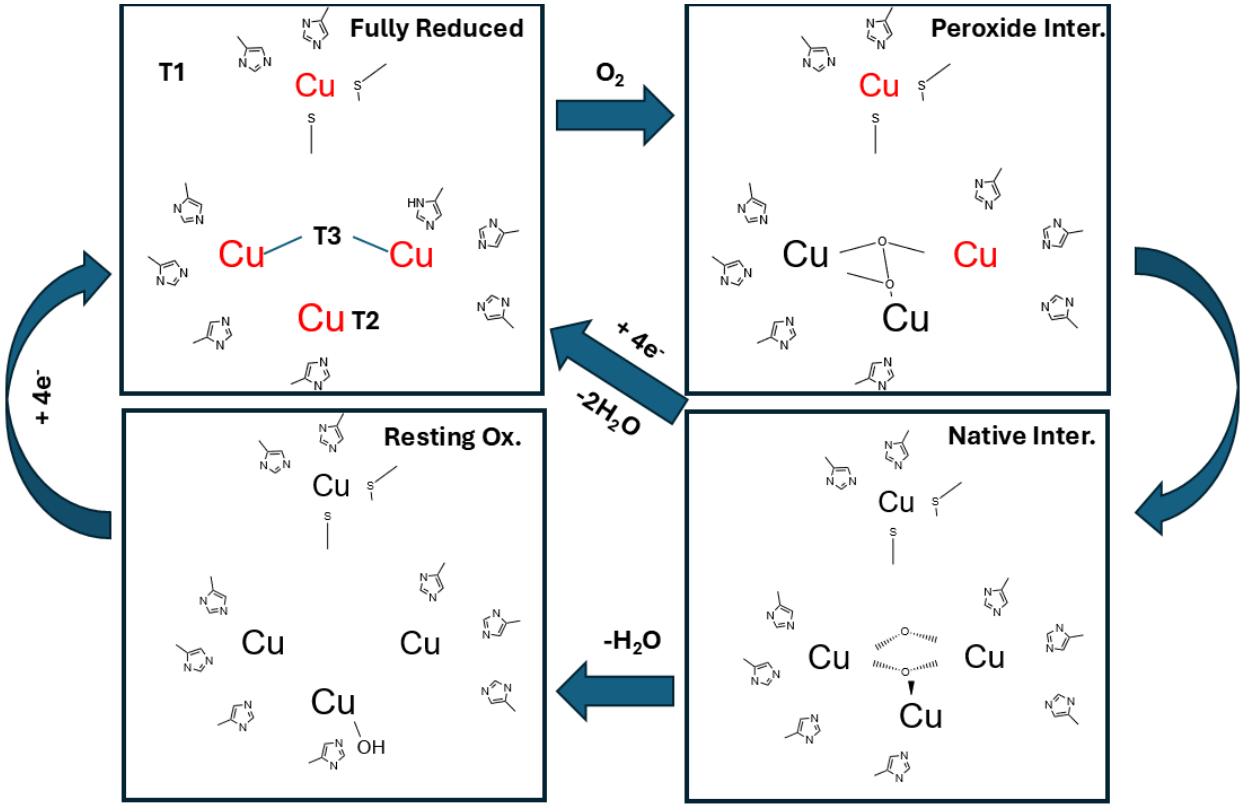

Figure 7 Laccase catalytic reduction of oxygen cycle. reduced Cu(1+) in red and Cu(2+) are in black

The specific laccase chosen to base the library off is from the organism *Bacillus Subtillis*. This mutant is a low redox laccase, having been shown to have a redox potential of

450mV vs NHE at the T1 copper site.[7] This species of laccase possesses very few native cysteine residues compared to laccase from other species. It only has one unbonded, and solvent exposed cysteine at the C35 position in its wild type (WT) form; this will be mutated away to design the rest of the library. Three other cysteines are expressed within the native enzyme, however, two are occupied with a disulfide bridge and the other is held deep within the active site, comprising part of the Cys-His bridge. Therefore, less mutations are needed to be done to design the single cysteine library compared to other laccase species. Laccase from *bacillus subtilis* overexpression in e. coli has already been established and was used as a guide for expression.[17]

Protein Library Design

The design of the cysteine modified laccase library started with the crystal structure and sequence of the wild type (WT) CotA laccase enzyme from *Bacillus Subtillis* for which is identified in PDB 1gsk. The WT laccase naturally carries 4 cysteine residues; three of which must be conserved and are required for proper folding. The native cysteine at the C35 position is not necessary for laccase activity and will later be removed to design the rest of the library. This position is ~31Å from the T1 cluster and 25Å from the TNC active site using the β-carbon on the C35 residue. The WT enzyme will be used within experiments as a part of the immobilized library. WT's cysteine location nearest to the TNC makes it more likely to interact with this moiety. However, it is quite far from either and the bridging hydrophobic amino acids could be quite insulating towards electron transfer. To design the rest of the library from a single cysteine lacking enzymes this residue was replaced with a serine amino

acid to form the mutant C35S. The sequence, plasmid, and design of C35S was used to design the three other laccase mutants.

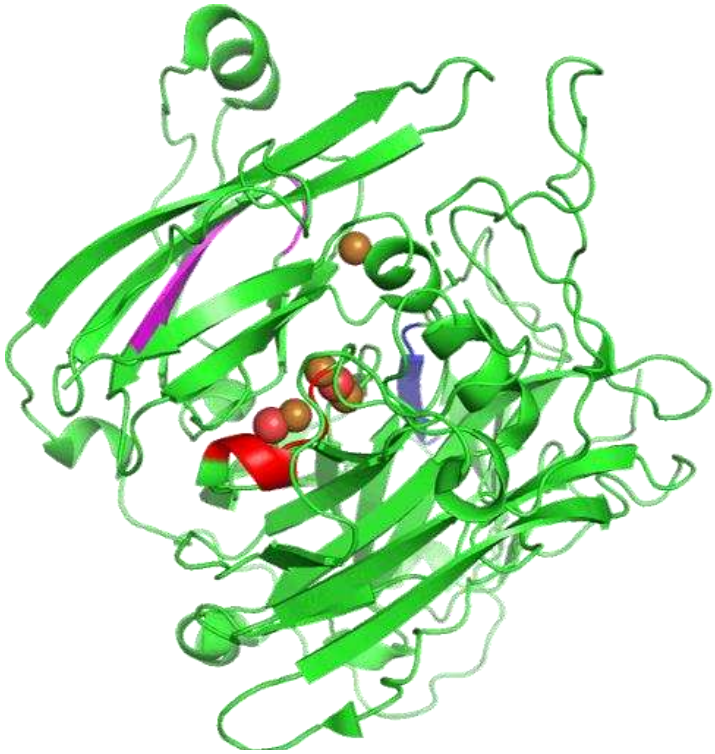

Figure 8 Laccase regions of interest for mutations. The red alpha helix is where D113C is located, the purple Beta sheet is where the H470C is chosen and the blue loop in the back where N264C is located.

To design these mutants, attention was given to avoid cysteine interactions with the active sites or forming a disulfide bond with the T1 bound cysteine. Avoiding the disulfide region was also done to not confuse the disulfide bonds being formed. Multiple secondary structures from the laccase crystallographic data were identified as regions of interest (ROI) and can be seen in figure 8. These ROI's differed in locations near the T1 or tri nuclear copper active sites and by their secondary structures. They were mainly chosen due to their locations near either active sites or substrate pathways. The regions were tabulated and compared on these metrics. Potential mutations were also assisted by previous literature surrounding mutating laccases near the active site. A solvent exposure calculation was

performed on the beta carbon on every amino acid in these chosen regions to keep things uniform, even if the chosen amino acid has longer side-branches. The solvent exposure comparisons can be seen at the end of the chapter in fig 13 and full laccase library in fig 12.

Assessing the mutations individually, mutant D133C is located most closely to the TNC active site out of all the mutated locations. Being roughly 15Å from the TNC active site and 25Å away from the T1 active site it is predicted to be a potential site for DET with the TNC. The alpha helix that the D113 residue is within participates in the protonation of oxygen and the removal of water from the active site after reduction. Its neighboring aspartic acid residue D116 has been shown to take part directly in the proton shuttling for the formation of water at the T2 copper. D113 is the last aspartic acid residue in the loop and is separated by a serine as well from the D116 residue. The hypothesis is that this particular residue (D113) does not participate in proton shuttling in an essential way so that the enzyme becomes deactivated. Coupling to this region could be helpful for DET with the other charged aspartic acid residues within the loop participating in proton transfer with how closely this loop participates in the catalytic process with the TNC. DET in this location could be helpful in the ORR, being able to bypass the T1 site entirely. Conversely, wiring in this location could be beneficial in oxidizing a variety of reagents at the T1 site in an anaerobic, or semi-anaerobic environment lacking oxygen.

The H470C mutant is located at the end of a series of parallel B sheets. Its neighboring anti-parallel β sheet contains several histidine residues that take part in the bonding of the T1 active site. This H470 locations is the closest engineered site in proximity

to the T1 active site and its location would orient this active site very close to the electrode surface. Much of the literature involving laccase orientation focus on orienting the T1 site to the electrode surface and have found success doing so. Being around 10Å from the T1 site there is a risk this mutant could become inactivated by the cysteine either interacting with the active site or the cysteine- as part of the cys-his bridge between the active sites. There is also a methionine residue nearby that takes part in bonding with the T1 site and its substrates that could be perturbed by interacting sulfurs. It is also fear that this active site could be possess significant steric hinderance being placed so close to an electrode surface or SAM. This binding orientation could be ideal for shuttling electron for the ORR at the TNC using the T1 site as a bridge for electron transfer. Orienting by this site would also leave the alpha helix possessing the aspartic acid D116 which helps provide protons for oxygen reduction most into the bulk solvent, allowing for expulsion of water into the bulk instead near the electrode surface.

The final mutant, N264C, is not located near either active site, almost equally. Its location is at the end of a globular regime of the laccase structure. It is 18Å away from the T1 active site and 21Å from the TNC. This location was chosen to be ambiguous with its preferred site for electron transfer. There should also be no expected steric hinderance from this site since the T1 cluster will be directed away from the electrode surface. The packing density of the mutants should also be slightly different and directing the most globular region of the protein to the electrode surface could aid in packing density. Figure 9 shows the three D113C, N264C, and H470C with their cysteine residues oriented towards the flat plane in order to show their expected orientations.

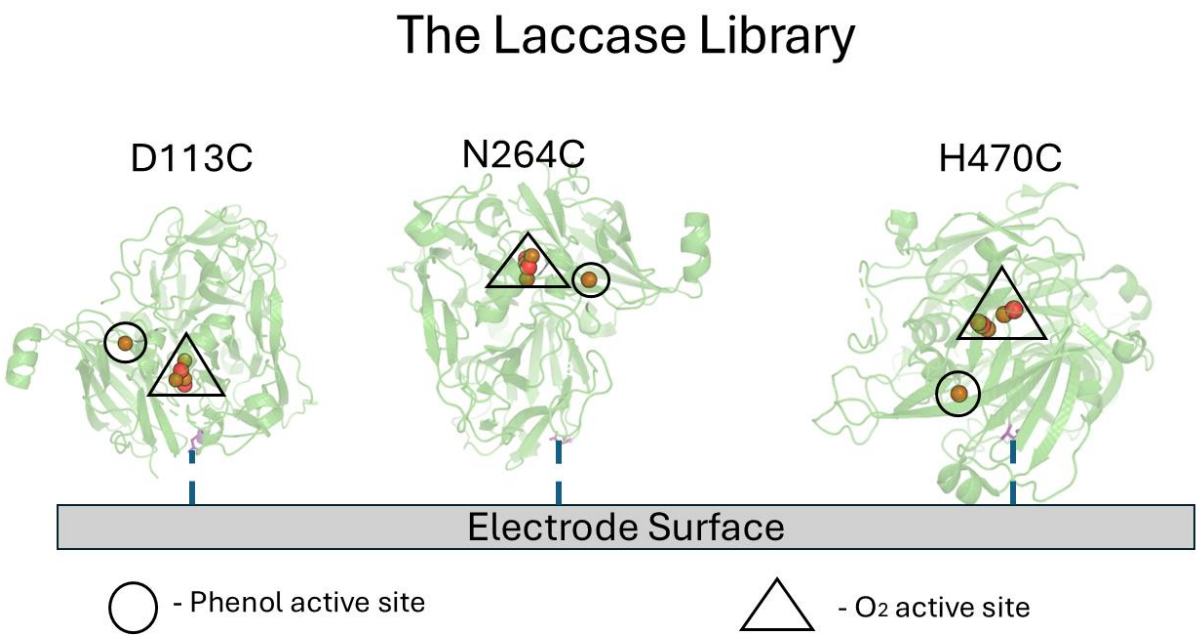

Figure 9 The laccase mutants with their mutated locations oriented toward the electrode surface with active sites T1 (circle) and the TNC (Triangle)

Plasmid Design

The sequence for the laccase WT protein was obtained from the PDB 1gsk. Amino acids codons were optimized for e. coli expression and the terminal His and Strep tags were added to the C and N terminus, respectively. Next the WT cysteine was mutated out in order to produce the mutant. From this DNA sequence the D113C, H470C, and N264C sequences were designed. Gene blocks were edited into Pet20B(+) plasmids using the Bamh1 restriction sites. The Pet20B(+) plasmid has been shown to be good plasmid structures for protein overexpression. The Pet20B(+) plasmid also comes with a T7 promoter region for using T7 RNA Polymerase optimized e. coli cell lines and encodes for ampicillin antibiotic resistance. The sequence for each mutant can be found at the end of the chapter.

Materials and Methods

Materials

5mL His columns and 1mL Strep Column were purchased from cytiva. Luria Broth, Agar, copper sulfate, and sonicating probes were purchased from Fisher Scientific. Tryptone was obtained from IBI scientific and Yeast extract from Acros organics BCA quantifying reagents from bio-vision, and IPTG was obtained by goldbio. PBS was made using premade packets, Glycerol, Bovine serum Albumin, .22micron filters are from VWR. Millipore water (MP H2O) made by in-house Nanopure water purifying system. ABTS and propargyl maleimide were purchased by Chem-Impex. Imidazole, ampicillin, bugbuster, methanol, and acetic acid were purchased from sigma Aldrich. T7 and DH5A cells were purchased from NEB. Plasmids were made by Addgene. NaOH was purchased from oakwood chemical, cysteine HCl was purchased from thermo-scientific, Measure-IT from invitrogen, Ellmans reagent from Biosciences, Page gels were purchased from BioRad, and ethanol from pharmco.

Instruments

Uv-Vis spectrophotometer used for measuring the absorption at ~610nm from the T1 active site was the Varian CARY 500scan UV-VIS-NIR spectrophotometer. Plate reader for UV-Vis analysis of the ABTS activity was an Accuris Smartreader 96. Fluorescence experiments were performed on the BioTek SynergyMX. Potentiostat used for electrochemical measurements was a CHI 630D. PAGE gels were run on a Invitrogen PowerEase Touch 350W.

Laccase Library Expression and Purification

Laccase expression was primarily based on previously established methods.[17] Plasmids containing the laccase library were separately transformed into DH5α strain of e. coli cells for expression of individual plasmids. Three individual colonies were placed into 5mL of LB respectively and grown over night with the ampicillin at 50 µg/ml. Using a commercially available midi prep kit the plasmid was extracted, and portion was sent out for sequencing for plasmid confirmation. After sequencing, individual plasmids were transformed into T7 strain of e. coli cells and streaked onto agar plates. Three colonies were isolated and added to 5mL of LB for overnight expression. The Lac-T7 frozen stocks were made by mixing 500µL of overnight LB with 50% glycerol solution with MP H2O and placed into a –80C° freezer for long term storage. The remaining 4.5mL of the overnight culture was centrifuged to separate cells from the rest of supernatant and this pellet was then used with a midi prep kit to isolate the Laccase plasmid DNA. These plasmids were sent out for sequencing to confirm the identity of –80 stock of cells. These frozen stocks were used to inoculate starter cultures for expression for the individual mutants of laccase WT, D113C, N264C, and H470C respectively.

Laccase expressing cultures were made by inoculating a stab of the frozen stocks into 7mL of LB with ampicillin antibiotics at ug/mL and were grown overnight with an incubating temperature of 37C° at 250RPM. The next morning 1L of terrific broth within a 5L shaking flask containing ampicillin at a concentration of 50 µg/mL was inoculated with the full 7mL the Lac-T7 overnight culture. The 5L flask was incubating with a shaking speed of 250RPM at 37C until OD reached 0.8 or higher, at which point expression was induced using

an inoculation to a final working concentration of 0.1mM IPTG and 1mM CuSO4. During induction, Lac-T7 cells were shaking at 180RPM at 25C for 5 hrs, followed by a resting period at 28C for 24 hrs. During induction and expression, a microaerobic environment is produced in-situ while expressed laccase reacts with naturally occurring polyphenols and dissolved oxygen. Cells were harvested by centrifugation at 14,000 RPM for 20 min at 4C°, and Lac-T7 cell pellet was further lysed with Bugbuster® protein Extraction Reagent and cold probe sonication for 10 minutes in 3 sec on/ 7 sec off cycles. Cell lysate was diluted with 200mL of PBS and vigorously agitated to allow for laccase enzymes to dissolve into the PBS. The cell lysate and PBS mixture was centrifuged at 14,000 for 20 minutes and the PBS-Lysate and TB supernatant were combined and then vacuum filtered through a .22-micron filter. The cell supernatant was chilled and imidazole was added to a final concentration of 25mM.

Laccase purification was done using a 5mL Ni Sepharose His-column. To remove 20% ethanol storage solution millipore water was flushed through the column at a rate of 3mL/min for 5 min totaling 3 bed volumes. Next a running buffer comprised of 25mM imidazole in PBS at pH 7 was passed through the column for a total of 5 bed volumes at 3mL/min. The combined Lac-PBS and Lac-TB supernatant solution with 25mM imidazole was passed through the His-column at a rate of 3mL/min until. Once completed the column was rinsed with a 25mM Imidazole solution PBS at pH 7 for 3 bed volumes. Bound laccase protein was eluted out of the column using 250mM imidazole solution in PBS at pH 7 for 2 bed volumes. Imidazole was immediately removed via membrane dialysis with PBS to a concentration below .1mM and then concentrated using 30kDa spin columns. The concentration of enzyme was determined via BSA methods since laccase has been shown

to have activity towards Coomassie used in the more conventional bradford assay. The concentrated laccase enzyme was distributed into 500ul aliquots then flash frozen over LN2 and then lyophilized over night until properly freeze-dried and stored in the freezer in airtight storage until further use. To reconstitute laccase enzymes 500ul of mp water was added to the lyophilized powder and a small amount ~5µl was added to 1mM abts solution to superficially check for laccase activity.

Library ABTS Activity Testing

(2,2'-azino-bis(3-ethylbenzothiazoline-6-sulfonic acid) is a common substrate and redox shuttle used with many oxidoreductases. Using Michaelis-Menten methodologies the activity of each laccase mutant was tested using the Accuris Smartreader 96 using a 96-well plate. The activities were tested using citrate buffer at pH 5 with a range of ABTS concentrations including 0.01mM, 0.03mM, 0.05mM, 0.09mM, 0.12mM, 0.15mM, 0.2mM, 0.25mM, 0.3mM and 0.4mM ABTS. Wells were loaded with their respective concentration of ABTS, followed by the addition 10µL of .1mg/mL of each respective laccase. Laccase concentrations were confirmed using copper BSA protein assay.

PAGE

20µL of each of the laccase mutants was mixed with 5µL of 4x loading buffer. This mixture was heated to 95 to fully unfold laccases. All 25 µL were loaded into a Bio-Rad TGX PAGE gel with 7 µL of the Bio-Rad protein ladder. MOPS was used as the running buffer and the electrophoresis ran at 180V for 60 minutes. The gels were stained with Coomassie dye and subsequently destained with destain solution (MeOH, Acetic Acid, H2O) 1:1:2 ratios.

Cysteine-Thiol Determination

The determination and quantification of free cysteine residues was tested via multiple methods. Since the monitoring of cysteine residues can carry significant noise the use of multiple tools was used to find an average between them. Measure-IT was used as a fluorescent tag using reduced glutathione as a standard. Unfortunately, the laccase sample could made in a concentration to be within the working range for using Ellmans reagent. All laccases expressed in this experiment began crashing out of solution beyond a concentration of .5mg/mL.

Measure-IT kit was prepared first by making glutathione stock and working solutions at 110mM and 110µM respectively. A standard assay was prepared ranging from 0µM-55µM free thiol from the glutathione working solution. Laccase enzymes were prepared at a 0.5mg/mL concentrations, corresponding to a 8µM solution. Low on the end of the standard, but still within working range. Excitation for the Measure-IT reagent was set to 494 and emission was set for 517nm.

Proteomics LC-MS-MS

Proteomics was performed in conjunction with the CSU Analytical Resource Center, Research Resource ID (SCR_021758). Before samples were sent off for proteomics and sequencing, 1mL of .350mg/mL of laccase N264C was placed in 100uL of TCEP gel and vortex 15 times over 10 min. TCEP gel was pelleted out by centrifugation of at 10,000RPM. Supernatant was removed and added to a 1.5mL Eppendorf. Reduced N264C reacted with 25µM propargyl maleimide at 4˚C for 4 hours. The resulting solution was moved to a 30kDa

spin column, diluted by 5mL of PBS, and then centrifuged at 3,000 RPM in 10-min increments until 1mL solution remained. 5mL of PBS was added followed by further centrifugation at 3,000 RPM. This step was followed 3 more times. At the final centrifugation step the solution was reduced to a final volume of 100µL. This solution was frozen at -20 and submitted to proteomics along with N264C enzymes not modified by propargyl maleimide.

For proteomics preparation samples were digested using the EasyPep Mini MS Sample Prep Kit following the manufacturer's instructions. Briefly, 90uL was aliquoted from the sample and raised to 100ul with lysis buffer. Reduction and alkylation solutions were sequentially added followed by incubation at 95˚C for 10 min. After cooling to room temperature, 50µg of a 0.2µg/µL Trypsin/LysC mixture was added and samples were digested with shaking at 37˚C for 2 hours. The enzymes were then deactivated with the Digestion Stop Solution and contaminants removed using mixed mode peptide clean up columns. Peptide eluate was dried in a vacuum evaporator and resuspended in 3% acetonitrile/0.1% formic acid.

Reverse phase chromatography was performed using water with 0.1% formic acid and 80% acetonitrile with 0.1% formic acid . A total of 1µg of peptides was purified and concentrated using an on-line enrichment column (Thermo Scientific PepMap Neo C18). Subsequent chromatographic separation was performed on a Vanquish Neo (Thermo Scientific) on a reverse phase nanospray column with integrated silica emitter (ionopticks Aurora Ultimate Gen 3 C18 45°C) using a 90 minute method at a flow rate of 300 nanoliters/min: 1-6%B over 3 minutes followed by 6-35%B over 70 minutes, 35-45%B over 5

minutes ending in 12 minutes of washing at 500 nanoliters/minute, 99%B. Peptides were eluted directly into the mass spectrometer (Orbitrap Eclipse, Thermo Scientific) equipped with a Nanospray Flex ion source (Thermo Scientific) and spectra were collected over a m/z range of 375–2000 under positive mode ionization. Ions with charge state +2 or higher were accepted for MS/MS using a dynamic exclusion limit of 1 MS/MS spectra of a given m/z value with an exclusion duration of 60 s. The instrument was operated in FT mode for MS detection (profile; resolution of 6 240,000) and ion trap mode for MS/MS detection with a normalized HCD collision energy set to 30% and data centroided. Proteome Discoverer 3.0 was used for data processing (Thermo Scientific).

Laccase MWCNT Electrodes

Inspired by many MWCNT laccase electrode experiments,[18,19] glassy carbon electrodes were cleaned and polished with alumina from sizes 3-1 μm, and rinsed thoroughly with DI water. 5mg of MWCNT are dissolved in 500 μL DMF and sonicated for 15 minutes until fully dispersed. 20μL of the DMF-MWCNT mixture was dropped onto the GC electrode and allowed to dry. A second layer of MWCNT was formed by adding another 20μL of MWCNT working solution and was left to dry. Lyophilized laccase was dissolved to a concentration of 300μg/mL and distributed into 150uL increments into 1.5mL Eppendorf tubes. The MWCNT functionalized GC electrodes were placed MWCNT side down into the Eppendorf tube and left there overnight in the fridge at 4C.

Electrochemical measurements were performed in pH 4 citrate buffer saturated with oxygen by vigorous bubbling. Cyclic voltammetry measurements were taken from 0.7V to

0.1V vs Ag/AgCl with a scan rate of 5mV/s. The reference electrode was a Ag/AgCl electrode paired with a platinum wire electrode as a counter electrode.

Results and Discussion

T1 active site and Library ABTS Activity

Using UV-Vis to observe the T1 active site the WT laccase shows its ubiquitous peak absorbance at 607nm. Comparing the mutants to the WT enzyme they seem to share this feature with few differences. Seen in Figure 10 D113C and H470C show a very slight red shift

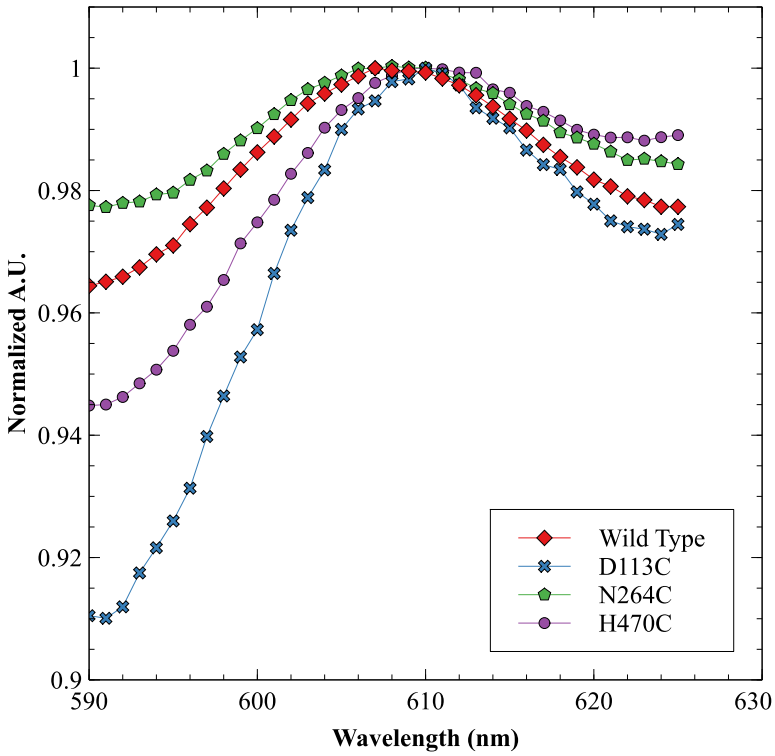

Figure 10 Laccase library's T1 active sites absorption in UV-Vis : WT (red diamond, D113C(blue x), N264C(green pentagon), and H470C(purple circle).

in their peaks absorbances to 610nm and 611nm respectively. With the location of the H470C mutant so close to the T1 active site, at nearly 10Å away, this could be explained by the alteration of the secondary solvation sphere surrounding the active site. Strangely this

change in Abs_{max} is also observed in the D113C mutant which holds its cysteine closest to the TNC being over 25Å away from the T1 site. Being only 15Å away from the TNC it could be interacting with that active site, which in turn could extend into the Cys-His bridge affecting the T1 site, but without EPR or crystallographic information little can be said about the true cause and electronic effects of this shift. N264C being so far away from both active sites it makes sense this mutant has little effect on the T1 active site.

The chemical activity appeared to be maintained in some capacity by the entire engineered library. The individual reaction rates for the library can be seen at the end of the chapter in figure 14 with their Lineweaver-Burke plots in figure 15. The WT laccase maintained the highest activity toward ABTS at 1510μM/min. There was a drop in activity for the rest of the mutants, but ABTS activity was retained. D113C and H470 had nearly identical activities at 952 μM/min and 918 μM/min respectively. The lowest activity for ABTS was the N264C mutant, which had maintained an activity of 253 μM/min. This is not the trend that was predicted for these mutants. N264C is the furthest cysteine from both active sites, and it was predicted that this mutation would have the least effect on the activity of the enzyme. Conversely the D113C is very close to the arginine at D116C which participates in the evacuation of water from its TNC active site. The Arginine it replaced must be far enough away from the active site to not participate in a truly essential manner. Even H470C, which had the greatest chances for affecting binding at the T1 site kept similar activity for ABTS. This is promising for further mutations that could be explored in the future. When comparing electrochemical activities of these mutants it will be interesting to see if any of these trends change with the aid of the electrode for electron exchange. Being able to study oxidation and

reduction separately it will be interesting to see if the lowering of activity in H470C or D113C could be explained by their interactions with their neighboring active sites, T1 and TNC respectively.

Using any thiol determination technique led to no clear understanding or even direction of an agreed upon free cysteine on the laccase library. For this reason, proteomics was explored to confirm the location and identity of the cysteines in the mutants. N264C was chosen for the proteomics experiment since its mutation is furthest from either of the active site. Through proteomics the identity and structure of the N264C was confirmed, but unfortunately the binding of the N264 cysteine by the propargyl maleimide was not found. During the proteomics all the cysteines were identified by being carbamidomethylated during the digestion process of the sample preparation rather than binding to propargyl maleimide. The proteomics experiments show the mutated cysteine could not be as solvent accessible as we might hope. It is not believed to interact with the Cys-His bridge or even replacing one of the cysteines taking part in the disulfide bonds. Any Cys-His interactions would be very unlikely given its distance from the T1 active site and in proteomics analysis neither cysteine participating in the disulfide bond could be identified, this suggests this bond survived digestion remained as larger, hard to identify fragments. Not being able to bind to any of the proposed cysteine locations appears troublesome moving forward with protein immobilization using maleimide.

MWCNT Electrochemistry

The MWCNT experiments were essential in knowing whether the library would be useful for moving forward. Despite the rudimentary nature of the experimental design a

small yet distinct electrochemical response for the reduction of oxygen was found for each mutant. In Figure 11 each mutant is compared to the blank that was prepared alongside it. The WT and N264C laccases show a clear sigmoidal shape indicative of a catalytic response with dissolved oxygen. Since this species of laccase has an expected T1 reduction potential at 450mV and both the WT and its mutant seem to have an onset potential around 350mV vs Ag/AgCl. This shows we are operating at around a 100mV overpotential from expected catalysis, which is promising given the unstable immobilization techniques. The mutants

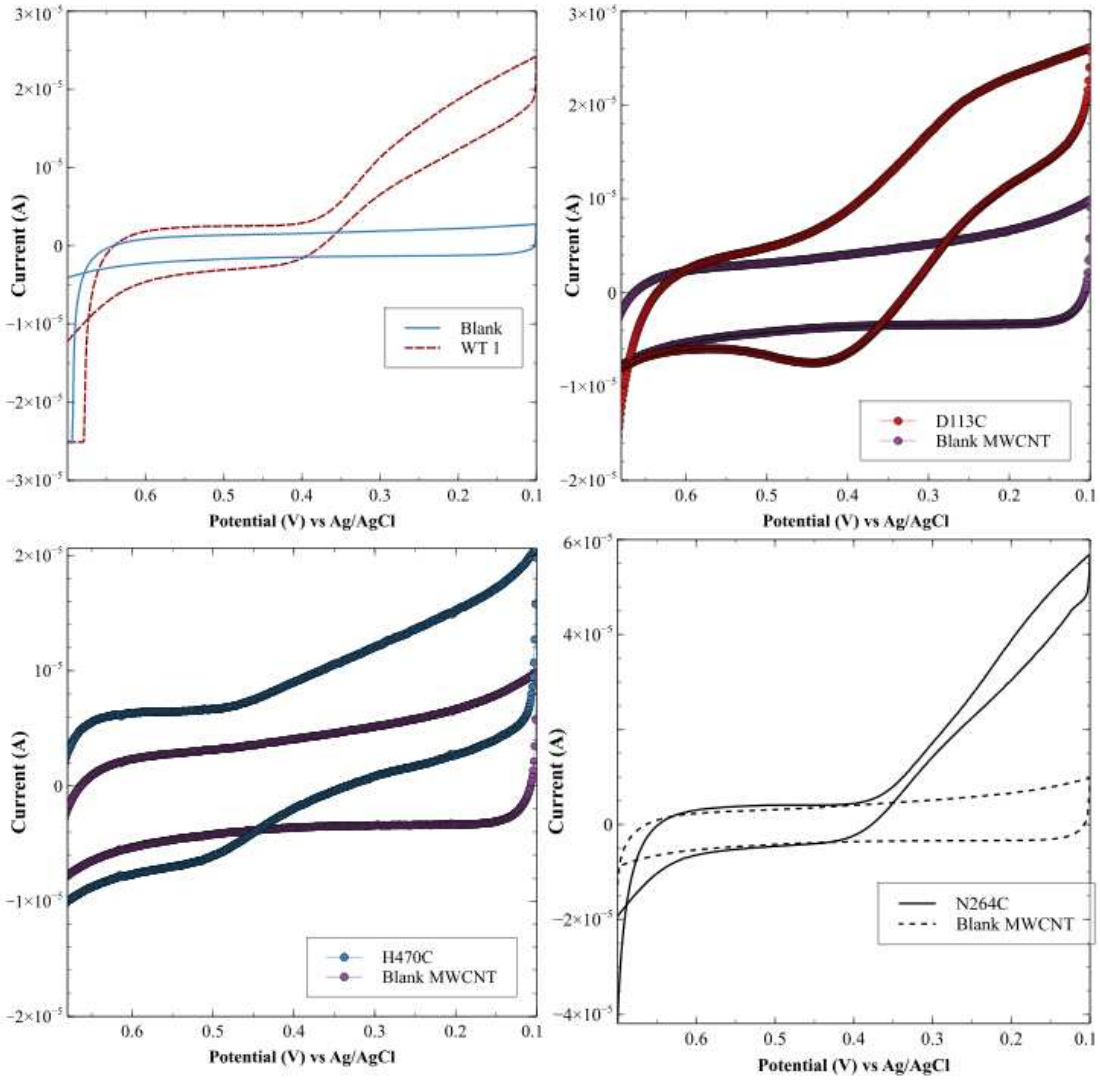

Figure 11Electrocatalytic reduction of oxygen on MWCNT modified graphene electrodes in citrate buffer pH 4. WT (top left), D113C(top right), H470C(bottom left), N264C(bottom left). Scan rate 5mV/s

D113C and H470C on the other hand do not show the same sigmoidal shape expected for electrochemical catalysis. Neither show “duck” shaped curves expected for a reversible redox process either. Instead, they are both thicker linear curves, still displaying catalysis.

Strangely the onset potential for the reduction of oxygen appears sooner for the H470C and D113C mutants compared to the WT laccase. The H470C mutant appears to begin reduction at 460mV Ag/AgCl while the D113C begins reduction near 500mV vs Ag/AgCl. The cause of this is unclear, it could be caused by changes to the reduction potentials of the T1 active caused by the mutation, or by the orientations of the enzymes around and within the MWCNT’s. Since the H470C mutation site is so close to the T1 active site it is expected that this mutation would influence the active site. A higher potential for the reduction of the T1 active site is certainly possible from this mutation. The D113C mutation is closest to the TNC and could also influence catalysis at this site. Since the D116 aspartic acid is known to help provide the protons to the TNC active site, the removal of the D113 aspartic acid might affect the overall proton channel. If this were the case one would expect a greater shift toward lower reduction potential, meaning it is necessary to apply more work than predicted to force the catalysis to happen. The change in reduction potential of the T1 active can further be investigated via EPR to probe this moiety individually. Unfortunately, there is no similar experimentation to know any changes of the active site for the TNC without a crystal structure.

Pairing the UV-Vis data of the T1 active site with electrochemical measurements using MWCNT, it appears that there could be a link between the red-shifting of the T1

absorbance with the electrochemical catalysis. Both the D113C and H470C mutants show this red shift in the t1 active site as well as a change in onset potentials in the same direction as well as appearing to have a non-sigmoidal shape to its CV. Again, this change is easily explainable for the H470C mutant given how close it is to the T1 active site, but the D113C changes are more peculiar.

Future Directions

More must be known about the structure of the mutants and the location of the single cysteine. Further proteomics determinations would aid in this for the rest of the library aside from the ones currently tested. Attaching propargyl maleimide to the cysteine and getting it identified by proteomics would be a good check to see the proper attachments is being made with the gold electrodes. Since this library has been shown to require higher heat for denaturing, warming laccase to partially break hydrogen bonds and see if any of the reagents can react with the cysteine's thiol without much harm to the protein. EPR measurements would also help elucidate the redox potential of the T1 copper active site. Growing crystals of each mutant would also elucidate the location of the free thiols for the entire library. However, crystallization of the laccase library have been fruitless only leading to precipitation of the enzymes.

The innovations surrounding predicting enzyme structures and simulating enzyme interactions have grown tremendously over the past decade and all future enzyme/protein work should be done alongside these technologies. Using in-silica experimentation can save researchers time and resources on protein expression and further testing.[20,21]

Computational protein design using community accessible tools like Rosetta, ProteinMPNN, RFdiffusion, and AlphaFold2 are now capable of predicting cascading effects regarding single site mutations on a protein or enzyme. Predicting mutation sites and choosing the best substituting amino acids are now common endeavors.[22] Having in silica coordinating data suggesting a mutation with reactive amino acids like cysteine, selenocysteine, and methionine will not interact in such a way so that it negatively affects the activity or becomes solvent/reagent inaccessible. Having misfolded or inactive proteins through computation design is still a regular occurrence, but the guiding hand of folding predictive software is a profoundly helpful tool. Giacobelli et al.[22] used computational methods to simulate the binding of the substrate to the laccase POXA1b. After simulations identified binding regimes, they next did Monte Carlos simulation on this entire moiety to substitute every native amino acid with every possible mutation by natural amino acids and identified laccase mutants. Four were chosen to express in the lab and only half of the expressed mutants held activity for the substrate 2,4 diamino benzenesulfonic acids. Future research should include computational designs of the laccase enzyme interacting with different surfaces and topographies to choose sites that would properly orient themselves near these surfaces with solvent accessible mutations.

Conclusions

Laccase from *Bacillis subtillis* was chosen as a model system to study enzyme orientation on planar gold electrodes. The design of the library of mutants was done visually, based on the solvent exposure, calculated from crystallographic data of the native amino acids before mutation. Literature was investigated to search for previously expressed amino

acid mutations. The single cysteine mutants N264C, D113C, and H470C were expressed and isolated from commercially available e. coli cells. The expression of the laccase library successfully produced a library of 4 catalytically active enzymes with a single cysteine motif designed to bind to gold electrode architectures. The wild type Laccase remained the most active towards oxidation of the common oxidoreductase substrate ABTS while the mutants D113C and H470C maintained 65% of this activity and N264C maintained only 18% of this activity while in solution. Out of the library the most notable mutation is D113C near the TNC active site. Mutations near this site have been known to completely inactivate laccase enzymes and only losing a small 20% of its activity was surprising.

While trying to quantify the free cysteine to make sure the thiols are solvent accessible with finding all commercially available products to be unsuccessful, proteomics was used to confirm the total sequence of the laccase with no information on its secondary and tertiary structures. Proteomic analysis suggests cysteine sulfur atom remained as a thiol rather than oxidizing to a sulfenic or sulfinic acids. Proteomics also suggests the N264C mutation is not interacting with the other cysteines in the laccase native structure.

Confirming the electrocatalytic activity of the laccase library was done using randomly oriented multi walled carbon nanotubes onto a glassy carbon electrode. The laccase enzymes were allowed to intercalate into MWCNT matrix in a pseudo-entrapment and adsorption mechanism. These electrodes showed profound differences between the MWCNT functionalized electrodes in terms of onset potentials and current densities with different laccase enzymes embedded within. Due to the nature of these electrodes'

engineering, no further experimentation or data analysis was performed on these electrodes to investigate these differences since it is not in the scope of this thesis. The onset potential for these reactions occurs at the expected potential of the T1 active site for WT and N264C laccases. While the D113C and H470C both show a higher onset potential, this could be corresponding to a similar red shift of the T1 active site UV-Vis absorbance for the D113C and H470C mutants.

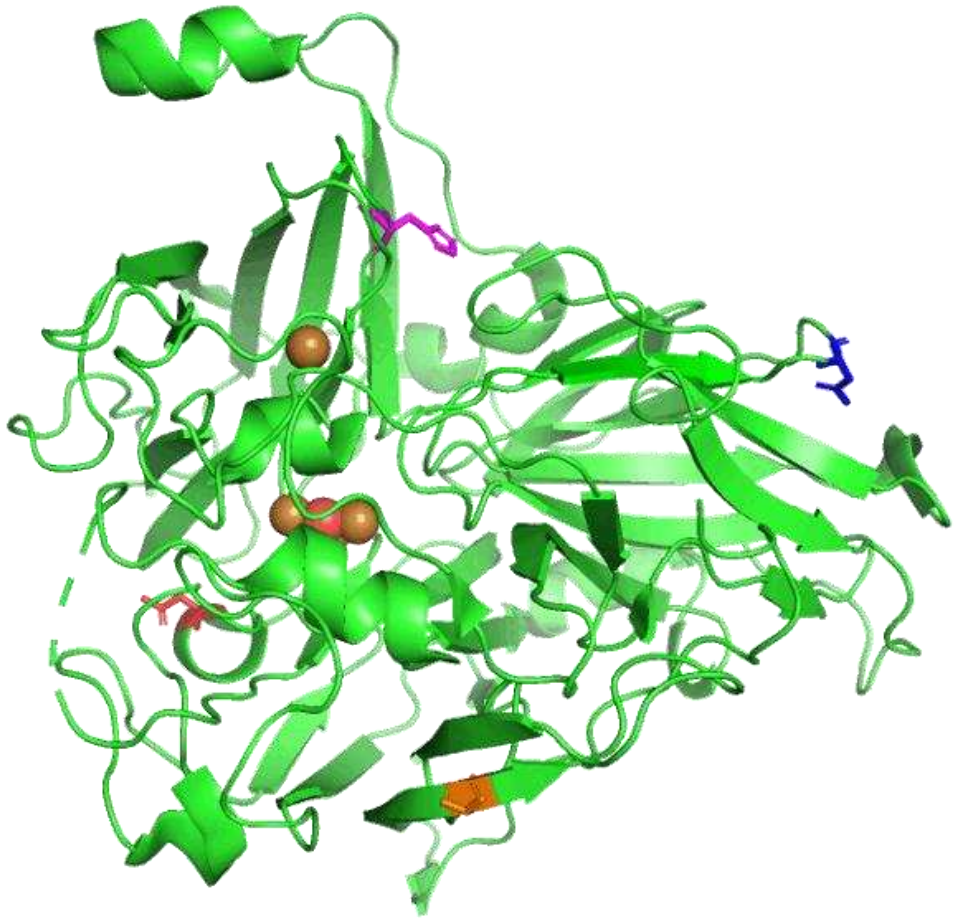

Figure 12 Laccase enzyme with all four cysteines highlighted. WT (orange), N264C (blue), H470C(pink), and D113C(orange)

Figure 13 Tables of the solvent exposure (SE) and distance in angstroms from the T1 and TNC

PDDSD Trinuclear CU sites			
	Trinuclear	Mono Cu	SE
P112C	14.4	25.7	30.4
D113C	14.0	23.6	42.77
D114C	14.7	25.4	37.54
S115C	13.8	24.8	.772
D116C	9.5	21.1	5.98
Wild Type			
	Trinuclear	Mono Cu	SE
WT	22.8	30.4	

YNLSL Substrate Pathway 1			
	Trinuclear	Mono Cu	SE
Y263C	18.0	16.4	.174
N264C	20.9	17.9	42.4
L265C	22.4	21.0	2.01
S266C	25.9	24.7	34.84
L267C	28.6	28.2	13.42

TIQAH Parallel Beta sheet 2			
	Tri	Mono	SE
T466C	8.8	11.9	.053
I467C	12.1	11.3	.213
Q468C	14.1	9.8	19.43
A469C	16.9	9.0	1.83
H470C	19.0	10.4	64.688

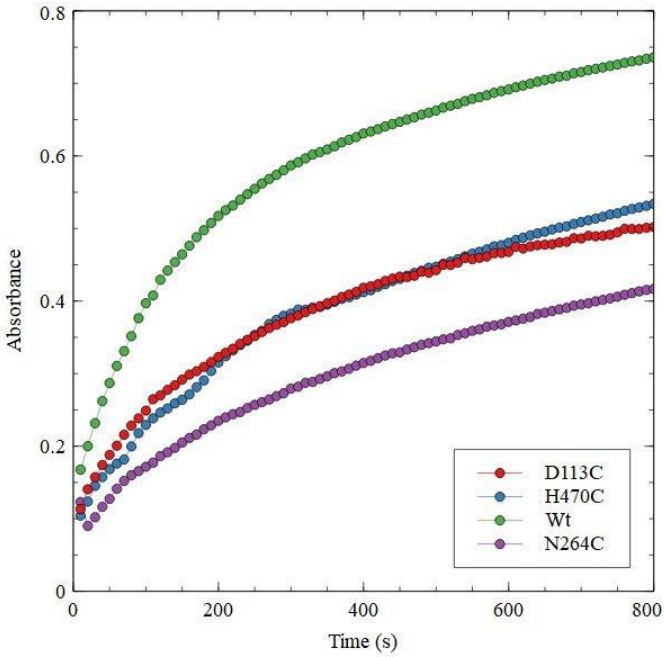

Figure 14 Laccase mutants reacting with .3mM ABTS in citrate buffer pH4

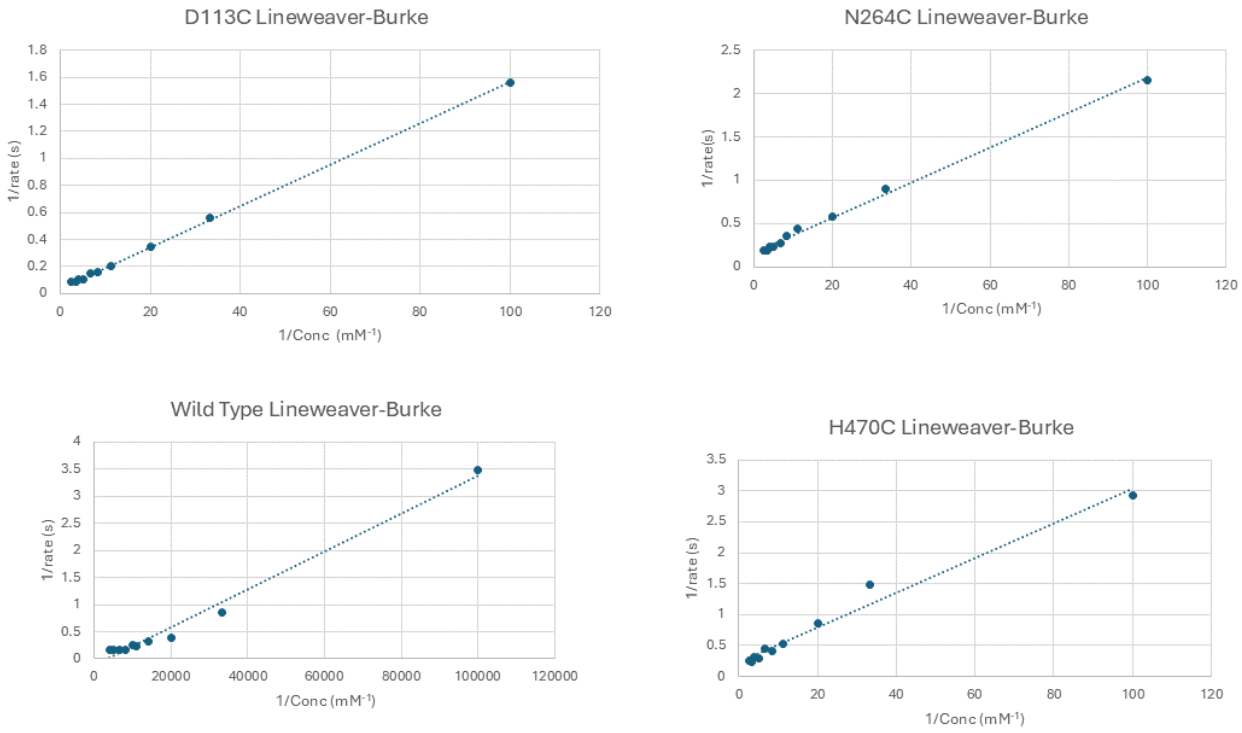

Figure 15 Laccase library Lineweaver-Burke plot used to calculate ABTS activity

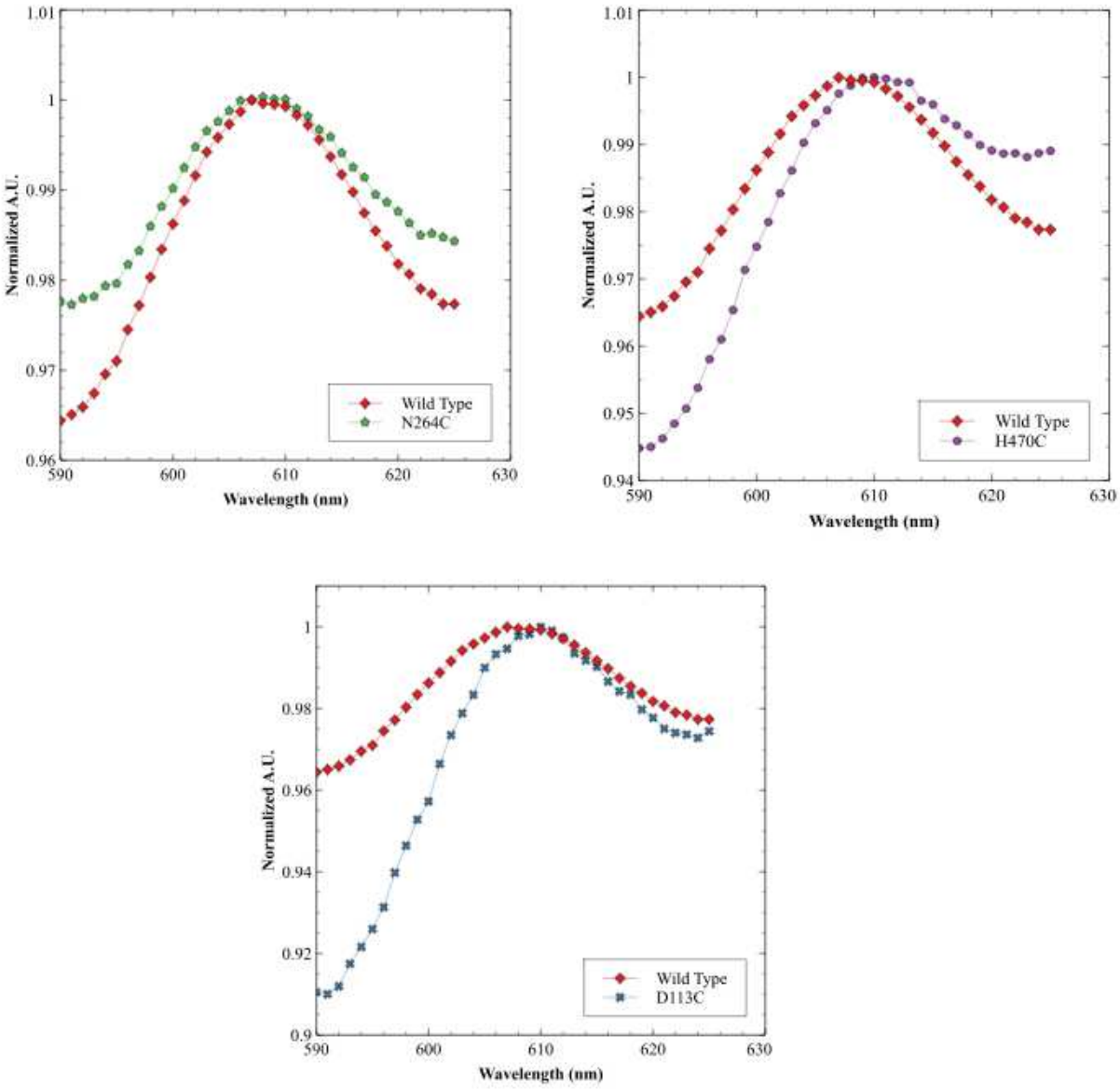

Figure 16 T1 active sites compared to the wild type laccase

Laccase Library Sequences- Mutation sites are highlighted

Wild Type Laccase Insert Sequence

atgaccctggagaaatttgtggatgcgctgccgattccagacacactgaagccggttcagcagagcaaagaaaagacatattacgaagtg
accatggaggaatgcacgcatcagctgcaccgcgatctgccgccaacccgcctctggggctataatggtctgttcccgggcccgacaatcg
aagtcaaacgcaacgagaatgtgtacgttaagtggatgaacaacctgcctagcacacattttctgccgattgaccacaccatccatcattct
gattcccagcacgaagaaccggaggtgaaaaccgtggttcatctgcacggtggcgtcacaccagatgacagcgatggttatccggaagcc
tggttcagcaaagactttgaacagacgggcccgtacttcaaacgtgaggtgtatcactacccaaaccagcagcgtggtgcaattctgtggt
atcatgatcacgccatggcgttaacacgcctgaacgtttacgctggcctggtgggtgcgtatatcattcacgatccgaaagaaaaacgcctg
aagctgccgtctgacgaatacgatgtgccactgttaattactgatcgtaccatcaatgaggacggctccctgttttatccgagcgcaccgga
aaacccgtccccaagcctgccgaacccatctattgttccggcgttttgcggtgaaacaatcctggtgaacggcaaagtctggccatacctgg
aagtggaaccgcgcaaatatcgtttccgtgtgatcaacgccagcaacacccgtacctacaacctgtccttggataatggtggcgaatttatt
caaatcggtagcgatggcggtctgctgcctcgtagcgtgaaactgaactctttcagcctggcaccggccgagcgctatgacattattatcga
ttttactgcgtacgaaggcgaaagcattattctggccaattccgcgggttgcggcggtgacgttaacccggagaccgatgcaaatatcatgc
agttccgtgtgaccaaaccgctggcgcaaaaagatgaaagccgcaaaccaaaatatctggcctcttacccgagcgtccagcacgaacgc
attcaaaacattcgtaccttgaaactggcgggcactcaggacgagtatggccgcccggtgctgctgctgaataacaaacgttggcatgatc
cagttaccgaagcgccgaaggtgggtactaccgaaatctggagcattatcaacccgacgcgcggcacccatccgattcacctgcatctggt
gtcctttcgcgttctggatcgccgcccattcgacatcgcccgctaccaagagagcggtgaactgagctatacgggcccggcggtgccgcca
ccgccgagcgaaaaaggttggaaggataccattcaagcccatgcgggcgaggtcctgcgtatcgccgcgacatttggtccgtactccggc
cgctatgtgtggcactgccacattctggaacatgaagactatgatatgatgcgtccaatggatattaccgatccgcacaaa

C35S

atgaccctggagaaatttgtggatgcgctgccgattccagacacactgaagccggttcagcagagcaaagaaaagacatattacgaagtg
accatggaggaaagcacgcatcagctgcaccgcgatctgccgccaacccgcctctggggctataatggtctgttcccgggcccgacaatc
gaagtcaaacgcaacgagaatgtgtacgttaagtggatgaacaacctgcctagcacacattttctgccgattgaccacaccatccatcattc
tgattcccagcacgaagaaccggaggtgaaaaccgtggttcatctgcacggtggcgtcacaccagatgacagcgatggttatccggaagc
ctggttcagcaaagactttgaacagacgggcccgtacttcaaacgtgaggtgtatcactacccaaaccagcagcgtggtgcaattctgtgg
tatcatgatcacgccatggcgttaacacgcctgaacgtttacgctggcctggtgggtgcgtatatcattcacgatccgaaagaaaaacgcct
gaagctgccgtctgacgaatacgatgtgccactgttaattactgatcgtaccatcaatgaggacggctccctgttttatccgagcgcaccgg
aaaacccgtccccaagcctgccgaacccatctattgttccggcgttttgcggtgaaacaatcctggtgaacggcaaagtctggccatacctg
gaagtggaaccgcgcaaatatcgtttccgtgtgatcaacgccagcaacacccgtacctacaacctgtccttggataatggtggcgaatttat
tcaaatcggtagcgatggcggtctgctgcctcgtagcgtgaaactgaactctttcagcctggcaccggccgagcgctatgacattattatcg
attttactgcgtacgaaggcgaaagcattattctggccaattccgcgggttgcggcggtgacgttaacccggagaccgatgcaaatatcatg
cagttccgtgtgaccaaaccgctggcgcaaaaagatgaaagccgcaaaccaaaatatctggcctcttacccgagcgtccagcacgaacg
cattcaaaacattcgtaccttgaaactggcgggcactcaggacgagtatggccgcccggtgctgctgctgaataacaaacgttggcatgat
ccagttaccgaagcgccgaaggtgggtactaccgaaatctggagcattatcaacccgacgcgcggcacccatccgattcacctgcatctgg
tgtcctttcgcgttctggatcgccgcccattcgacatcgcccgctaccaagagagcggtgaactgagctatacgggcccggcggtgccgcca
ccgccgagcgaaaaaggttggaaggataccattcaagcccatgcgggcgaggtcctgcgtatcgccgcgacatttggtccgtactccggc
cgctatgtgtggcactgccacattctggaacatgaagactatgatatgatgcgtccaatggatattaccgatccgcacaaa

D113C

atgaccctggagaaatttgtggatgcgctgccgattccagacacactgaagccggttcagcagagcaaagaaaagacatattacgaagtg
accatggaggaaagcacgcatcagctgcaccgcgatctgccgccaacccgcctctggggctataatggtctgttcccgggcccgacaatc
gaagtcaaacgcaacgagaatgtgtacgttaagtggatgaacaacctgcctagcacacattttctgccgattgaccacaccatccatcattc
tgattcccagcacgaagaaccggaggtgaaaaccgtggttcatctgcacggtggcgtcacaccatgcgacagcgatggttatccggaagc
ctggttcagcaaagactttgaacagacgggcccgtacttcaaacgtgaggtgtatcactacccaaaccagcagcgtggtgcaattctgtgg
tatcatgatcacgccatggcgttaacacgcctgaacgtttacgctggcctggtgggtgcgtatatcattcacgatccgaaagaaaaacgcct
gaagctgccgtctgacgaatacgatgtgccactgttaattactgatcgtaccatcaatgaggacggctccctgttttatccgagcgcaccgg
aaaacccgtccccaagcctgccgaacccatctattgttccggcgttttgcggtgaaacaatcctggtgaacggcaaagtctggccatacctg
gaagtggaaccgcgcaaatatcgtttccgtgtgatcaacgccagcaacacccgtacctacaacctgtccttggataatggtggcgaatttat
tcaaatcggtagcgatggcggtctgctgcctcgtagcgtgaaactgaactctttcagcctggcaccggccgagcgctatgacattattatcg
attttactgcgtacgaaggcgaaagcattattctggccaattccgcgggttgcggcggtgacgttaacccggagaccgatgcaaatatcatg
cagttccgtgtgaccaaaccgctggcgcaaaaagatgaaagccgcaaaccaaaatatctggcctcttacccgagcgtccagcacgaacg
cattcaaaacattcgtaccttgaaactggcgggcactcaggacgagtatggccgcccggtgctgctgctgaataacaaacgttggcatgat
ccagttaccgaagcgccgaaggtgggtactaccgaaatctggagcattatcaacccgacgcgcggcacccatccgattcacctgcatctgg
tgtcctttcgcgttctggatcgccgcccattcgacatcgcccgctaccaagagagcggtgaactgagctatacgggcccggcggtgccgcca
ccgccgagcgaaaaaggttggaaggataccattcaagcccatgcgggcgaggtcctgcgtatcgccgcgacatttggtccgtactccggc
cgctatgtgtggcactgccacattctggaacatgaagactatgatatgatgcgtccaatggatattaccgatccgcacaaa

H470C

atgaccctggagaaatttgtggatgcgctgccgattccagacacactgaagccggttcagcagagcaaagaaaagacatattacgaagtg
accatggaggaaagcacgcatcagctgcaccgcgatctgccgccaacccgcctctggggctataatggtctgttcccgggcccgacaatc
gaagtcaaacgcaacgagaatgtgtacgttaagtggatgaacaacctgcctagcacacattttctgccgattgaccacaccatccatcattc
tgattcccagcacgaagaaccggaggtgaaaaccgtggttcatctgcacggtggcgtcacaccagatgacagcgatggttatccggaagc
ctggttcagcaaagactttgaacagacgggcccgtacttcaaacgtgaggtgtatcactacccaaaccagcagcgtggtgcaattctgtgg
tatcatgatcacgccatggcgttaacacgcctgaacgtttacgctggcctggtgggtgcgtatatcattcacgatccgaaagaaaaacgcct
gaagctgccgtctgacgaatacgatgtgccactgttaattactgatcgtaccatcaatgaggacggctccctgttttatccgagcgcaccgg
aaaacccgtccccaagcctgccgaacccatctattgttccggcgttttgcggtgaaacaatcctggtgaacggcaaagtctggccatacctg
gaagtggaaccgcgcaaatatcgtttccgtgtgatcaacgccagcaacacccgtacctacaacctgtccttggataatggtggcgaatttat
tcaaatcggtagcgatggcggtctgctgcctcgtagcgtgaaactgaactctttcagcctggcaccggccgagcgctatgacattattatcg
attttactgcgtacgaaggcgaaagcattattctggccaattccgcgggttgcggcggtgacgttaacccggagaccgatgcaaatatcatg
cagttccgtgtgaccaaaccgctggcgcaaaaagatgaaagccgcaaaccaaaatatctggcctcttacccgagcgtccagcacgaacg
cattcaaaacattcgtaccttgaaactggcgggcactcaggacgagtatggccgcccggtgctgctgctgaataacaaacgttggcatgat
ccagttaccgaagcgccgaaggtgggtactaccgaaatctggagcattatcaacccgacgcgcggcacccatccgattcacctgcatctgg
tgtcctttcgcgttctggatcgccgcccattcgacatcgcccgctaccaagagagcggtgaactgagctatacgggcccggcggtgccgcca
ccgccgagcgaaaaaggttggaaggataccattcaagcctgcgcgggcgaggtcctgcgtatcgccgcgacatttggtccgtactccggc
cgctatgtgtggcactgccacattctggaacatgaagactatgatatgatgcgtccaatggatattaccgatccgcacaaa

N264C

atgaccctggagaaatttgtggatgcgctgccgattccagacacactgaagccggttcagcagagcaaagaaaagacatattacgaagtg
accatggaggaaagcacgcatcagctgcaccgcgatctgccgccaacccgcctctggggctataatggtctgttcccgggcccgacaatc

gaagtcaaacgcaacgagaatgtgtacgttaagtggatgaacaacctgcctagcacacattttctgccgattgaccacaccatccatcattc
tgattcccagcacgaagaaccggaggtgaaaaccgtggttcatctgcacggtggcgtcacaccagatgacagcgatggttatccggaagc
ctggttcagcaaagactttgaacagacgggcccgtacttcaaacgtgaggtgtatcactacccaaaccagcagcgtggtgcaattctgtgg
tatcatgatcacgccatggcgttaacacgcctgaacgtttacgctggcctggtgggtgcgtatatcattcacgatccgaaagaaaaacgcct
gaagctgccgtctgacgaatacgatgtgccactgttaattactgatcgtaccatcaatgaggacggctccctgttttatccgagcgcaccgg
aaaacccgtccccaagcctgccgaacccatctattgttccggcgttttgcggtgaaacaatcctggtgaacggcaaagtctggccatacctg
gaagtggaaccgcgcaaatatcgtttccgtgtgatcaacgccagcaacacccgtacctactgcctgtccttggataatggtggcgaatttatt
caaatcggtagcgatggcggtctgctgcctcgtagcgtgaaactgaactctttcagcctggcaccggccgagcgctatgacattattatcga
ttttactgcgtacgaaggcgaaagcattattctggccaattccgcgggttgcggcggtgacgttaacccggagaccgatgcaaatatcatgc
agttccgtgtgaccaaaccgctggcgcaaaaagatgaaagccgcaaaccaaaatatctggcctcttacccgagcgtccagcacgaacgc
attcaaaacattcgtaccttgaaactggcgggcactcaggacgagtatggccgcccggtgctgctgctgaataacaaacgttggcatgatc
cagttaccgaagcgccgaaggtgggtactaccgaaatctggagcattatcaacccgacgcgcggcacccatccgattcacctgcatctggt
gtcctttcgcgttctggatcgccgcccattcgacatcgcccgctaccaagagagcggtgaactgagctatacgggcccggcggtgccgcca
ccgccgagcgaaaaaggttggaaggataccattcaagcccatgcgggcgaggtcctgcgtatcgccgcgacatttggtccgtactccggc
cgctatgtgtggcactgccacattctggaacatgaagactatgatatgatgcgtccaatggatattaccgatccgcacaaa

References

(1) Yoshida, H. LXIII.—Chemistry of Lacquer (Urushi). Part I. Communication from the Chemical Society of Tokio. *J. Chem. Soc., Trans.* **1883**, *43* (0), 472–486. https://doi.org/10.1039/CT8834300472.

(2) Mano, N.; de Poulpiquet, A. O2 Reduction in Enzymatic Biofuel Cells. *Chem. Rev.* **2018**, *118* (5), 2392–2468. https://doi.org/10.1021/acs.chemrev.7b00220.

(3) Turner, A. Biosensors: Then and Now. *Trends in Biotechnology* **2013**, *31* (3), 119–120. https://doi.org/10.1016/j.tibtech.2012.10.002.

(4) Khatami, S. H.; Vakili, O.; Movahedpour, A.; Ghesmati, Z.; Ghasemi, H.; Taheri-Anganeh, M. Laccase: Various Types and Applications. *Biotechnology and Applied Biochemistry* **2022**, *69* (6), 2658–2672. https://doi.org/10.1002/bab.2313.

(5) Filgueira, D.; Fernández-Costas, M. C.; Gouveia, S.; Bolaño Losada, C.; Moldes, D. Laccases for Wood Treatment: From Composites Manufacturing to Surface Modification. In *Laccase: Applications, Investigations and Insights*; 2017; pp 181–206.

(6) Jeon, J.-R.; Baldrian, P.; Murugesan, K.; Chang, Y.-S. Laccase-Catalysed Oxidations of Naturally Occurring Phenols: From in Vivo Biosynthetic Pathways to Green Synthetic Applications: Laccases and Natural Phenols for Organic Synthesis. *Microbial Biotechnology* **2012**, *5* (3), 318–332. https://doi.org/10.1111/j.1751-7915.2011.00273.x.

(7) Jones, S. M.; Solomon, E. I. Electron Transfer and Reaction Mechanism of Laccases. *Cell. Mol. Life Sci.* **2015**, *72* (5), 869–883. https://doi.org/10.1007/s00018-014-1826-6.

(8) Bento, I.; Silva, C. S.; Chen, Z.; Martins, L. O.; Lindley, P. F.; Soares, C. M. Mechanisms Underlying Dioxygen Reduction in Laccases. Structural and Modelling Studies Focusing on Proton Transfer. *BMC Structural Biology* **2010**, *10* (1), 28. https://doi.org/10.1186/1472-6807-10-28.

(9) Piontek, K.; Antorini, M.; Choinowski, T. Crystal Structure of a Laccase from the Fungus Trametes Versicolor at 1.90-A Resolution Containing a Full Complement of Coppers. *J Biol Chem* **2002**, *277* (40), 37663–37669. https://doi.org/10.1074/jbc.M204571200.

(10) Xu, F. Oxidation of Phenols, Anilines, and Benzenethiols by Fungal Laccases: Correlation between Activity and Redox Potentials as Well as Halide Inhibition. *Biochemistry* **1996**, *35* (23), 7608–7614. https://doi.org/10.1021/bi952971a.

(11) Janusz, G.; Pawlik, A.; Świderska-Burek, U.; Polak, J.; Sulej, J.; Jarosz-Wilkołazka, A.; Paszczyński, A. Laccase Properties, Physiological Functions, and Evolution. *International Journal of Molecular Sciences* **2020**, *21* (3), 966. https://doi.org/10.3390/ijms21030966.

(12) Pita, M.; Gutierrez-Sanchez, C.; Olea, D.; Velez, M.; Garcia-Diego, C.; Shleev, S.; Fernandez, V. M.; De Lacey, A. L. High Redox Potential Cathode Based on Laccase Covalently Attached to Gold Electrode. *J. Phys. Chem. C* **2011**, *115* (27), 13420–13428. https://doi.org/10.1021/jp203643h.

(13) Shleev, S.; Christenson, A.; Serezhenkov, V.; Burbaev, D.; Yaropolov, A.; Gorton, L.; Ruzgas, T. Electrochemical Redox Transformations of T1 and T2 Copper Sites in Native Trametes Hirsuta Laccase at Gold Electrode. *Biochem J* **2005**, *385* (Pt 3), 745–754. https://doi.org/10.1042/BJ20041015.

(14) Frasconi, M.; Favero, G.; Boer, H.; Koivula, A.; Mazzei, F. Kinetic and Biochemical Properties of High and Low Redox Potential Laccases from Fungal and Plant Origin. *Biochimica et Biophysica Acta (BBA) - Proteins and Proteomics* **2010**, *1804* (4), 899–908. https://doi.org/10.1016/j.bbapap.2009.12.018.
(15) Marcus, R. A.; Sutin, N. Electron Transfers in Chemistry and Biology. *Biochimica et Biophysica Acta (BBA) - Reviews on Bioenergetics* **1985**, *811* (3), 265–322. https://doi.org/10.1016/0304-4173(85)90014-X.
(16) Warren, J. J.; Lancaster, K. M.; Richards, J. H.; Gray, H. B. Inner- and Outer-Sphere Metal Coordination in Blue Copper Proteins. *Journal of Inorganic Biochemistry* **2012**, *115*, 119–126. https://doi.org/10.1016/j.jinorgbio.2012.05.002.
(17) Wang, T.-N.; Zhao, M. A Simple Strategy for Extracellular Production of CotA Laccase in Escherichia Coli and Decolorization of Simulated Textile Effluent by Recombinant Laccase. *Appl Microbiol Biotechnol* **2017**, *101* (2), 685–696. https://doi.org/10.1007/s00253-016-7897-6.
(18) Giroud, F.; Minteer, S. D. Anthracene-Modified Pyrenes Immobilized on Carbon Nanotubes for Direct Electroreduction of O2 by Laccase. *Electrochemistry Communications* **2013**, *34*, 157–160. https://doi.org/10.1016/j.elecom.2013.06.006.
(19) Bourourou, M.; Elouarzaki, K.; Lalaoui, N.; Agnès, C.; Le Goff, A.; Holzinger, M.; Maaref, A.; Cosnier, S. Supramolecular Immobilization of Laccase on Carbon Nanotube Electrodes Functionalized with (Methylpyrenylaminomethyl)Anthraquinone for Direct Electron Reduction of Oxygen. *Chemistry – A European Journal* **2013**, *19* (28), 9371–9375. https://doi.org/10.1002/chem.201301043.
(20) Coluzza, I. Computational Protein Design: A Review. *J. Phys.: Condens. Matter* **2017**, *29* (14), 143001. https://doi.org/10.1088/1361-648X/aa5c76.
(21) Goldenzweig, A.; Fleishman, S. J. Principles of Protein Stability and Their Application in Computational Design. *Annual Review of Biochemistry* **2018**, *87* (Volume 87, 2018), 105–129. https://doi.org/10.1146/annurev-biochem-062917-012102.
(22) Giacobelli, V. G.; Monza, E.; Lucas, M. F.; Pezzella, C.; Piscitelli, A.; Guallar, V.; Sannia, G. Repurposing Designed Mutants: A Valuable Strategy for Computer-Aided Laccase Engineering – the Case of POXA1b. *Catal. Sci. Technol.* **2017**, *7* (2), 515–523. https://doi.org/10.1039/C6CY02410F.

Chapter 3: Gold Electrode Design and Electrochemical Measurements

Introduction

The use of planar electrodes is important in being able to make meaningful statements about the orientation of the laccase library of enzymes with respect to the electrode surface. This can be done by using single crystal gold electrodes, commercially available or made in the lab. The use of single crystal gold can confidently obtain atomically flat regions of the electrode with high precision.[1] However, over large areas, millimeters are larger, these electrodes are anything but atomically flat; terraces and stair steps are common for crystalline electrodes, and since these single crystal electrodes are made from a bulk material these features can be on the scale of tens of nanometers.[2,3] In many aspects of electron transfer it has been shown that defect sites like these promote electron transfer more than the bulk material and this could affect the activity of enzymes near these domains and would complicate data analysis. [4] For this reason planar and atomically flat electrodes are preferred to study enzyme orientation without the cluttered electrochemical response from large surface defects.

Since single crystalline gold in any phase is very costly to purchase or prepare in the lab. To limit the cost of experiments an alternative electrode architecture was considered. The primary option considered was using gold thin films with well-defined and uniform surfaces with defects smaller than 2nm in size. Gold thin film microscope slides are

commonly used in microscopy to help with staining and spectroscopy, particularly useful in surface enhanced Raman spectroscopy (SERS).[5] While searching for proof of concept with a reasonable budget short 10nm thick film microscope slides were chosen to be valid candidates for these experiments. There are several suppliers making 10nm gold microscope slides, however deposition research laboratories incorporated (DRLI) seemed to have the best product after atomic force microscope was used to analyze surface roughness.

On this 10nm gold surface self-assembled monolayers (SAM) were grown to help bind the laccase mutants. The growth of SAM's onto gold electrodes has been well studied for the functionalization and protection of gold surfaces. [6–8] The engineering of two different SAMs will be investigated for the controlled binding of the laccase mutants. First a SAM of dithiobismaleimidoethane (DTME) will be grown onto the 10nm gold surface. This monolayer will bind to the gold surface with its sulfhydryl group which in turn is bound to a maleimide moiety. This maleimide moiety will be pointed out into the solvent to bind to the individual laccase mutant's single cysteine.[9,10] The maleimide-thiol bond is very strong and hold the enzyme in place during electrochemical processes.

The second SAM will be designed using Azido-propyl thioacetate. The acetate group protecting the sulfur can be removed via reaction with potassium hydroxide.[11–13] This leaves a gold surface modified by Gold-sulfur monolayer capped with an azido group that can further be modified easily. Propargyl maleimide will then be used to react with the terminal azido group using the Copper (I) catalyzed azide-alkyne cycloaddition (CuAAC) click

reaction.[14,15] This click reaction combines azide and alkynes into a very stable triazole ring. After the CuAAC reaction the surface is then capped with a maleimide moiety similar to that made by the DTME SAM.

The two SAMs both bring the enzyme very close to the electrode surface. The DTME SAM will bind the laccase's cysteine group less than 1nm from the electrode surface. The Azido modified SAM after CuAAC functionalization will bind to the laccases' cysteine a little over a 1nm from the electrode surface, based on standard bond distances. The azido-thioacetate comes in a variety of alkyl lengths, ranging up to octyl varieties, allowing for future studies on bond distances in the future. Figure 17 below shows the predicted scheme for the SAM's from DTME and Azido-propyl thioacetate. DTME can be bound directly to the laccase enzyme while the azido group must react with propargyl maleimide before laccase enzymes can be bound to them.

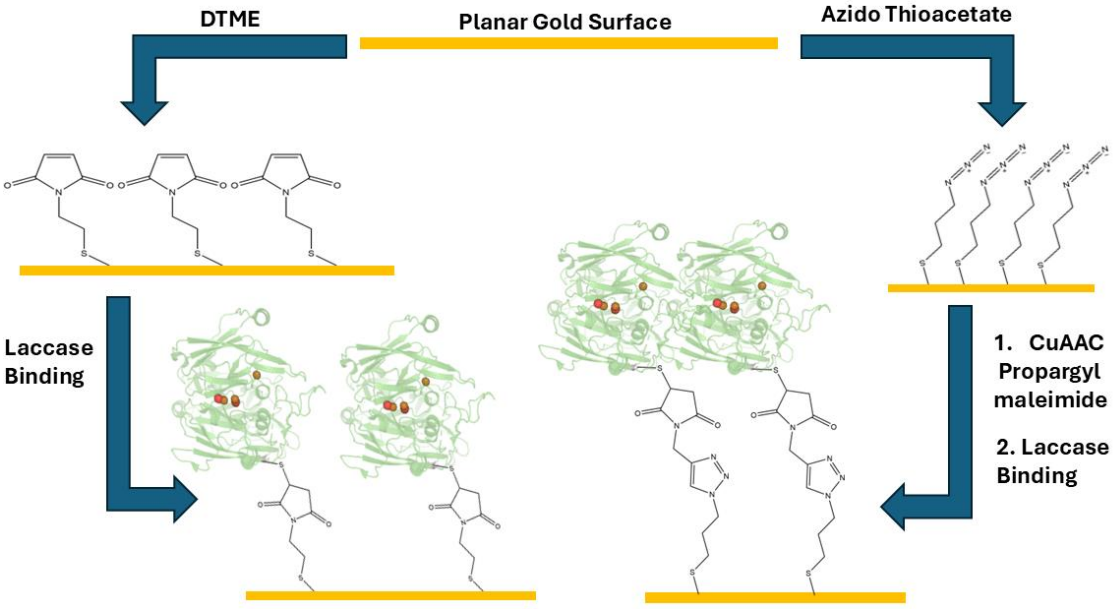

Figure 17 Scheme to functionalize the gold electrode with the SAM's DTME and azido propyl thioacetate followed by their binding with the laccase enzyme

There has been a myriad of publications pointing to the complications involved in doing electrochemistry with enzymes bound to planar or atomically flat surfaces.[16,17] One way to increase the topography of the electrode is by roughening the surface or by using nanoporous gold electrodes.[16,18,19] Nanoporous gold electrodes have become very popular in electrochemistry due to its increased surface area over unmodified bulk gold electrodes. These nanoporous electrodes are expensive to purchase mainly due to their destructive approach to produce them.[20] They are made generally by alloying gold with other metals like zinc or copper and then etching away all the added metals using strong acids. To produce an electrode with higher surface area and rougher topography to test the effects of surface conditions on enzyme catalysis a novel technique was produced using our 10nm gold microscope slides and gold 144 (Au144) water soluble gold clusters synthesized in the lab.

Au144 clusters are stable, atomically precise nanomaterials with a known geometric structure. Gold materials have been shown to be aurophilic and has a proclivity to bind to other gold materials. This ended up providing a novel bottom-up approach to produce a gold electrode with higher topography similar to nanoporous gold electrodes, we are referring to as a 3D SAM. These electrodes were tested electrochemically like the two SAMs and laccase modified 10nm gold electrodes as well as by atomic force microscopy(AFM). Figure 18 displays the scheme and AFM data from this electrode architecture. Without the use of large amounts of strong acids or any halogenated organic solvents in the production of the gold

clusters this can also be seen as a “green” technique in order to add topography to thin films compared to the production of nanoporous gold.

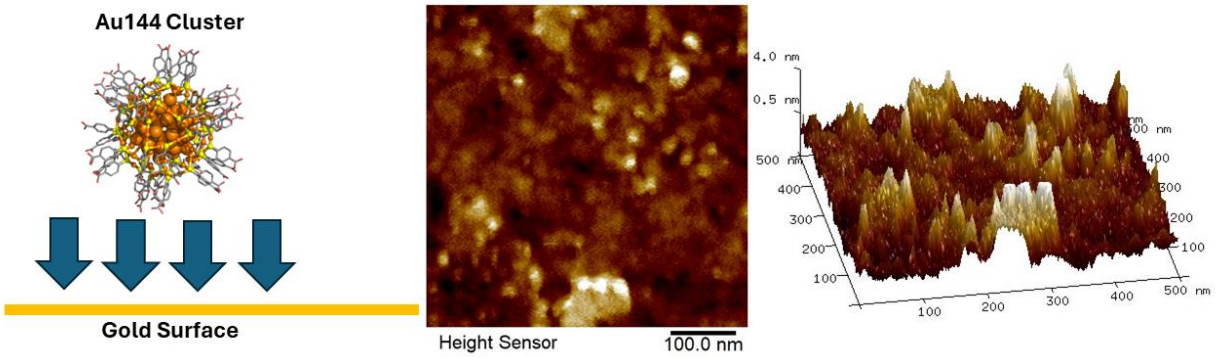

Figure 18 Scheme and topographical results for the gold cluster Au144 3D SAM

Materials and Methods

Materials

10nm Gold electrodes were purchased from Deposition Research Labs inc. Ethanol was purchased from Pharmco. Azido propyl, gold chloride, p-Mercaptobenzoic acid, $NaBH_4$, azido butyl acetate and sodium ascorbate were purchased from Sigma Aldrich. Propargyl maleimide was purchased from kerafast. Oxygen was purchased from Airgas. 2,2'-azino-bis(3-ethylbenzothiazoline-6-sulfonic acid) (ABTS) and Dithiobismaleimidoethane (DTME) were purchased from chem impex intl. MP H_2O was made using Millipore sigma water purifier to 18MΩ. Copper sulfate, Methanol, DMSO, ammonium acetate, and sodium citrate were purchased from fisher chemical. PBS was prepared using pre-mixed packets from VWR. TCEP dithiol reducing gel was purchased from Thermo scientific. NaOH was purchased from oakwood chemicals.

Instruments

Electrochemical measurements were taken on a CHI 630D potentiostat. The electrochemical cell used for gold electrode analysis was a BM EC 15mL- Bottom Mount electrochemical cell from redox.me. The cell is top mounted and keeps a nominal exposure area of 1cm^2. Making post processing and current densities easy to normalize between samples. This electrochemical cell also comes with a pre-engineered gas bubbling inlet and outlet system to control aerobic or anaerobic atmospheres during catalysis. Saturated Ag/AgCl electrodes were used as a reference electrode and a platinum wire counter electrode were used for all electrochemical measurements.

For surface characterization the ATR-IR data was obtained with aid from the Krummel Lab's Bruker Hyperion 3000 with a germanium anvil tip #793129809/ECOO. 256 scans were averaged at 2 wavenumber resolution and baseline correction was performed using Bruker analysis software. The water droplet analyzer is a Kruss DSA10 drop shape analyzer contact angle goniometer using 18MΩ water was used for the water droplet measurements. Finally, the AFM was a Bruker Bioscope Resolve AFM System. Brukers Sharp Nitride Lever (SNL) SNL-10 probe was chosen for these experiments and tip "A" was used exclusively. The Nanoscope's in house ScanAsyst was used to collect topographic data only. A scan area of 500nm x 500nm area was taken.

Methods

Electrode Preparations and Modifications

10nm Gold microscope slides were turned into electrodes and functionalized with the native cysteine, DTME, azido propyl thioacetate, and azido butyl thioacetate SAM's. No

matter the SAM applied every gold slide was cleaned the same way. A full 3x1 inch gold coated microscope slide was cleaned using piranha solution, a 5:1 solution of Sulfuric acid and 40% peroxide. This mixture is very reactive and dangerous, take extra care to use appropriate PPE and by having a work area clean of carbon-carbon bonds. Gold microscope slides were left in piranha solution for 20 min or until bubbles stopped being produced. Containers with gold microscope slides and piranha solution were agitated (carefully) every 5 min to remove accumulating bubbles on the electrode surface. After piranha cleaning the gold microscope slides were cleaned in DI H_2O until the pH of the rinsing solution stabilized. The microscope slides were then rinsed with 200 proof ethanol and dried by nitrogen gas. The cleaned microscope slides were cut into 1cmx1cm squares and used for further functionalization within one hour of cleaning.

For the formation of propyl and butyl thioacetate SAM's previously described methods were used.[12] 2mM thioacetate solutions reacted with 2.5mM KOH in 200 proof ethanol for 30min to deprotected the thioacetate and promote thiol formation. Over these 30 min the smell of thiols became more pronounced, so take care that these reactions are performed in an appropriate ventilated space, preferably a fume hood. After 30 min, gold electrodes were placed directly into the ethanolic solution used to convert thioacetates into thiols and left for 24 h. The next day the thiol containing ethanol solution was removed and the gold microscope slides were rinsed with 200 proof ethanol three times followed by 10 min in a sonicating bath until no lingering smell remained.

The CuAAC reaction was adapted by previously described methods.[21] The azido functionalized electrodes were added to a small microscope staining container for functionalization. An aqueous solution containing 100μM copper sulfate, 150μM sodium ascorbate and 2mM Propargyl maleimide was added to the azide functionalized electrodes. The reaction was left to react for 24 h to fully functionalize the electrodes. The solution was agitated periodically over 24 h at 4°C. To clean up post CuAAC, the electrodes were rinsed with 200 proof ethanol moved to a large microscope staining flask and sonicated in ethanol for 10 min.

DTME functionalized gold electrodes were synthesized by previously established methods.[22] After cleaning, gold slides were placed into a slide staining flask containing 2mM DTME within DMSO or ethanol. Ethanol became preferred for this functionalization since DMSO can leave unwanted residues on the containers and electrodes. Microscope slides were left to react with DTME for 24 hrs followed by rinsing with three times with 200 proof ethanol followed by 10 min sonicating bath within ethanol. Electrodes were used within 24 hrs of formation.

Laccase Modified Electrodes

To modify electrodes with Laccase, freeze-dried enzymes were rehydrated with MP H_2O and agitated until fully dissolved. Before immobilization to the electrode the laccase library was assured to be reduced using commercially available TCEP gel. 100uL of TCEP gel was added to the 500uL laccase and spun for 15 min. Gel was separated from laccase using centrifuge at 10000 RPM for 3 min. Laccase was removed and depending on the addition method different attempts were made. For Bare gold electrodes, reduced laccase was

added to the gold electrode and placed into the fridge at 4°C overnight. For maleimide capped electrodes formed by DTME and post CuAAC reaction, reduced laccase samples were combined to make 1mg laccase and were added to 7mL PBS to react with multiple electrodes within a small microscope slide staining container. The container was stored at 4°C and left for 12 h, shaking and agitating solution frequently. To remove unbound laccase from the surface the electrodes were sonicated in PBS for 15 min at 4°C three times, replacing the PBS each time.

Synthesis and Cleanup of Au144(pMBA)60

A 95.2 mM solution of *p*-MBA was prepared in a solution 0f 0.3 M NaOH in MP H_2O and was left to vortex overnight. The next day, a 28 mM solution of $HAuCl_4 \cdot H_2O$ was prepared in MP H_2O. To prepare the Au-*p*MBA oligomer solution, 4.5 mL of the *p*MBA solution and 5.14 mL of the $HAuCl_4 \cdot H_2O$ solution was added to a 50 mL conical tube. MP H_2O and methanol were added so the total volume reached 48 mL. At this point the solution was 53% aqueous and 47% methanol. The Au-*p*MBA solution was left to vortex overnight. Prior to vertexing, the Au-pMBA solution was a transparent, golden yellow color. After the overnight mixing, the solution was a translucent, pale yellow color. The next day, a 150 mM solution of $NaBH_4$ was prepared. 480 µL of the $NaBH_4$ solution was added to the Au-*p*MBA solution to reduce the Au^+ ions into zero-valent Au and promote cluster formation. This solution was left to vortex for a maximum of two hours. Within the two hours, the solution transitioned from an opaque gray color to an opaque dark brown color.

The crude product was split evenly into eight 15 mL conical tubes. To assist in precipitation, 500 µL of 5 M ammonium acetate was added to each conical tube. Each tube

was filled to a final volume of 14 mL with methanol. The crude product was cleaned up via centrifugation at 4,000 rpm for 10 min at 4°C. The clear supernatant was decanted, and the remaining black pellet was redissolved in minimal MP H_2O. Fractional precipitation was then used to further purify the cluster sample. A 40% cluster, 60% methanol solution was prepared in a 15mL conical tube with the addition of 500 µL of 5M ammonium acetate. The solution was centrifuged at 4,000 rpm for 10 min at 4°C. The black pellet was separated from the translucent, gray supernatant. More methanol was added to the supernatant until the total volume was roughly 14mL. 500µL of 5M ammonium acetate was also added again. The same centrifugation step was repeated. The black pellet was separated from the translucent, gray supernatant again and additional methanol and 5M ammonium acetate was added. The centrifugation step was repeated for a final time to produce a black pellet and a transparent, colorless supernatant. The supernatant was discarded, and the black pellet was redissolved in MP H_2O.

3D Self Assemble Monolayers

To see the effects of ions on the gold clusters collapsing onto the gold electrode and forming a 3D SAM, deposition was tested with and without salts and buffers. For this 20mg of $Au_{144}(pMBA)_{60}$ was dissolved into 20mL of MP H2O with 20% glycerol to limit self-aggregation of clusters. This solution was added to a microscope staining flask with a freshly cleaned 10nm gold microscope slide. The solution was left stirring at 4°C for 12 h. For the formation of gold electrodes in the presence of salts, buffers and with the laccase enzyme 20mg of $Au_{144}(pMBA)_{60}$ was dissolved into 20mL PBS with 20% glycerol to prevent aggregations and precipitation of clusters. For laccase functionalized 3D SAM's 0.8mg of

lyophilized protein was added to the Au144(pMBA)60 solution. 1cm x 1cm microscope slides were placed into solution and left to stir at room temperature for 2 hours followed by 12 hours of stirring at 4°C. Functionalized electrodes were rinsed in PBS and placed into a sonicating bath in PBS at 4°C and sonicated for 3 cycles of 15 min each, replacing PBS each time.

Results and Discussion

IR-ATR Thiol SAM

The use of attenuated total reflection was necessary to study the SAMs on the gold electrode due to their low concentration at the electrode surface. DTME and azido propyl thioacetate functionalized gold electrodes were directly studied with a germanium anvil. There are no unique spectroscopic features to the DTME SAM, since the carbonyl bonds in maleimide are not as unique as for the azido SAM's. DTME IR spectra can be seen at the end of the chapter in figure 23. The azido propyl thioacetate SAM did show a distinctive peak at 2100 wavenumbers typical for azide moieties. After CuAAC reaction combining propargyl

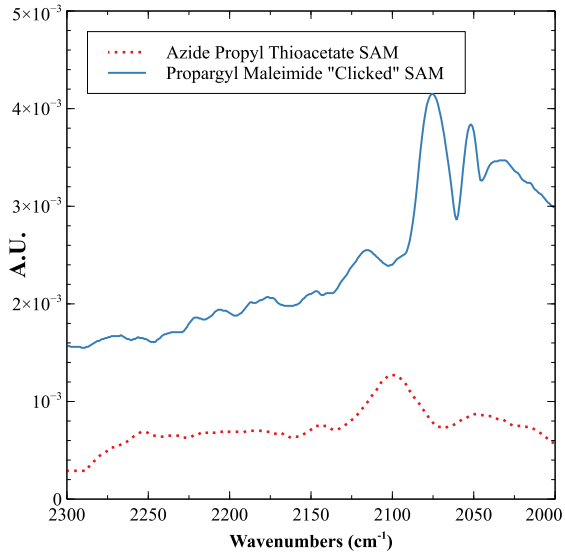

Figure 19 IR-ATR of the Azido thioacetate SAM before and after CuAAC reaction with propargyl maleimide. Signs of the Azide peak at 2100 cm^{-1} appears to disappear.

maleimide with azide-capped SAM the peak at 2100 disappears and other signals typical for other carbonyl compounds appear in the absorption region. The before and after CuAAC reaction can be seen in figure 19. Although the regions do not absorb in the same way the absorbance units are within the same realm and with the CuAAC no sign of lingering azides can be seen.

DTME and Azido SAM Electrochemistry

The electrochemical measurements were taken in pH 5 citrate buffer, common conditions for laccase electrochemistry. Looking into the working window of the SAM's, cyclic voltammetry was applied with a wide voltage range. In Figure 25, reduction of the SAM can be seen to take place after -500mV followed by the rapid reduction of water and subsequent destruction of the 10nm gold base layer. Oxidation of the SAM occurs at higher potentials beyond 800mV vs Ag/AgCl. This correlates well with established working window of thiol based SAM's.[23] This gives a working window of these electrodes to be 0.7V to -0.3V vs Ag/AgCl. This window accommodates the redox potential of ABTS as well as what we achieved for the laccase library on MWCNT where the whole library began reduction at potentials lower than 0.4V vs Ag/AgCl.

For the reduction of oxygen to water using the laccase library on the SAM modified gold electrodes the furthest negative any experiment went was to -200mV vs Ag/AgCl. With the oxygen catalysis with MWCNT occurring just beyond 400mV vs Ag/AgCl a 600mV overpotential between electrodes was maintained during experimentation. Especially since the graphite modified electrodes react with ABTS within 200mV as the gold modified electrodes. Unfortunately, no conditions were found that showed any of the laccase library

through any binding motif whether it be directly bound to gold, by DTME, or by the clicked SAMs. No combination of laccase mutant or electrode architecture was able to show any electrochemical response indicating a catalytic reaction was taking place. Many attempts were made including changing acidic buffers from PBS at PKA1 (pH 3), acetate buffers, and citrate buffers and no reduction of oxygen was seen. Since enzyme stability needs to be considered during direct electron transfer, slow sweep rates were maintained never exceeding 10mV/s during experimentations in concordance with much of the active literature.[16,24] We experimented with oxygen reduction in the presence of 1mM ABTS in solution as well. This also resulted in no sign of electron transfer with the laccase enzyme.

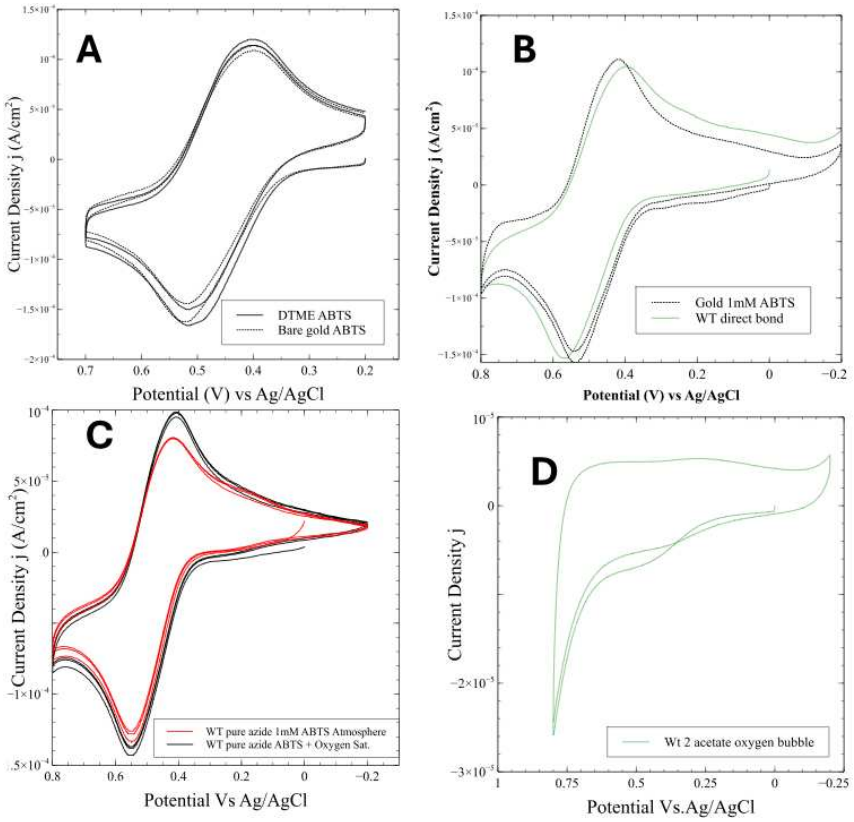

Figure 20 Electrochemical experiments with WT laccase in different cyclic voltammetry conditions. (A) shows the redox CV of ABTS by the bare gold electrode and the DTME monolayer. (B) Is he gold electrode and WT modified electrode through a direct bond to the gold combining the redox chemistry of ABTS with the reduction of oxygen in more negative potentials. (C) WT laccase on the Azide modified electrodes during the redox of ABTS with and without oxygen present. (D) WT laccase on DTME with a CV in the presence of oxygen. No catalysis was ever observe using these architectures.

Some of these electrochemical measurements can be seen in figure 20. All of this is very unexpected since once these electrodes are placed into a solution with ABTS the solution will slowly change color indicating there are laccase enzymes on the electrode surface.

For the oxidation of ABTS unfortunately the story is the same as for the catalytic reduction of oxygen by the laccase library. Many conditions and environments were tested and yet there was no catalytic response in any of them. Strangely the bare gold electrode surface and electrodes show similar current responses for the redox of ABTS. This continues after laccase enzymes are thought to be immobilized onto the electrode surface where minimum changes to the "duck shape" of ABTS occurs. Given the complications involving quantifying the free thiol concentration there was whether the laccase library was not binding to the maleimide tail groups. This is a possibility, yet the color change that occurs when laccase exposed electrodes are placed into solutions containing ABTS is unexpected. And even happens after taping the glass side of the microscope slide so that the any adsorbed enzymes on the glass are not contributing to any color change.

3D SAM Oxygen Reduction

When using the 3D SAM with Au144 to create topographic features in the presence of laccase there is a clear difference in currents between electrodes with and with laccase WT attached seen in Figure 21. In oxygen saturated citrate buffer, the WT laccase enzyme began reduction of at -100mV vs Ag/AgCl a full 100mV before a bare gold electrode began its reduction of water. The Au144 modified gold microscope slides without laccase followed

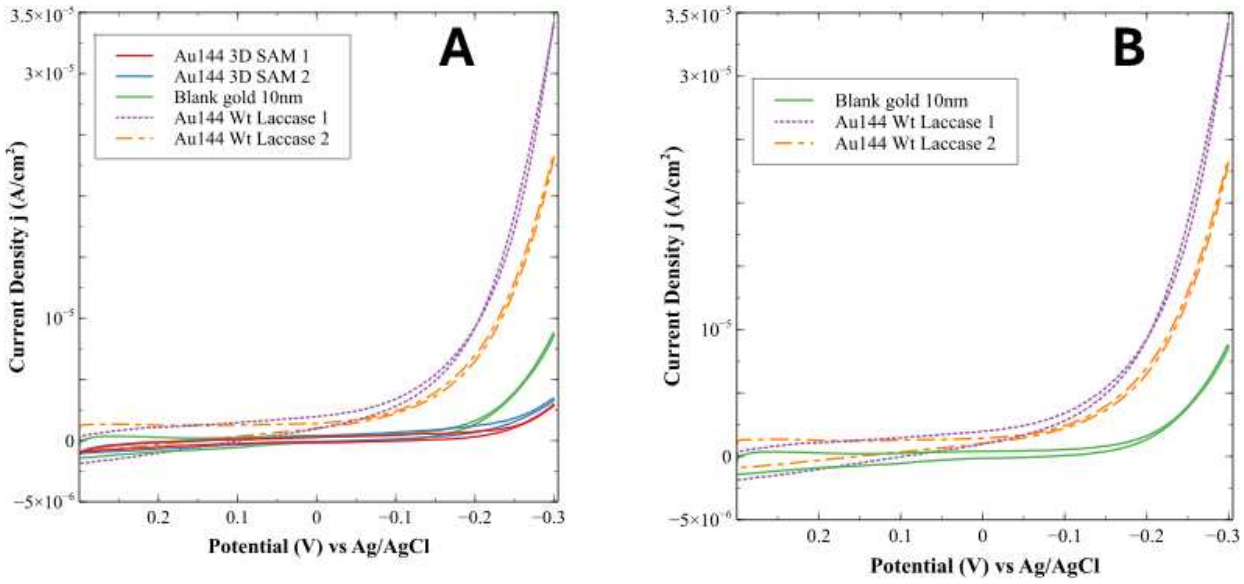

Figure 21 Cyclic voltammograms of the Au144 functionalized electrodes and their reduction of oxygen. (A) all the electrodes combined and (B) just the laccase modified electrodes compared to the blank bare gold electrode electrode.

with an onset potential of -300mV vs Ag/AgCl. With the Au144 clusters possessing a propanoic acid SAM before attaching to the gold electrode it appears this SAM remains and is having an insulating effect on the electrodes ability to reduce diatomic oxygen. Unfortunately, there has only been enough time to make small samples of these electrodes due to how labor intensive it is to prepare the Au144 modified 3D SAM's. The surface roughness of gold electrodes has been shown to have a great effect on the onset potential for the laccase reduction of oxygen. After roughening up their gold electrode found a 200mV difference in their onset potential.[16] Comparing this information with the known working window of the DTME and thioacetate SAM there is a chance that any oxygen reduction reactions performed by the laccase library could have occurred after the reduction of the gold sulfur bond begins using a 10nm gold base layer. The gold sulfur bond has been shown to be very prone to reduction and oxidation, having a small electrochemical window.[23] For

this reason we did not extend the reduction window further for the catalytic reduction of oxygen by this electrode reduction trial.

Atomic Force Microscopy of Au144(PMBA)60 3D SAM's

The atomic force microscopy of the gold surface showed a stark difference in the electrodes topography after being exposed to the Au144 clusters and can be seen in Figure 22. The bare gold with no modifications showed that the 10nm gold microscope slide from deposition research laboratory shows a flat surface with no major features over 2nm throughout the 500nm x 500nm search area. A maximum change of ±3nm was observed, yet overall, the surface appears nearly flat. The addition of the Au144 clusters without any salts used to help stabilize any charges or help chelate clusters into place showed only a slight addition of randomly placed pillars rising upwards of 7nm from the surface. These pillars are thin as well only ranging 50nm in width at the thickest. Once PBS is used to help buffer the pH and provide some charge stabilization with the addition of salts within the PBS showed a stark difference in topography obtained. The electrodes modified in the presence of PBS showed motifs more similar to mountain ranges rather than the pillars obtained without the use of salts. Long connections of steeply rising pillars act like walls. Forming motifs similar to mountains and valleys, this greatly increased the surface area of the electrodes with peaks of 7nm from the surface average. The mixture of WT laccase with Au144 clusters provided electrodes with even greater change in topography where these mountain-like morphologies now rise 30nm above the surface. This makes sense as the laccase enzymes are 5nm in diameter at places and this would greatly increase the size of the building blocks of these topologies. There are no obvious shapes that make appear to be enzymes alone so

there is no way of knowing whether the laccase enzymes are embedded in the added topography or sitting on top. Chances are the laccase enzymes are held within these structures in a combination of entrapment and covalent methods.

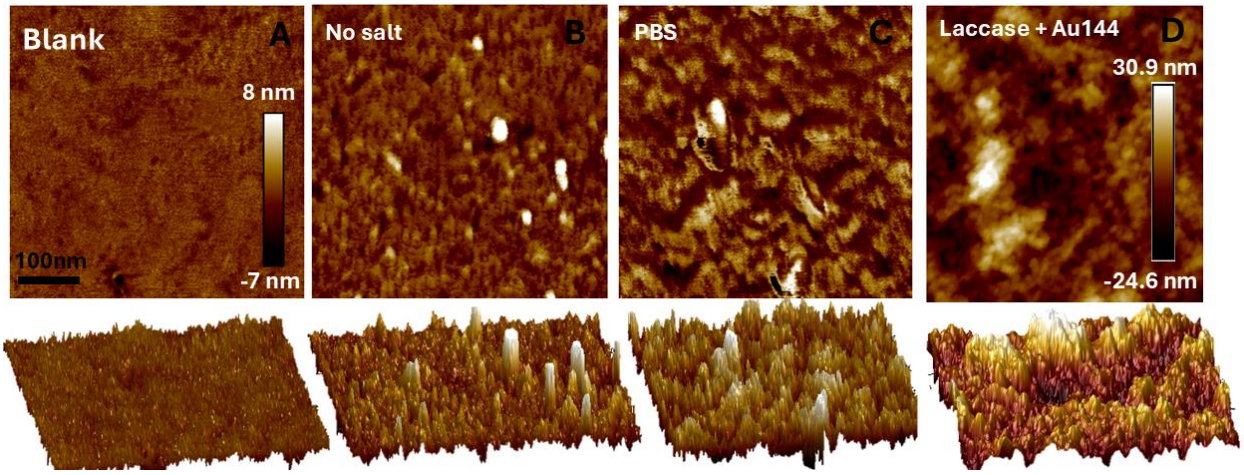

Figure 22 Atomic Force Microscope of the Au144 modifed electrodes. A-C use the initial scale bar while D has its own scale bar for clarity. (A) bare gold electrode (B) Au144 modification without salts (C) Au144 modification in the presence of PBS (D) Au144 modified electrodes in the presence of WT laccase

Future Directions

Not obtaining the any electrochemical catalysis with any of the laccase library on the 10nm gold electrodes was challenging, yet there are a few more things worth trying with this novel electrode setup. With such a low onset potential for the 3D SAM compared to the oxygen reduction using MWCNT there appears to be some significant resistance towards electron transfer with these electrodes. This could be caused by the thin 10nm gold film being resistant towards electron transfer with bound catalysts. Gold films of different thickness should be tested to see if the thickness influences the gold-enzyme interactions. Thin film gold microscope slides come in 50nm, 100nm, and 500nm variants are commercially available products. Atomic Force microscopy is not sensitive enough to

distinguish a protein on an electrode surface. Typically the carbon based structures do no give the same repulsion as hard metallic surfaces. Scanning tunnelling microscope(STM) on the other hand is sensitive to distinguish these features.

Scanning tunnelling microscope is very similar to AFM in their design and analytical setup. The main difference between the two is that STM measures the currents achieved by a surface with sub nanometer resolution is some cases.[11] STM has already been used on many laccase surfaces successfully.[24,26,27] This would be a beneficial analytical tool for both the planar gold electrodes and the 3D SAM electrodes. For the planar electrodes it would be interesting to see if there are 5nm sized features with poor electron conductance compared to the surrounding gold electrode, if the laccase library continues to be poorly conducting toward electron transfer. For the 3D SAM it would be interesting to see where laccase enzymes are held within the collapsed gold cluster architectures, if there are any on the surface, or if we can find any held within the large topographic features.

Binding alkynes and carbonyls to gold surfaces has recently become an intriguing topic in surface chemistry for modifying gold for both nanoscale and bulk materials.[27] These bonds have been demonstrated to be more stable than Au-S bonds, which are prone to disorder, oxidation, and reduction, while Au-C seem to have wider working windows before degradation occurs.[28] Forming SAM of propargyl maleimide, 1,4 diethynyl Benzene, or any other short chain di-alkyne would be interesting to test for improved electron transfer between the laccase library.

The spontaneous collapsing of gold nanoclusters onto bulk gold material is very interesting and a novel way to add topography to thin films. This area requires much more experimentation to understand the underlying mechanism and establish different control conditions. Few conditions were established for the functionalization of these electrodes and more conditions (pH, salt concentrations, applied potentials, and Buffers) should be explored in order to optimize these conditions. PBS was chosen as the buffer as a default due to its compatibility with biological substrates and other biological buffers could result in different topologies and features due to differences in pH and chelating strengths. Sulfonated and aminated buffers interact with gold nanostructures differently than phosphate groups, which have been shown to be strongly chelating to gold.[29] Different topologies leading to a myriad of pore sizes, pillar heights, and topological features could interact with different proteins with more favorable interactions over other topologies.

Since there are so few water-soluble clusters available, exploring these functionalizing techniques with organo-soluble clusters would introduce different sized building blocks to explore new topological features. This would not longer be considered as "green" chemistry, but would allow for more options for electrode modification. Organo-soluble clusters range in sizes from sub nanometer to ~ 2.0nm clusters and can be functionalized with a myriad of different SAM's.[30,31] Sulfides, phosphines, and alkynes are functional groups that have been shown to form stable SAM's with gold clusters. Since there are no reported alkyne functionalized water-soluble clusters, this would be the only way to form alkynyl bonds to this style of electrode formation. Since we have evidence of SAM retention on the 3D SAM's after electrode formation this would allow for more

immobilization strategies outside of entrapment and adsorption. Using propargyl maleimide or DTME as SAM's for gold clusters would allow for a cysteines thiol to bind to the terminal maleimide groups after electrode formations. This would be requires since the laccase enzyme would certainly denature in organic solvents. Introducing the enzyme at different times of 3D SAM formation would aid in this endeavor.

Conclusions

Multiple electrode architectures were designed to grow on to 10nm gold microscope slides. These architectures were intended to bind to the library of Laccase enzymes designed to orient themselves in different ways on the electrode surface with the intention understanding the effect enzyme orientation has on the electrochemical properties. Alkyl thiols were used to form self-assembled monolayers (SAMs) on the gold surface. Two different SAM's were used: one using dithiobismaleimidoethane (DTME) and the other using azido propyl thioacetate. Both SAM designs have a maleimide group tail group exposed to the electrolyte solvent. Laccase enzymes were immobilized onto these electrodes using the laccase' single cysteine residue. Cyclic voltammograms were taken with two of laccases substrates 2,2'-azino-bis(3-ethylbenzothiazoline-6-sulfonic acid) (ABTS) and gaseous oxygen. Many attempts were made to obtain an electrochemical response from these electrodes, yet nothing was achieved. Buffers, pH, scan rate, and scan windows were all tested with every enzyme in the library to no avail. This was always peculiar because electrodes which showed no electrochemical response, once placed in solutions containing ABTS, the cause a color change indicative of ABTS oxidation by laccase enzymes. Strangely this suggests that there are at least laccase enzymes adsorbed to the electrode

surface. Using the laccase library adsorbed onto multi-walled carbon nanotubes (MWCNT) we obtained a clear catalytic response by every enzyme tested. This library has shown even through adsorption they are able to demonstrate direct electron transfer with the electrode without any mediators. The complex 3D structure of the MWCNT could aid in this electron transfer. The 10nm planar electrode intentionally does not have many 3D on the order of the size of the enzyme or larger.

There is a growing body of literature pointing to the complex nature of obtaining electron transfer with planar electrodes[16,26,32] In attempts to understand whether the planar nature of the electrode was having an effect on the electron transfer, we engineered a topographically complex surface using water soluble gold clusters. The spontaneous adsorption of the gold clusters onto the gold electrode and subsequent collapsing into them seems to be a feature of the aurophilic nature of gold and a novel technique to functionalize gold electrodes.[33,34] The resulting surface is being referred to as a 3D SAM, since the gold electrode seem to be maintaining some the clusters' original mercaptobenzoic acid protecting monolayer. The intercalation of laccase into this 3D structure during its formation led to a clear catalytic response towards the reduction of oxygen for the wild type laccase. The reduction of oxygen while imbedded in the 3D SAM occurs at an overpotential nearly 400mV past the onset potential achieved using the MWCNT. This suggests the gold electrode is operating under higher resistance than expected for electron transfer to the laccase catalysts. This is most likely caused by the capacitive nature of the electrolyte double layer formed during electrode polarization. Knowing that increasing the topography in planar electrodes can have an effect of hundreds of millivolts on the onset potential of

similarly designed electrodes, there is a chance that the potential for electron transfer given the electrode design could be occurring beyond the reduction of the thiol SAM. These are still preliminary results and more needs to be done to study the 3D SAM formation, the working window of the electrode, as well as introduce the rest of the library to the new electrode design.

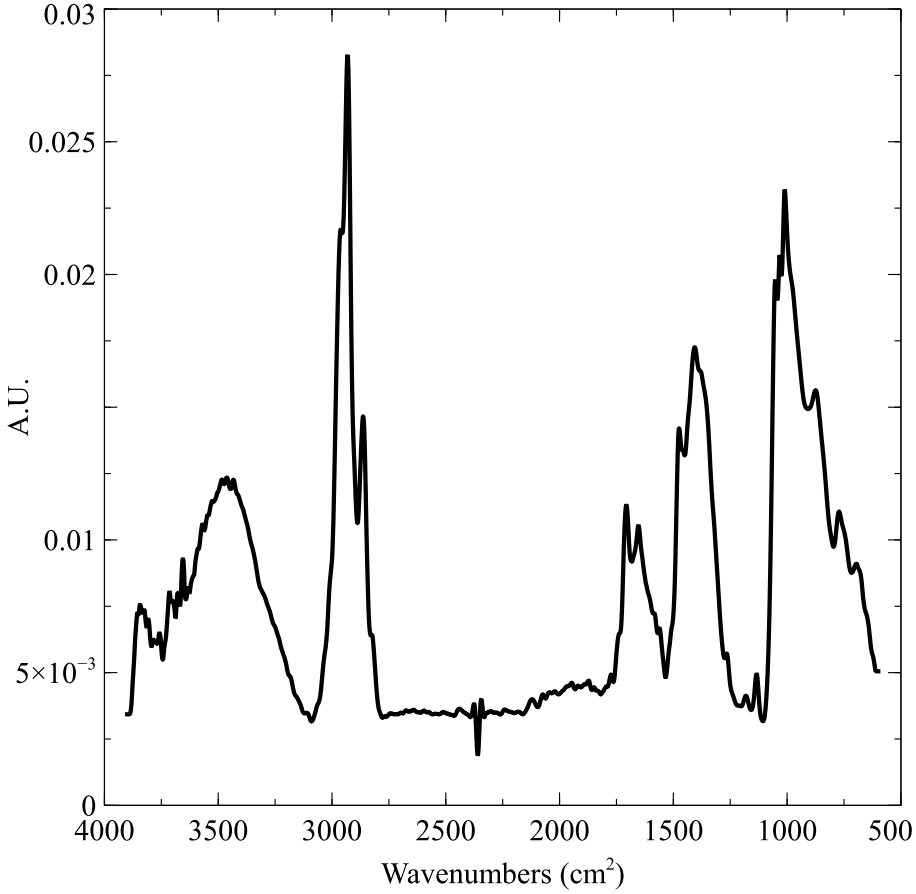

Figure 23IR-ATR of the DTME SAM electrode

Figure 24 Electrodes not electrochemically active still exhibit signs that laccase enzymes are present on the electrode.Whether they were directly bound versus adsorbed is unknown

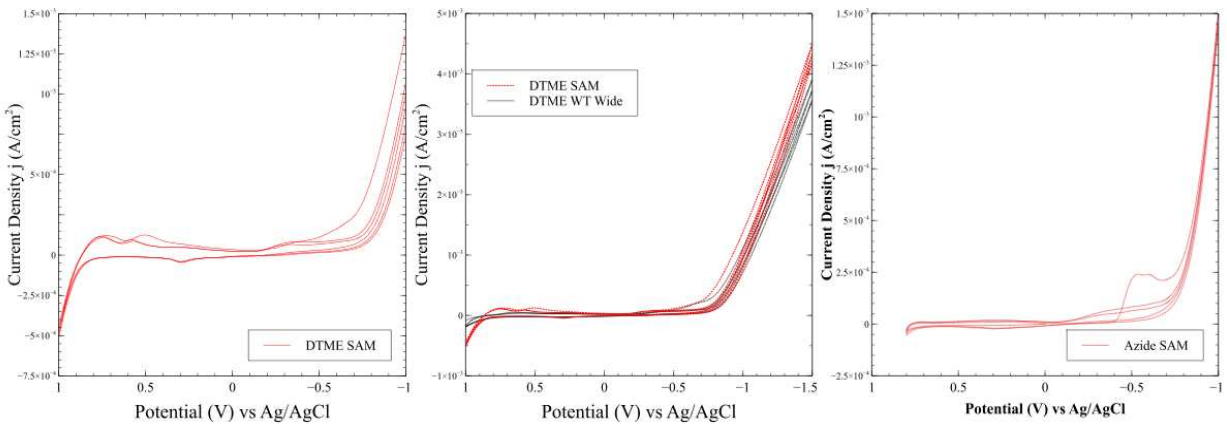

Figure 25 Electrochemical working window of the DTME and Azido propyl thioacetate SAM's

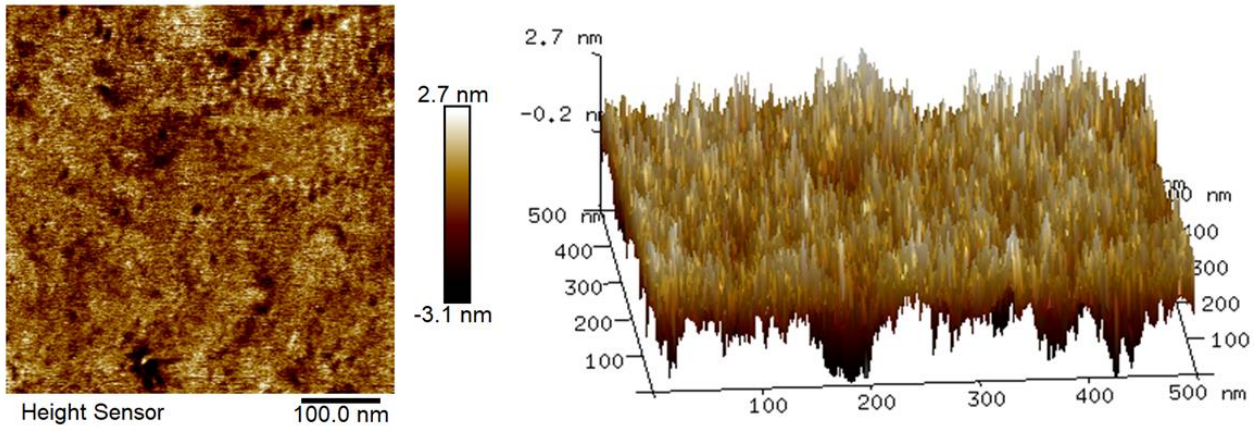

Figure 26 Bare gold electrode Atomic Force Spectroscopy

References

(1) Tominaga, M.; Ohtani, M.; Taniguchi, I. Gold Single-Crystal Electrode Surface Modified with Self-Assembled Monolayers for Electron Tunneling with Bilirubin Oxidase. *Phys. Chem. Chem. Phys.* **2008**, *10* (46), 6928–6934. https://doi.org/10.1039/B809737B.

(2) Wandelt, K. Properties and Influence of Surface Defects. *Surface Science* **1991**, *251–252*, 387–395. https://doi.org/10.1016/0039-6028(91)91021-O.

(3) Krakow, W. The Direct Observation of Atomic Surface Structure and Inclined Planar Defects in Au(111) Films. *Thin Solid Films* **1982**, *93* (3), 235–253. https://doi.org/10.1016/0040-6090(82)90129-8.

(4) Che, G.; Li, Z.; Zhang, H.; Cabrera, C. R. Voltammetry of Defect Sites at a Self-Assembled Monolayer on a Gold Surface. *Journal of Electroanalytical Chemistry* **1998**, *453* (1), 9–17. https://doi.org/10.1016/S0022-0728(97)00246-5.

(5) López-Lorente, Á. I. Recent Developments on Gold Nanostructures for Surface Enhanced Raman Spectroscopy: Particle Shape, Substrates and Analytical Applications. A Review. *Analytica Chimica Acta* **2021**, *1168*, 338474. https://doi.org/10.1016/j.aca.2021.338474.

(6) Hasan, M.; Bethell, D.; Brust, M. The Fate of Sulfur-Bound Hydrogen on Formation of Self-Assembled Thiol Monolayers on Gold: 1H NMR Spectroscopic Evidence from Solutions of Gold Clusters. *J. Am. Chem. Soc.* **2002**, *124* (7), 1132–1133. https://doi.org/10.1021/ja0120577.

(7) A. Canaria, C.; So, J.; R. Maloney, J.; J. Yu, C.; O. Smith, J.; L. Roukes, M.; E. Fraser, S.; Lansford, R. Formation and Removal of Alkylthiolate Self-Assembled Monolayers on Gold in Aqueous Solutions. *Lab on a Chip* **2006**, *6* (2), 289–295. https://doi.org/10.1039/B510661C.

(8) Hostetler, M. J.; Templeton, A. C.; Murray, R. W. Dynamics of Place-Exchange Reactions on Monolayer-Protected Gold Cluster Molecules. *Langmuir* **1999**, *15* (11), 3782–3789. https://doi.org/10.1021/la981598f.

(9) Silva, R.; Muniz, E. C.; Rubira, A. F. Maleimide Immobilized on a PE Surface: Preparation, Characterization and Application as a Free-Radical Photoinitiator. *Langmuir* **2009**, *25* (2), 873–880. https://doi.org/10.1021/la802309u.

(10) Park, C. S.; Lee, H. J.; Jamison, A. C.; Lee, T. R. Robust Maleimide-Functionalized Gold Surfaces and Nanoparticles Generated Using Custom-Designed Bidentate Adsorbates. *Langmuir* **2016**, *32* (29), 7306–7315. https://doi.org/10.1021/acs.langmuir.6b01299.

(11) Park, T.; Kang, H.; Ito, E.; Noh, J. Self-Assembled Monolayers of Alkanethioacetates on Au(111) in Ammonium Hydroxide Solution. *Bulletin of the Korean Chemical Society* **2021**, *42* (2), 252–257. https://doi.org/10.1002/bkcs.12189.

(12) Singh, A.; Dahanayaka, D. H.; Biswas, A.; Bumm, L. A.; Halterman, R. L. Molecularly Ordered Decanethiolate Self-Assembled Monolayers on Au(111) from in Situ Cleaved Decanethioacetate: An NMR and STM Study of the Efficacy of Reagents for Thioacetate Cleavage. *Langmuir* **2010**, *26* (16), 13221–13226. https://doi.org/10.1021/la100103k.

(13) Béthencourt, M. I.; Srisombat, L.; Chinwangso, P.; Lee, T. R. SAMs on Gold Derived from the Direct Adsorption of Alkanethioacetates Are Inferior to Those Derived from the Direct Adsorption of Alkanethiols. *Langmuir* **2009**, *25* (3), 1265–1271. https://doi.org/10.1021/la803179q.
(14) Devaraj, N. K.; Collman, J. P. Copper Catalyzed Azide-Alkyne Cycloadditions on Solid Surfaces: Applications and Future Directions. *QSAR Comb. Sci.* **2007**, *26* (11–12), 1253–1260. https://doi.org/10.1002/qsar.200740121.
(15) Hein, J. E.; Fokin, V. V. Copper-Catalyzed Azide–Alkyne Cycloaddition (CuAAC) and beyond: New Reactivity of Copper(i) Acetylides. *Chem Soc Rev* **2010**, *39* (4), 1302–1315. https://doi.org/10.1039/b904091a.
(16) Thorum, M. S.; Anderson, C. A.; Hatch, J. J.; Campbell, A. S.; Marshall, N. M.; Zimmerman, S. C.; Lu, Y.; Gewirth, A. A. Direct, Electrocatalytic Oxygen Reduction by Laccase on Anthracene-2-Methanethiol-Modified Gold. *J. Phys. Chem. Lett.* **2010**, *1* (15), 2251–2254. https://doi.org/10.1021/jz100745s.
(17) Hitaishi, V. P.; Clement, R.; Bourassin, N.; Baaden, M.; De Poulpiquet, A.; Sacquin-Mora, S.; Ciaccafava, A.; Lojou, E. Controlling Redox Enzyme Orientation at Planar Electrodes. *Catalysts* **2018**, *8* (5), 192. https://doi.org/10.3390/catal8050192.
(18) Siepenkoetter, T.; Salaj-Kosla, U.; Xiao, X.; Belochapkine, S.; Magner, E. Nanoporous Gold Electrodes with Tuneable Pore Sizes for Bioelectrochemical Applications. *Electroanalysis* **2016**, *28* (10), 2415–2423. https://doi.org/10.1002/elan.201600249.
(19) Xiao, X.; Si, P.; Magner, E. An Overview of Dealloyed Nanoporous Gold in Bioelectrochemistry. *Bioelectrochemistry* **2016**, *109*, 117–126. https://doi.org/10.1016/j.bioelechem.2015.12.008.
(20) Qiu, H.; Xue, L.; Ji, G.; Zhou, G.; Huang, X.; Qu, Y.; Gao, P. Enzyme-Modified Nanoporous Gold-Based Electrochemical Biosensors. *Biosensors and Bioelectronics* **2009**, *24* (10), 3014–3018. https://doi.org/10.1016/j.bios.2009.03.011.
(21) Fehr, J. M.; McKenas, C. G.; Liu, B.; Lockett, M. R. Azide-alkyne Click Reactions to Prepare Chemically Modified Amorphous Carbon Electrodes. *Applied Surface Science* **2019**, *480*, 1109–1115. https://doi.org/10.1016/j.apsusc.2019.02.151.
(22) Mak, L. H.; Sadeghi, S. J.; Fantuzzi, A.; Gilardi, G. Control of Human Cytochrome P450 2E1 Electrocatalytic Response as a Result of Unique Orientation on Gold Electrodes. *Anal. Chem.* **2010**, *82* (12), 5357–5362. https://doi.org/10.1021/ac101072h.
(23) Ovchinnikova, S. N.; Medvedev, A. Zh. Desorption of Octanethiol from Gold Electrode Surface during Its Electrochemical Cleaning. *Russ J Electrochem* **2015**, *51* (4), 287–293. https://doi.org/10.1134/S1023193515040084.
(24) Traunsteiner, C.; Sek, S.; Huber, V.; Valero-Vidal, C.; Kunze-Liebhäuser, J. Laccase Immobilized on a Mixed Thiol Monolayer on Au(111) – Structure-Dependent Activity towards Oxygen Reduction. *Electrochimica Acta* **2016**, *213*, 761–770. https://doi.org/10.1016/j.electacta.2016.07.111.
(25) Farneth, W. E.; Diner, B. A.; Gierke, T. D.; D'Amore, M. B. Current Densities from Electrocatalytic Oxygen Reduction in Laccase/ABTS Solutions. *Journal of*

Electroanalytical Chemistry **2005**, *581* (2), 190–196. https://doi.org/10.1016/j.jelechem.2005.03.025.
(26) Climent, V.; Zhang, J.; Friis, E. P.; Østergaard, L. H.; Ulstrup, J. Voltammetry and Single-Molecule in Situ Scanning Tunneling Microscopy of Laccases and Bilirubin Oxidase in Electrocatalytic Dioxygen Reduction on Au(111) Single-Crystal Electrodes. *J. Phys. Chem. C* **2012**, *116* (1), 1232–1243. https://doi.org/10.1021/jp2086285.
(27) Zaba, T.; Noworolska, A.; Bowers, C. M.; Breiten, B.; Whitesides, G. M.; Cyganik, P. Formation of Highly Ordered Self-Assembled Monolayers of Alkynes on Au(111) Substrate. *J. Am. Chem. Soc.* **2014**, *136* (34), 11918–11921. https://doi.org/10.1021/ja506647p.
(28) Guo, L.; Ma, L.; Zhang, Y.; Cheng, X.; Xu, Y.; Wang, J.; Wang, E.; Peng, Z. Spectroscopic Identification of the Au–C Bond Formation upon Electroreduction of an Aryl Diazonium Salt on Gold. *Langmuir* **2016**, *32* (44), 11514–11519. https://doi.org/10.1021/acs.langmuir.6b03206.
(29) Konishi, K.; Iwasaki, M.; Shichibu, Y. Phosphine-Ligated Gold Clusters with Core+exo Geometries: Unique Properties and Interactions at the Ligand–Cluster Interface. *Acc. Chem. Res.* **2018**, *51* (12), 3125–3133. https://doi.org/10.1021/acs.accounts.8b00477.
(30) Sokolowska, K.; Hulkko, E.; Lehtovaara, L.; Lahtinen, T. Dithiol-Induced Oligomerization of Thiol-Protected Gold Nanoclusters. *J. Phys. Chem. C* **2018**, *122* (23), 12524–12533. https://doi.org/10.1021/acs.jpcc.8b02988.
(31) Abroshan, H.; Li, G.; Lin, J.; Kim, H. J.; Jin, R. Molecular Mechanism for the Activation of Au25(SCH2CH2Ph)18 Nanoclusters by Imidazolium-Based Ionic Liquids for Catalysis. *Journal of Catalysis* **2016**, *337*, 72–79. https://doi.org/10.1016/j.jcat.2016.01.011.
(32) Shleev, S.; Pita, M.; Yaropolov, A. I.; Ruzgas, T.; Gorton, L. Direct Heterogeneous Electron Transfer Reactions of Trametes Hirsuta Laccase at Bare and Thiol-Modified Gold Electrodes. *Electroanalysis* **2006**, *18* (19–20), 1901–1908. https://doi.org/10.1002/elan.200603600.
(33) Dreier, T. A.; Wong, O. A.; Ackerson, C. J. Oxidative Decomposition of Au25(SR)18 Clusters in a Catalytic Context. *Chem. Commun.* **2014**, *51* (7), 1240–1243. https://doi.org/10.1039/C4CC07832B.
(34) Anderson, I. D.; Riskowski, R. A.; Ackerson, C. J. Observable but Not Isolable: The RhAu24(PET)181+ Nanocluster. *Small* **2021**, *17* (27), 2004078. https://doi.org/10.1002/smll.202004078.

Chapter 4 Auxiliary Projects and Final Conclusions

Amorphous materials stability and toxicity

Introduction

The exploration of rigid, amorphous metal-rich (RAMETRIC) materials in the Ackerson lab has led to the discovery of a class of materials unique for their combination of metallic and polymer-like properties.[1] Coinage metals are well known for their binding properties with thiols to form covalently bound molecules[2,3] and metallopolymer hydrogels with 1D[4,5] and 2D extended structures[6]. 2D sheets can stack in the third dimension forming fibers that entangle and trap solvent to form "metallophillic" hydrogels.[7] These materials have demonstrated interesting antibiotic properties; however, their physical properties limit their applications.[8] An extended 3D system is novel in this space and exhibits unique properties from this large, interconnected network, displaying greater strength and structural rigidity over 1D and 2D materials.

We have reported a soft material with high metal content and polymer-like rigidity. The material is comprised of interconnected Ag and cysteine amino acids in a unique mixed phase material. With the introduction of an antisolvent immediately after mixing reagents together forms a colloidal solution of ~50nm silver nanoparticles.[9] Upon desolvation the nanoparticles colloids coalesce to form a rigid amorphous metal-rich (RAMTERIC) phase. This coalescence of colloidal solutions is similar to how sol-gels transition. Figure 27 displays a model of the RAMETRIC structure and interactions that give it such unique

properties. This shows the interactions within the silver colloids and intermolecular forces holding the materials together through different states of hydration.

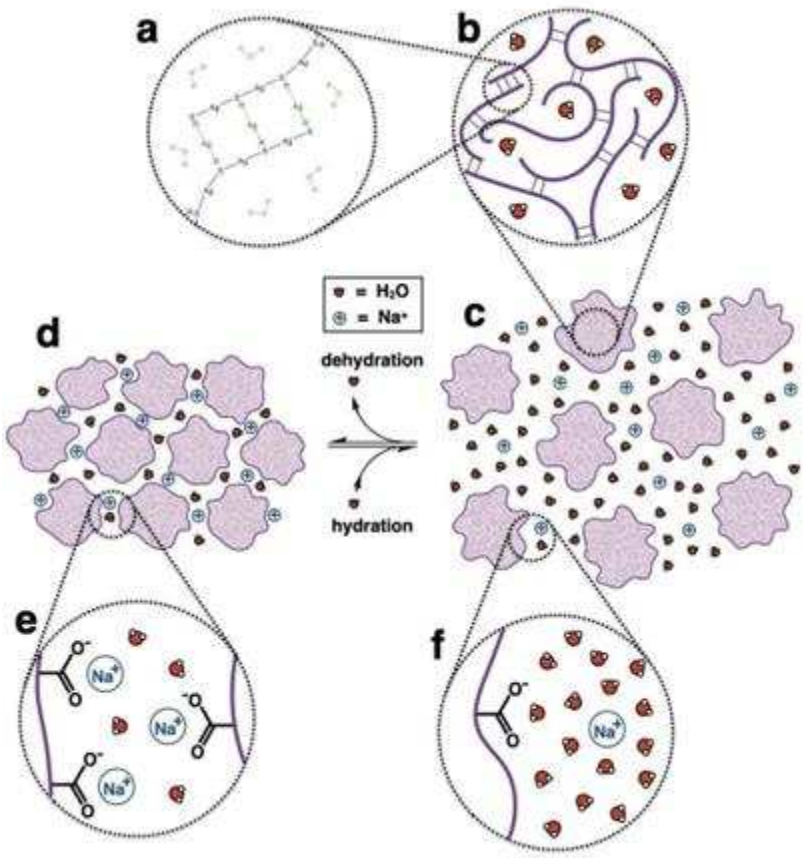

Figure 27 scheme for the predicted structures of the silver-cysteine RAMETRIC materials. (a) silver and cysteine interactions (b) silver and cysteine forming chains, (c & f)fomation of colloids and solvation at higher water content, and (d & e) solvation at lower

The RAMETRIC materials share properties with both gel phases and glass materials yet cannot be classified as either. Gels tend to have hydration content upwards of 95% by mass, while RAMETRIC only has around 5% hydration by mass and forms a rigid amorphous material. This makes it seem more like a glass material; however, glasses are characterized by defined phase transitions. The RAMETRIC material phase has no such temperature-based transitions; rather, it is a near-amorphous solid at lower temperatures and decomposes at higher temperatures. Rheology experiments suggest RAMETRIC belongs to

a unique class of materials. Figure 28 shows the Ashby chart of Youngs modulus vs density compared to many engineered materials pulled from our original work on the material.[9] Not overlapping with any other material on how it reacts to stimuli. RAMETRIC has similar densities to polymers and elastomers, while having the young modulus of natural materials and foams. This means the RAMETRIC material has similar elasticities, or response to axial compression, as materials like rubber, polystyrene foam, and cells. [10]

Silver based antimicrobial and disinfecting compounds have been explored for centuries.[11] Colloidal silver and other silver compounds are more commonly being used as

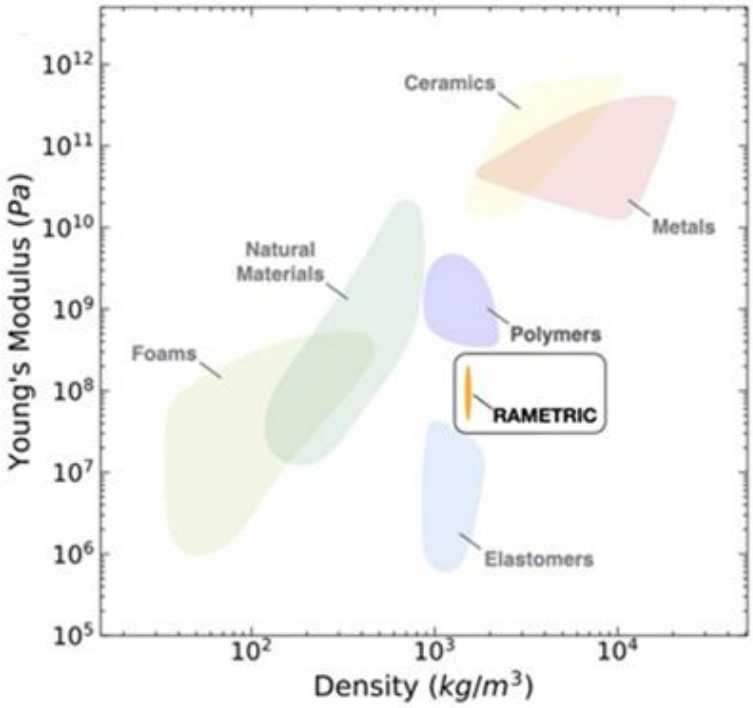

Figure 28 Ashby chart of the physical properties of RAMETRIC compared to many other materials.

topicals and coatings. Silver nanoparticles are also of pharmaceutical interest for drug delivery and disinfections.[12] Most of the silver antimicrobial materials are water and skin soluble.[13] After their application to surface the dried material can also aerosolize and be

inhaled. And through cross contamination with food and hands silver antimicrobial materials can be ingested. Luckily the LD50 for silver is very high even through inhalation at 5.15mg/L.[13] As a new class of material, RAMETRIC needs to be studied in order to understand its antibiotic properties as well as its toxicity towards mammalian life.

In a yet to be published manuscript we tested the antibacterial properties of AgCys RAMETRIC material. In figure 29 We compared the zones of inhibition of the RAMETRIC material with silver ions on e. coli cells using agar plates as a substrate. This experiment suggests that AgCys RAMETRIC produces a larger zone of inhibition than that produced by similar concentrations of $AgNO_3$. This is particularly due to silver ions binding to chloride ions within the media that the e. coli was grown upon. RAMETRIC appears to be less affected by the presence of chloride ions in the media. This is hypothesized to be caused by the strong binding between the silver ions and the cysteines sulfur and amino groups while chloride ions stay outside the colloids within the regime where water and sodium bridges between colloids.

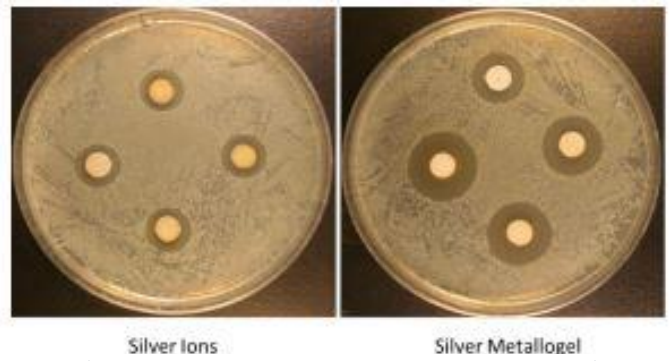

Figure 29 Zone of inhibition study using AgNO3 and AgCys RAMETRIC. The concentration of material starting at the top, moving clockwise are 10, 20, 30, and 40 mg/mL.

Here we extend this experiment to study the toxicity of AgCys RAMETRIC on mammalian cells. For this experiment HeLa and U937 lymphatic cells were used to test the

cell viability in the presence of AgCys. HeLa cells are well established human mimics while U937 is a newer cell line. FlouroBlue was used with a 96 well plate fluorimeter to track the cell viability at different RAMETRIC concentrations.

Methods

Materials

RPMI 1640 medium, Dulbecco's Modified Eagle Medium (DMEM), Trypsin-EDTA, penicillin and streptavidin solution, PBS sterile solution and fetal bovine serum were obtained by Gibco. Cell Counter is a Bio-Rad Tc20 automated cell counter, using BIORAD dual chamber cell counting slides. Trypan blue stain 0.4% from Bio-Rad was the stain used to count the cells. HeLa cells and U937 cell lines were purchased from atcc. HeLa cells were originally taken from Henrietta Lacks in 1951without her consent. $AgNO_3$, DL-Cysteine, and 1,2 dimethoxyethane (Diglyme) were purchased from Sigma Aldrich. CO_2 was purchased from Airgas. FlouroBlue was purchased from Thermos Scientific. The fluorimeter was a BioTek Synergy mx microplate reader.

RAMETRIC synthesis

The synthesis of RAMETRIC requires the preparation of 5 mL 100mM $AgNO_3$ solution in MP H_2O, 10mL of a 100mM cysteine solution in 0.3M NaOH, and 15mL of 1,2-dimethoxyethane (diglyme). In a 50 mL falcon tube with a stir bar the 2.5 mL $AgNO_3$ solution and 7.5mL cysteine solution were combined followed by the immediate addition of the diglyme. The $AgNO_3$ and alkaline cysteine start forming a blue/black color that quickly goes away and becomes a clear, colorless solution. This solution is stirred vigorously for 20 min before stir bar was removed and the solution was centrifuged at 5000 rpm for 15 min. The

result is a yellow precipitation of the gel phase with a single phased clear, colorless supernatant which is gently decanted away. The precipitate is pipetted away using small transfer pipettes and collected in a 1.5mL Eppendorf tube. The resulting materials is subjected to LN until completely frozen and placed in a lyophilizer at .420mbar until completely freeze-dried, 24h later. Lyophilized materials were placed in an airtight container, wrapped in foil, and stored in the freezer. The silver in the RAMETRIC is light sensitive while liquid and as a powder.

Mammalian Cell Growth

All Cell work was done in sterile biological safety cabinets. Proper sterilizing procedures must be taken to avoid contamination. All materials must be sterile, and containers are cleaned with 70% ethanol. Hela Cells were first started from frozen -80 stocks glycerol stocks. Once warmed up cells were pelleted using a centrifuge at 400rpm for 5 minutes. The supernatant was removed and replaced with 500µL of DMEM media. The pellet and media were aspirated gently with a pipette. 1mL of cells were added to the added to 7 mL of DMEM media supplemented with 10% Fetal Bovine Serum (FBS), penicillin (2µg/mL), and streptavidin (0.5µg/mL). Cells were left to incubate in 5% CO_2 solutions at 37°C. After 3 days cell lines were subcultured by removal of the DMEM followed by a wash with10 mL of PBS to remove trace serum. 3.0mL of Trypsin-EDTA solution to the flask and let sit for 5 min. 8mL of media was added and cells were aspirated by gentle pipetting. Cells were transferred to 50mL falcon tubes and centrifuged at 500 rpm for 5 min to form a loose pellet. Supernatant was removed and Eagle media was added to cells followed by a gentle aspiration to loosen pellet. Cells were counted and roughly one million cells were added to

a 75cm^2 flask with 7mL of DMEM with 10% FBS and antibiotics and left to grow at 37°C with 5% CO_2.

U937 cells were thawed from-80°C frozen stocks. Once Thawed the cells were centrifuged at 400rpm for 5 min. The supernatant was removed and replaced with RPMI-1640 media supplemented with 2mM L-glutamine, 5% FBS, penicillin (2µg/mL), and streptavidin (0.5µg/mL). 1mL of cells were added to a 75cm flask with 9mL of growth media. Cells were grown at 37°C with 5% CO_2 in the atmosphere. Subculturing of U937 cells is done by transferring U937 cells from the grown flask to a 50mL sterile falcon tube. Cells were gently pelleted by centrifugation at 500 RPM for 5 minutes. After centrifugation, supernatant was removed and replaced by supplemented RPMI-1640. Cells were counted and roughly 1 million cells were added a new 75cm^2 flask containing 7mL of supplemented RPMI-1640 media.

Toxicity study

HeLa cells were removed from growth flask by removing DMEM media followed by a wash with PBS. 3mL of Trypsin was added to the flask and left to sit for 5 min. Trypsin was neutralized with DMEM media and cells were transferred to a sterile 50mL falcon tube. Cells were centrifuged for 5 min at 500RPM to form a loose pellet. Supernatant was removed and cells were dispersed in DMEM media. Cells were counted and 2000 cells were added to each well in the 96 well plate. Each well was made to a final volume of 100 µL each using supplemented DMEM media. For U937 cells, the RPMI-1640 media was removed, and the cells were gently centrifuged for 5 min at 500RPM to form a loose pellet. After centrifugation the supernatant was removed, and the cells were resuspended in fresh supplemented

RPMI-1640. Cells were counted and 40,000 cells were added to each well in a 96-well plate. Larger quantities of U937 were used to try to maximize the signal obtained. Each well volume was filled to be 100µL using supplemented RPMI-1640. Plates were left to incubate at 37°C at 5% CO_2 for 24 h.

Lyophilized RAMETRIC was ground in a mortar and pestle and the powder was weighed to make working solutions of the AgCys material. A serial dilution of RAMETRIC was made making solution ranging from .1-5mg/mL in MP water. Using these working solutions cells were introduced to AgCys RAMETRIC ranging from .01 to .5 mg/mL of Ag/Cys in solution run in triplicate. Cells were again incubated at 37°C at 5% CO_2 for 24 h.

Plate Reader

To study cell viability cells incubated with AgCys RAMETRIC were removed from the incubator and 20uL of FlouroBlue was added to each well. This mixture was left to incubate at 37°C at 5% CO_2 for one hour. Plates to added to the BioTek fluorimeter and each well was measured using 410nm as the excitation wavelength and 455nm as the emission wavelength.

Results and Discussion

Hela and U937 cell lines were grown up to confluency in their respective media. 2000 cells of each were added to wells in a 96-well plate. After 24 h they were exposed to RAMETRIC AgCys in concentrations ranging from 0.01mg/mL to .5mg/mL. During experimental setup it became abundantly clear that the silver within the RAMETRIC materials was not compatible with the chloride ions required for cell homeostasis. Notably

chloride interacting with silver ions happened more aggressively at lower concentrations of AgCys, once added to the DMEM or RPMI 1640 media, the silver ions separated from the material matrix and began crashing out as a white precipitate of insoluble AgCl. The precipitate made data collection difficult and the results quite noisy. However, we did obtain enough data to get an idea of the toxicity for the RAMETRIC AgCys material. In figure 30 the fluorescence count vs RAMETRIC material added to HeLa and U937 cells. The increase of cells did result in a larger background of counts for the fluorescence measurements, but the difference between maximum and minimum still only varied by 15000 counts by the detector.

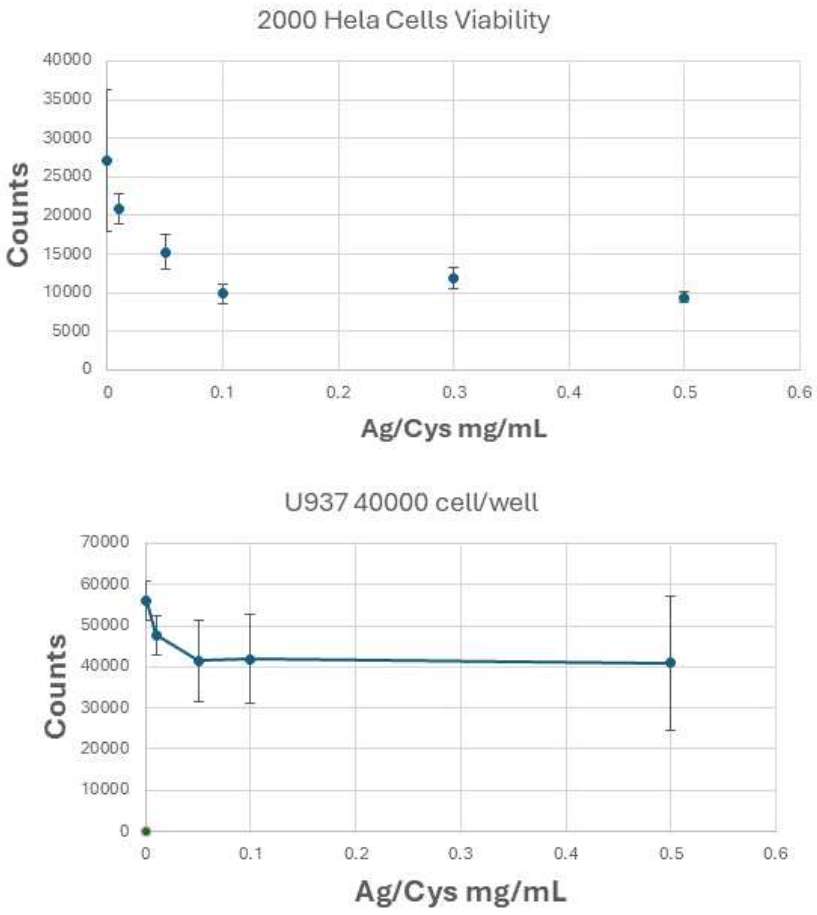

Figure 30 Fluorescence study for the cell viability of HeLa cells and U937 cells exposed to AgCys Rametric.

We do seem to lose most of the counts in cells by 0.5mg/mL for the U937 cells and 0.1mg/mL for the HeLa cells. Still the error bars are significant for these measurements. Unfortunately, chloride is unavoidable in biology, and this makes the measurements of its toxicity complicated. Compared to silver nanoparticles the AgCys RAMETRIC seems to be more susceptible to chloride ion. Silver nanoparticles are more densely bound, consisting of mostly silver, and protected by monolayer of organic molecules. The monolayer seems to keep the silver nanoparticles from reacting with nearby molecules.[14,15] The colloidal silver cysteine seems to be less protected by the ligated cysteines and therefore more prone to react with its environment. Having the more dilute RAMETRIC solutions crash out of solution faster than the more concentrated solutions is a sign of this. Once diluted the colloids are either so small the surface tension cannot hold them together or begin acting as small silver-cysteine molecules or clusters rather than the protected colloids. Operating in single cells environments with RAMETRIC materials appears to be unfeasible so we will attempt to test for AgCys toxicity in larger organisms.

Conclusion

The Ackerson Lab has discovered a novel class of materials rigid, amorphous metal rich material (RAMETRIC). RAMETRIC materials have unique physical properties unlike any material to date, of this metal rich composition. AgCys RAMETRIC is an interesting delivery tool of silver ions, beneficial for their antimicrobial properties. We sought to test the AgCys RAMETRIC safety by finding its toxicity with the single celled mammalian cell lines heLa and

U937. The presence of AgCys RAMETRIC clearly has an effect of mammalian cell viability. This can be see by the rapid decay of the fluorescence signal with higher RAMETRIC concentrations. Chloride ions were a major hinderance in experimental setup. Unfortunately, chloride ions are necessary for cellular function. Moving forward we hope to study the effects of AgCys RAMETRIC on larger organisms not requires to live in aqueous halide heavy environments.

Final Conclusions

Based on the results from the electrochemical measurements there appears to be more nuance required for the use of planar electrodes for use in direct electron transfer(DET) with enzymes. Planar electrodes directly bound to proteins or linked via DTME or azide-alkyne coupling never showed signs of catalysis from the laccase library. The electron transfer with the glassy carbon shows there are some interactions with the laccase library that will allow for DET. Although there was no sign of electron transfer with the electrode surface there were signs that the laccase enzymes were on the electrode surface. When electrodes cleaned by sonication and placed in solutions containing ABTS the solution slowly changes color suggesting ABTS oxidation. Since the gold surface on the electrodes were only 10nm on average roughening of the surface needed to be done by constructive means rather than destructive means to preserve full electrode conductivity. For this purpose, the water soluble Au144 cluster was used to add topography to the electrode surface. Utilizing the aurophilic nature of gold materials Au144 spontaneously adsorbed onto the clean gold electrode surface. Electrochemical measurements suggest the self-assembled monolayer on originally on the cluster was retained after addition onto the electrode surface.

Mixing the laccase WT enzyme with the Au144 clusters in the presence of freshly cleaned gold electrodes produced a catalytically active electrode for oxygen reduction. The onset potential for this reduction was far more negative than that obtained by MWCNT with

the same laccase enzyme –100mV vs Ag/AgCl and 400mV vs Ag/AgCl respectively. This suggests there is still significant resistance towards electron transfer even with these new 3D interfaces. The 400mV or more difference in onset potentials demonstrates how favored 3D interfaces are for electron transfer with enzymes. With such a negative onset potential it is now clear there is a chance that the reduction of oxygen by the planar gold electrodes functionalized with the conventional SAM (DTME and Azido-propyl thioacetate) could be occurring beyond the potential in which we begin getting electrode degradation.

There is a consensus in the literature than flat electrodes are less active more studying to understand the preferred environments to study DET[16–18] This is believed to be caused partly by the capacitive nature of the Hemholtz double layer being formed upon electrode polarization. There is also work showing how the roughness of the surface has a profound effect on surfaces ability to provide rapid electron transfer. To explore this more, the 3D SAM's obtained by here need to be investigated further to optimize the surfaces they form when they collapse onto the planar gold electrode. This no longer allows for control of the enzyme orientation in the same ways as a planar electrode but was the only gold interface studied here that obtained an electrochemical response. As a novel electrode functionalization technique it is not yet clear the full advantages of this style of architecture.

References

(1) Compel, W. S. Metallogels through Glyme Coordination. *Dalton Trans.* **2016**, *45* (11), 4509–4512. https://doi.org/10.1039/C6DT00255B.

(2) Anderson, I. D.; Riskowski, R. A.; Ackerson, C. J. Observable but Not Isolable: The RhAu24(PET)181+ Nanocluster. *Small* **2021**, *17* (27), 2004078. https://doi.org/10.1002/smll.202004078.

(3) Kuda-Singappulige, G. U.; Window, P. S.; Hosier, C. A.; Anderson, I. D.; Aikens, C. M.; Ackerson, C. J. Chiral and Achiral Crystal Structures of Au25(PET)180 Reveal Effects of Ligand Rotational Isomerization on Optoelectronic Properties. *Chemistry – A European Journal* **2024**, *30* (2), e202202760. https://doi.org/10.1002/chem.202202760.

(4) Leung, B. O.; Jalilehvand, F.; Mah, V.; Parvez, M.; Wu, Q. Silver(I) Complex Formation with Cysteine, Penicillamine, and Glutathione. *Inorg. Chem.* **2013**, *52* (8), 4593–4602. https://doi.org/10.1021/ic400192c.

(5) Veselska, O.; Guillou, N.; Diaz-Lopez, M.; Bordet, P.; Ledoux, G.; Lebègue, S.; Mesbah, A.; Fateeva, A.; Demessence, A. Sustainable and Efficient Low-Energy Light Emitters: A Series of One-Dimensional D10 Coinage Metal–Organic Chalcogenolates, [M(o-SPhCO2H)]n. *ChemPhotoChem* **2022**, *6* (5), e202200030. https://doi.org/10.1002/cptc.202200030.

(6) Chen, L.-J.; Yang, H.-B. Construction of Stimuli-Responsive Functional Materials via Hierarchical Self-Assembly Involving Coordination Interactions. *Acc. Chem. Res.* **2018**, *51* (11), 2699–2710. https://doi.org/10.1021/acs.accounts.8b00317.

(7) Odriozola, I.; Ormategui, N.; Loinaz, I.; Pomposo, J. A.; Grande, H. J. Coinage Metal–Glutathione Thiolates as a New Class of Supramolecular Hydrogelators. *Macromolecular Symposia* **2008**, *266* (1), 96–100. https://doi.org/10.1002/masy.200850618.

(8) Boonkaew, B.; Kempf, M.; Kimble, R.; Supaphol, P.; Cuttle, L. Antimicrobial Efficacy of a Novel Silver Hydrogel Dressing Compared to Two Common Silver Burn Wound Dressings: Acticoat™ and PolyMem Silver®. *Burns* **2014**, *40* (1), 89–96. https://doi.org/10.1016/j.burns.2013.05.011.

(9) Armstrong, J.; Shea, P.; Cornell, C. C.; Bryson, T.; Mason, H. E.; Morrison, K. D.; Tofanelli, M.; Lewicki, J. P.; Wood, B. C.; Guilliams, B. F.; Compel, W. S.; Ackerson, C. J. Surpassing the Strength of Metallogels with a Rigid, Amorphous Metal-Rich Material Formulation. *CR-PHYS-SC* **2023**, *4* (12). https://doi.org/10.1016/j.xcrp.2023.101738.

(10) Lee, J.; Jha, K.; Harper, C. E.; Zhang, W.; Ramsukh, M.; Bouklas, N.; Dörr, T.; Chen, P.; Hernandez, C. J. Determining the Young's Modulus of the Bacterial Cell Envelope. *ACS Biomater. Sci. Eng.* **2024**, *10* (5), 2956–2966. https://doi.org/10.1021/acsbiomaterials.4c00105.

(11) Kim, J. S.; Kuk, E.; Yu, K. N.; Kim, J.-H.; Park, S. J.; Lee, H. J.; Kim, S. H.; Park, Y. K.; Park, Y. H.; Hwang, C.-Y.; Kim, Y.-K.; Lee, Y.-S.; Jeong, D. H.; Cho, M.-H. Antimicrobial Effects of Silver Nanoparticles. *Nanomedicine: Nanotechnology, Biology and Medicine* **2007**, *3* (1), 95–101. https://doi.org/10.1016/j.nano.2006.12.001.

(12) Kim, T.-H.; Kim, M.; Park, H.-S.; Shin, U. S.; Gong, M.-S.; Kim, H.-W. Size-Dependent Cellular Toxicity of Silver Nanoparticles. *Journal of Biomedical Materials Research Part A* **2012**, *100A* (4), 1033–1043. https://doi.org/10.1002/jbm.a.34053.
(13) Mijnendonckx, K.; Leys, N.; Mahillon, J.; Silver, S.; Van Houdt, R. Antimicrobial Silver: Uses, Toxicity and Potential for Resistance. *Biometals* **2013**, *26* (4), 609–621. https://doi.org/10.1007/s10534-013-9645-z.
(14) Zheng, K.; Setyawati, M. I.; Leong, D. T.; Xie, J. Antimicrobial Silver Nanomaterials. *Coordination Chemistry Reviews* **2018**, *357*, 1–17. https://doi.org/10.1016/j.ccr.2017.11.019.
(15) Koch, M.; Kiefer, S.; Cavelius, C.; Kraegeloh, A. Use of a Silver Ion Selective Electrode to Assess Mechanisms Responsible for Biological Effects of Silver Nanoparticles. *J Nanopart Res* **2012**, *14* (2), 646. https://doi.org/10.1007/s11051-011-0646-y.
(16) Schneider, E. Oriented Attachment of Cytochrome P450 2C9 to a Self-Assembled Monolayer on a Gold Electrode as a Biosensor Design, UC Berkeley, 2011. https://escholarship.org/uc/item/1m67k8mm (accessed 2019-09-18).
(17) Thorum, M. S.; Anderson, C. A.; Hatch, J. J.; Campbell, A. S.; Marshall, N. M.; Zimmerman, S. C.; Lu, Y.; Gewirth, A. A. Direct, Electrocatalytic Oxygen Reduction by Laccase on Anthracene-2-Methanethiol-Modified Gold. *J. Phys. Chem. Lett.* **2010**, *1* (15), 2251–2254. https://doi.org/10.1021/jz100745s.
(18) Shleev, S.; Pita, M.; Yaropolov, A. I.; Ruzgas, T.; Gorton, L. Direct Heterogeneous Electron Transfer Reactions of Trametes Hirsuta Laccase at Bare and Thiol-Modified Gold Electrodes. *Electroanalysis* **2006**, *18* (19–20), 1901–1908. https://doi.org/10.1002/elan.200603600.